The Role of High Sugar Diets in Colitis

by

Sabitha Rajaruban

A thesis submitted in partial fulfillment of the requirements for the degree of

Master of Science

Department of Medicine
University of Alberta

Abstract

There is an increase in the prevalence of inflammatory bowel disease (IBD) worldwide, and this appears to be associated with an increase in the consumption of a Western diet high in fat and sugar, and low in fiber. Previous work shows that two-day exposure to high sugar diets increases the severity of Dextran Sulfate Sodium (DSS)-induced colitis and impair recovery after removal of DSS. High sugar diets were found to decrease short-chain fatty acids (SCFA), which play a role in gut barrier integrity and promote an anti-inflammatory environment. The purpose of this thesis was to determine whether the increased severity and lack of repair were due to the high sugar content or the altered fiber content of high sugar diets. Mice were given chow diet with 15% glucose, 15% fructose, or control water. Water, food, and caloric intake were assessed, as well as the concentration of SCFAs in cecum contents and stool. Intestinal permeability was measured with plasma lipopolysaccharide (LPS) levels and lactulose/mannitol ratio, and gastroduodenal permeability was assessed with sucrose excretion in the urine. Mice on the high glucose water treatment had increased water intake, making this experimental model inappropriate for use with DSS. No differences in fecal or cecal SCFA levels or small intestinal permeability were observed. Gastroduodenal permeability was higher in mice on high glucose water treatment. In a second study, mice were given chow, 50% glucose, 50% fructose or 50% sucrose diets. DSS was added to drinking water after 2 days. After 5 days, the DSS water was replaced with regular drinking water. Consumption of high sugar diets for 2 days caused a reduction in butyric acid concentration. Mice on the glucose, fructose, and sucrose diets experienced worse disease severity and histological changes and greater concentration of pro-inflammatory cytokines IL-1β and IL-6 in the colon. Significant changes in *Lachnospiraceae* and *Enterobacteriaceae* were observed. During the recovery period, high sugar diet-fed mice had

greater *Enterobacteriaceae* and *Akkermansia*, and lower amounts of SCFA-producing bacteria such as *Lachnospiraceae* and *S24-7*. In conclusion, a lack of fermentable fibers in the high sugar diets was associated with microbial alterations, reduced levels of butyrate-producing microbes, increased susceptibility to DSS-induced colitis and delayed recovery. These results suggest that a lack of fiber rather than the presence of high levels of sugar was responsible for the increased disease susceptibility.

Preface

This thesis is an original work by Sabitha Rajaruban. The research project, of which this thesis is a part, received research ethics approval from the University of Alberta Research Ethics Board, Project Name “Probiotic bacteria and epithelial cells and breeding colony,” No. AUP00000293.

Acknowledgments

Firstly, I would like to express my sincere gratitude to my research supervisor Dr. Karen Madsen for accepting me as a Master's student in her lab. I am thankful for her support throughout my Master's program and for her guidance in writing this thesis.

I am dearly thankful to Naomi Hotte for her encouragement, continuous support, and for sharing her expertise and enthusiasm for research. I am thankful for the current and former students and post-docs in the lab for their friendship and assistance with my studies: Jenny Hyun, Wei Jen Ma, Jerry Dang, Valentin Mocanu, Zhengxiao Zhang, Hee Kuk Park and more.

I would like to thank Dr. Eytan Wine and Dr. Ben Willing for agreeing to be members on my supervisory committee, and for their advice and support. I am thankful for my graduate coordinator, Barb Thomson, for guiding me throughout the program.

Finally, I would like to thank my parents, grandmother, sister, family members, and the friends I have made in Edmonton for their patience, endless support and encouragement.

I would like to acknowledge the financial support provided by The Centre of Excellence for Gastrointestinal Inflammation and Immunity Research (CEGIIR), The Canadian Institutes for Health Research (CIHR), University of Alberta and Faculty of Medicine and Dentistry.

Table of Contents

List of Tables

List of Figures

List of Abbreviations

AUC	Area under the curve
CD	Crohn's Disease
DAI	Disease activity index
DHAP	Dihydroxyacetone phosphate
DSS	Dextran Sulfate Sodium
FITC-dextran	Fluorescein isothiocyanate-conjugated dextran
FOS	Fructo-oligosaccharides
HFCS	High fructose corn syrup
HPLC	High-Performance Liquid Chromatography
IBD	Inflammatory Bowel Disease
IEC	Intestinal epithelial cells
KC	Keratinocyte chemoattractant
KHK	Ketohexokinase
LacMan	Lactulose/mannitol ratio
LEfSe	Linear discriminant analysis effect size
LPS	Lipopolysaccharide
MARCO	Macrophage receptor with collagenous structure
MCT1	Monocarboxylate transporter 1
NF-κβ	Nuclear factor-kappa beta
PBS	Phosphate buffered saline
PCoA	Principle coordinates analysis
PPAR-γ	Peroxisome proliferator-activated receptor-gamma
PUFA	Polyunsaturated Fatty Acid
ROS	Reactive oxygen species
SCFA	Short-chain fatty acids
SEM	Standard error of the mean
SGLT1	Sodium-glucose cotransporter 1
SMCT1	Sodium-coupled monocarboxylate transporter 1
SPF	Specific pathogen-free

TER	Transepithelial electrical resistance
TFF3	Trefoil factor 3
TLR	Toll-like receptors
UC	Ulcerative Colitis
ZO-1	Zonula occludens 1

Chapter 1: Introduction

1.1. Inflammatory Bowel Disease

Inflammatory bowel disease (IBD) involves chronic inflammation of the gastrointestinal tract, resulting in symptoms such as weight loss, abdominal pain, diarrhea and rectal bleeding [1-2]. Individuals experience periods of relapses and remissions. The main forms of IBD are Crohn's Disease (CD) and Ulcerative Colitis (UC). Crohn's Disease is characterized by discontinuous, transmural inflammation that is commonly localized in the terminal ileum and colon. Ulcerative Colitis mainly involves inflammation of the mucosa of the colon and rectum [1-2].

Western countries such as Canada, the United States, Australia and those in Europe have the highest prevalence of IBD and a steady rise in incidence [3]. Currently, the prevalence of IBD in Canada is 0.7% of the population [4]. Adolescents and young adults make up the majority of newly diagnosed cases [4]. A rapid rise in the incidence of IBD in newly industrialized countries such as India and China suggests an influence of environmental factors corresponding to westernization [3]. The current understanding of IBD is that it involves an unregulated immune response against intestinal microbes in a genetically susceptible individual, and is influenced by environmental factors [1-2].

1.2. The Gastrointestinal Tract

The gastrointestinal tract extends from the mouth to the anus and consists of the esophagus, stomach, small intestine and large intestine [5]. The small intestine is longer and has a smaller diameter than the large intestine [5-6]. It consists of three sections, including the duodenum which is located closest to the stomach, the jejunum, and the ileum which is located closest to the large intestine. In humans, the large intestine consists of multiple sections including the cecum, ascending colon, transverse colon, descending colon, sigmoid colon and rectum [5-6]. The gastrointestinal tract in mice consists of a small intestine, cecum, and large intestine. Relative to the large intestine, the cecum is larger in mice than in humans [5]. In both mice and humans, the gut microbiota consists mainly of bacteria in the *Firmicutes* and *Bacteroidetes* phyla [5]. Humans also have a large proportion of bacteria from the *Proteobacteria* and *Actinobacteria* phyla [5-6]. The lack of oxygen in the large intestine promotes the presence of obligate

anaerobes [6]. The colon, especially the cecum, has the greatest microbial diversity in terms of bacterial richness and relative abundance [5-6]. The slow passage of luminal contents through the large intestine and the less acidic environment compared to the other regions of the gastrointestinal tract allows for increased growth of microbes and promotes microbial diversity [5].

1.3. The Intestinal Epithelial Barrier

The intestines are composed of a mucosa, submucosa, muscularis propria, and serosa [6-7]. The mucosa consists of a single epithelial layer, a basement membrane, the lamina propria, and muscularis mucosa. The muscularis mucosa and muscularis propria are two smooth muscle layers that are involved in peristalsis. The lamina propria is made up of connective tissue and contains blood vessels, lymph vessels and immune cells such as macrophages, B and T cells. The submucosa protects the mucosa during peristalsis. It resembles the lamina propria but holds larger blood vessels and adipose tissue [6-7].

The epithelial layer is lined with 4 types of cells: absorptive epithelial cells (enterocytes; IECs), enteroendocrine cells, Paneth cells, and Goblet cells [6,8]. Enterocytes have transporters on the apical and basolateral membrane to facilitate the transcellular transport of nutrients from the lumen to the blood. Enteroendocrine cells produce hormones involved in food intake, electrolyte secretion and blood flow. Goblet cells and Paneth cells maintain a boundary between the microbiota and the intestinal epithelial layer. Goblet cells produce mucin glycoproteins to form mucus layers [6,8]. They also produce trefoil factor 3 (TFF3), which is involved in repairing the intestinal epithelial barrier after damage [8]. Paneth cells are only found in the small intestine and produce antimicrobial peptides such as defensins, which damage bacterial cell walls [6,8].

Intestinal bacteria are separated from the epithelial barrier by the mucus layer [9]. The mucus layer is fragmented in the small intestine but exists as two separate layers in the colon. In the colon, bacteria are found in the thicker outer mucus layer located closest to the lumen. The inner mucus layer is dense and firmly attached to the epithelium due to an interaction between the carbohydrate component of mucins and mucin binding protein (MBP) on intestinal epithelial cell membranes [9-11]. It is devoid of bacteria due to the presence of antimicrobial agents such

as defensins, and IgA antibodies [9-10]. The mucus layers are mostly composed of a polymeric network of MUC2 mucin, which is produced by Goblet cells [10].

In the small intestine, the epithelial barrier consists of invaginations called crypts and projections called villi [6,12]. Enterocytes also have projections called microvilli which contain enzymes and transporters to digest and absorb nutrients. The microvilli form a "brush border" to maximize the surface area for nutrient absorption. Villi and microvilli are not present in the cecum and colon. The cecum and colon are mainly involved in the absorption of water and electrolytes, and transport of undigested food to the rectum [6,12]. The crypts contain pluripotent intestinal epithelial stem cells which can multiply and replace the IECs [6,8,12]. Paneth cells remain in the crypts whereas new enterocytes move towards the villus to replace older cells, which are lost every 4-5 days [7-10,12].

Tight junctions, adherens junctions and desmosomes maintain the epithelial barrier. Tight junctions regulate the paracellular transport of lumenal contents between the cells of the epithelial barrier [7,13]. Tight junctions consist of interactions between transmembrane proteins such as claudins and occludins, with the peripheral membrane protein zonula occludens 1 (ZO-1) and F-actin. Adherens junctions are located basolaterally to tight junctions and similarly involve the interaction of the transmembrane protein E-cadherin with β-catenin, catenin delta-1 and F-actin [7,13]. F-actin associates with myosin to form a perijunctional actomyosin ring [13]. Paracellular transport involves a nonselective leak pathway and a selective pore pathway. There are 27 genes for claudins in humans but the type of claudin present in the epithelial barrier varies depending on the location and local microenvironment. Certain claudins promote barrier integrity, such as claudin-1. Other claudins influence the selectivity of the pore pathway in terms of the charge and size of ions permitted across the intercellular space. For example, claudin-2 form pores for small cations. The expression of claudins is influenced by cytokines, such as TNF-α, which is associated with the upregulation of claudin-2 [7].

1.4. Fiber and Short Chain Fatty Acids

Bacteria in the intestine can produce short-chain fatty acids (SCFAs) from dietary fiber [14-16]. Dietary fibers are nondigestible, plant-derived carbohydrates such as resistant starch, cellulose, hemicellulose and lignin [14-15]. Fibers can be soluble, insoluble or have a combination of soluble and insoluble components [15]. Soluble fibers such as resistant starch and

pectin are quickly fermented by gut bacteria. Insoluble fibers such as lignin and wheat are poorly fermented [15]. The SCFAs produced are acetate, which is the most abundant SCFA found, as well as butyrate and propionate [14,15]. *Bifidobacteria* produce acetate, and *Akkermansia muciniphila* produce acetate and propionate [16]. Butyrate is produced by several bacteria including *Faecalibacterium prausnitzii*, *Roseburia* spp., and *Eubacterium rectale* [16]. Bacteria such as *Faecalibacterium prausnitzii* and *Eubacterium rectale* take part in cross-feeding to convert acetate into butyrate [17]. Most of the SCFAs enter IECs or immune cells by passive diffusion or through transporters such as monocarboxylate transporter 1 (MCT1) or sodium-coupled monocarboxylate transporter 1 (SMCT1) [16]. SCFAs can also trigger anti-inflammatory signaling pathways in IECs or immune cells by interacting with receptors on the cell surface such as GPR43, GPR41 and GPR109A [16]. Acetate, propionate and butyrate serve as ligands for GPR43 and GPR41 but butyrate serves as the only ligand for GPR109A [18]. Butyrate can promote epithelial barrier integrity by stimulating the expression of MUC2 [18-19] and tight junction proteins such as ZO-1 and claudin-1 [20]. SCFAs stimulate the production of regulatory T (Tregs) and IL-10 to promote an anti-inflammatory environment [18,21]. Tregs maintain mucosal tolerance by secreting IL-10 and TGF-β and preventing pro-inflammatory cytokine secretion and responses against commensal bacteria and dietary antigens [1]. Butyrate is metabolized by colonocytes for energy, propionate undergoes liver metabolism and acetate enters the blood where it interacts with several other organs [18].

1.5. Macrophages and Inflammation

Stem cells in the bone marrow generate monocytes, which then travel through the bloodstream to the lamina propria [22]. In the lamina propria, the monocytes mature into resident macrophages with a non-inflammatory phenotype, due to the presence of TGF-β produced by intestinal epithelial cells [23]. The phenotype of macrophages is influenced by the surrounding environments [24]. Macrophages take on an M1 phenotype when they are stimulated by IL-1β, IFN-γ and lipopolysaccharide (LPS). LPS, also known as endotoxin, is a component of the cell wall of gram-negative bacteria. M1 macrophages release reactive oxygen species (ROS) and pro-inflammatory cytokines such as IFN-γ and IL-6. M2 macrophages are stimulated by IL-4 and IL-10 and release anti-inflammatory cytokines such as TGF-β and IL-10 [24].

Unlike monocytes, intestinal resident macrophages lack certain innate immune receptors [23]. Pathogen-associated molecular patterns (PAMPs) are conserved microbial structures that induce an inflammatory response when they interact with innate receptors such as Toll-like receptors (TLRs) and NOD-like receptors (NLRs) [24]. Compared to monocytes, intestinal resident macrophages produce small amounts of pro-inflammatory cytokines, such as IL-6 and TNF-α, in response to microbial antigens such as LPS [22-23]. Despite the low levels of pro-inflammatory cytokines produced, the macrophages engage in phagocytosis and have high bactericidal activity. Under normal circumstances, the macrophages are able to clear infiltrating bacteria without initiating an inflammatory response [23].

Inflammatory processes may be triggered when intestinal immune cells sense cellular damage, through the release of cytokines by IECs, and the presence of microbial antigens across the epithelial barrier [24-25]. An impairment in tight junctions will increase intestinal permeability and increase the exposure of immune cells to microbial antigens [26]. Activation of innate immune receptors trigger signaling cascades, such as the nuclear factor-kappa β (NF-κβ) cascade, and increase the expression of inflammatory genes, chemokines and cytokines [26]. The release of chemokines leads to the recruitment of other immune cells, such as neutrophils and blood monocytes, to help clear out pathogens [25]. Infiltrating monocytes enter the lamina propria in a pro-inflammatory M1 state but later take on a non-inflammatory M2 phenotype after pathogens have been cleared [25].

In individuals with IBD, infiltrating monocytes continue to express a pro-inflammatory profile and produce pro-inflammatory cytokines [27]. There is an increase in the number of macrophages present in the lamina propria and surrounding environment. The high recruitment of immune cells and the production of pro-inflammatory cytokines can lead to tissue damage [27].

1.6. Wound Healing

Wound healing takes place when the intestinal epithelium has been damaged [28-29]. In a process known as epithelial restitution, nearby epithelial cells will move along the basement membrane to the site of injury to re-establish the barrier [28]. Epithelial restitution is stimulated by growth factors such as vascular endothelial cell growth factor (VEGF), trefoil factor peptides, mucins and cytokines such as IL-22 and IL-2 [29]. Growth factors and cytokines in the lamina

propria interact with the basolateral surface of epithelial cells to promote epithelial restitution. TFF3 and mucins interact with the apical surface of epithelial cells. Epithelial cells proliferate and undergo differentiation to replace damaged cells [29].

1.7. Genetic Factors of IBD

Twin studies indicate some influence of genetic factors on the development of IBD, more so with CD than UC [30]. For CD, the concordance rate in monozygotic twins is 20-50% and the rate in dizygotic twins is less than 10%. For UC, the rate is 16% in monozygotic twins and 4% in dizygotic twins [30].

Genome-wide association studies are used to identify genes linked to IBD [31-32]. More than 200 IBD-associated single nucleotide polymorphisms (SNPs) have been identified [31]. The genes include those involved in the sensing of bacteria and maintaining intestinal barrier integrity [31-32]. NOD2 is an innate receptor found in the cytosol of enterocytes, Paneth cells, monocytes, and macrophages [31]. Pro-inflammatory signaling cascades such as NF- κβ are stimulated when the receptor binds to muramyl dipeptide (MDP) found in the cell wall of bacteria [31]. NOD2 mutations lead to an impairment in the defense by the intestinal epithelium against gut microbiota by reducing the release of defensins by Paneth cells [31-32]. Mutations in genes encoding intestinal barrier components, such as E-cadherin, MUC3A, and MUC19, impair intestinal barrier integrity and are associated with IBD [31-32].

1.8. Environmental and Dietary Factors of IBD

Factors such as Westernization/urbanization and diet have been linked to IBD. Emigration to Western countries, especially at a young age, is associated with a higher risk of IBD [33-34]. Benchimol et al. (2015) found that the incidence of IBD was lower in South Asian immigrants compared to non-immigrants [35]. However, the incidence was similar between Ontario-born children of South Asian immigrants and children of non-immigrants.
Early-life exposure to factors linked to urbanization, such as better hygiene, greater use of antibiotics, Cesarean sections, and a Western diet may influence the gut microbiota and the development of the mucosal immune system [35-36].

A Western-style diet involves large amounts of carbohydrates and fats, but low amounts of fiber due to a lack of vegetables, fruits and whole grains [36-37]. The consumption of large

amounts of trans-unsaturated fatty acids [37], sugar and soft drinks with low vegetable intake is linked to a higher risk of UC [38]. Agus et al. (2016) demonstrated that when mice were fed a high sugar and fat diet, there was an increase in pro-inflammatory bacteria such as *Escherichia coli* and a decrease in SCFAs [39]. The mice developed a more severe case of Dextran Sulfate Sodium (DSS)-induced colitis compared to mice fed a conventional diet. They had a worse disease activity index (DAI) score and greater levels of pro-inflammatory cytokines such as IL-6 and IL-1β in the colon [39].

High fat diets can contribute to IBD by increasing intestinal permeability and promoting the infiltration of dendritic cells and Th17 cells into the lamina propria of the colon [40]. A high intake of n-6 polyunsaturated fatty acids (PUFAs) and low intake of n-3 PUFAs are linked to a higher risk of IBD [37,41]. N-6 PUFAs such as linoleic acid are found in red meat, margarine and cooking oils, and n-3 PUFAs like docosahexaenoic acid are found in oily fish such as salmon [41-43]. N-3 PUFAs inhibit activation of TLR2 and TLR4 whereas saturated fats promote activation [42]. Saturated fats from milk may promote the growth of *Bilophila wadsworthia* by increasing the amount of taurine-conjugated bile acids produced by the liver [44]. *B. wadsworthia* metabolizes the bile acids to produce hydrogen sulfide, which can damage the intestinal barrier and disrupt the mucus network at high amounts [44-45]. Hydrogen sulfide is also produced from the microbial fermentation of proteins and may be contributing to the higher risk of IBD with increased animal protein intake [46]. The high salt content and additives present in processed foods, such as emulsifiers, have also been found to increase intestinal permeability in mouse models [47].

A high intake of fruits and vegetables is associated with a lower risk of IBD [48-49]. They contain fiber, phytochemicals and ligands for aryl hydrocarbon receptors on immune cells such as indole metabolites [50-51]. These components are anti-inflammatory and promote gut barrier integrity by inducing tight junction protein expression and IL-22 production [50-51].

1.9. Microbial Factors of IBD

IBD patients, particularly those with CD, have lower gut microbiota diversity [52], a greater *Proteobacteria* population [53], and a smaller number of *Firmicutes* such as *Faecalibacterium prausnitzii* compared to healthy individuals [54]. There is an association between dysbiosis and IBD, though it is uncertain as to whether dysbiosis occurs before or after

disease onset [55]. Under normal circumstances, the colon is a hypoxic environment consisting mostly of obligate anaerobes that are able to produce SCFAs [56-57]. Butyrate maintains the hypoxic state by acting on the peroxisome proliferator-activated receptor-γ (PPAR-γ) receptor of epithelial cells and causing them to increase their consumption of oxygen. Epithelial cells rely on the β-oxidation of fatty acids and oxidative phosphorylation for energy. SCFAs also promote an anti-inflammatory environment in the colon by increasing the number of regulatory T cells [56-57]. When intestinal inflammation is present, the presence of pro-inflammatory cytokines such as IFN-γ causes epithelial cells in the colon to undergo anaerobic glycolysis [57]. This leads to a greater availability of oxygen in the colon. The abundance of M1 macrophages leads to an increase in the release of nitric oxide by macrophages. The nitric oxide gets converted to nitrate in the lumen and is utilized by facultative anaerobes such as *Proteobacteria*. The increased availability of oxygen and nitrate leads to the expansion of facultative anaerobes [57]. Facultative anaerobes also metabolize SCFAs when oxygen is present, preventing SCFA utilization by the host [55,57].

A Western diet and other environmental factors such as antibiotic use can promote dysbiosis [3,57]. They may reduce the levels of SCFAs in the colon, causing a decrease in regulatory T cells and high oxygen availability [57]. This would drive a pro-inflammatory environment and the expansion of facultative anaerobes [57].

IBD involves an immune response against gut microbes, as seen by studies involving germ-free mice and antibiotics. Sellon et al. (1998) looked for the spontaneous development of enterocolitis in IL-10 deficient mice housed in a germ-free or specific pathogen-free (SPF) environment [58]. They found that the SPF mice developed colitis whereas the germ-free mice did not. Seven weeks after birth, SPF mice experienced discontinuous colonic inflammation, weight loss, diarrhea, a reduction in the number of goblet cells, and infiltration of immune cells in the lamina propria. Germ-free mice resembled wild-type mice housed in SPF conditions [58]. IBD patients experience an improvement in their symptoms after receiving broad-spectrum antibiotic therapy [59]. Wang et al. (2012) conducted a meta-analysis of randomized control trials (RCT) involving antibiotic therapy or placebo with CD and UC patients. 56.1% of CD patients and 64.2% of UC patients who received antibiotic therapy experienced remission, compared to 37.9% of CD patients and 47.5% of UC patients in the placebo group [59]. These studies indicate that microbial factors play a role in the persistence of IBD.

1.10. Rationale for Focusing on Sugar

Meta-analyses show an association between the consumption of high sucrose diets and IBD [60-61]. High sugar diets are associated with microbial changes, impaired barrier function, and increased susceptibility to DSS-induced colitis [62-63]. Fedorak et al. (2016) demonstrated that when mice were fed a 50% high sugar (HS) diet for 28 days, their fecal microbiota differed from that of chow-fed mice [62]. HS-fed mice had less butyrate-producing *Lachnospiraceae* and higher amounts of pro-inflammatory *Enterobacteriaceae* and *Streptococcaceae*. HS-fed mice also had a lower expression of genes involved in barrier integrity, including β-defensin, MUC1, and ZO-1. DSS treatment was provided to induce colitis and replaced 5 days later with regular water. HS-fed mice experienced earlier disease onset, worse colitis symptoms and showed delayed recovery compared to chow-fed mice [62]. Short-term consumption of a high sugar diet was also associated with increased susceptibility to DSS-induced colitis [63]. Laffin et al. (2019) showed that when mice were fed a HS diet for 2 days, they had lower levels of cecal acetate compared to chow-fed mice. The HS diet-fed mice experience worse colitis symptoms and had greater levels of pro-inflammatory cytokines in the colon, including IL-1β and TNF-α. Administration of acetate through drinking water caused the colitis symptoms of HS diet-fed mice to resemble those of chow-fed mice [63]. The findings show that high sugar diets may increase susceptibility to DSS-induced colitis through changes in microbiota composition.

1.11. Intestinal Absorption of Sugars

Sucrose is a disaccharide composed of glucose and fructose [64]. It is catabolized by the enzyme sucrase-isomaltase, which is an α-glucosidase located on the brush border [64]. Sucrase-isomaltase is most present and active in the jejunum [65]. Glucose is transported across the apical surface of enterocytes and into the cytosol by the sodium-glucose cotransporter SGLT1 [64,66-67]. The active transport of glucose requires the presence of Na+/K+-ATPase on the basolateral membrane to maintain an electrochemical gradient for sodium ions [66]. SGLT1 couples the active transport of glucose with the movement of sodium ions down its electrochemical gradient [66]. Glucose may be transported paracellularly by solvent drag, however, this theory is under debate [68]. The passive transport of fructose into the cytosol of enterocytes involves the facilitative transporter GLUT5 [67]. Some of the fructose is phosphorylated by ketohexokinase (KHK) in the enterocytes [67,69-70]. KHK transfers a

phosphate from ATP to form fructose-1-phosphate, which can be catabolized by aldolase-B to form glyceraldehyde and dihydroxyacetone phosphate (DHAP) [67,69-70]. The metabolic intermediates formed from fructose-1-phosphate can trigger the synthesis of GLUT5 and KHK when fructose levels are high in the lumen [67,69]. Glucose and most of the fructose are moved across the basolateral surface of enterocytes and into the blood by GLUT2 [66-67].

1.12. Metabolism of Sugar by the Liver

Glucose and fructose enter the portal vein and are transported to the liver [71-74]. Approximately 30-60% of the glucose in the portal vein, and greater than 50% of the fructose are taken up by GLUT2 and metabolized by hepatocytes [73-75]. The rest of the glucose remains in the blood to be used by the cells of the body, such as the brain and skeletal muscle [74]. In the liver, most of the glucose is converted to glycogen, whereas excess glucose undergoes glycolysis to produce acetyl-CoA and fatty acids [73-74]. An increase in the level of glucose or fructose-1-phosphate in the hepatocyte causes the glucokinase regulatory protein (GKRP) to separate from glucokinase. Glucokinase becomes active and phosphorylates glucose to glucose-6-phosphate. Glucose-6-phosphate can be converted to glucose-1-phosphate to synthesize glycogen, or to fructose-6-phosphate to participate in glycolysis. An abundance of glucose-6-phosphate activates glycogen synthase. Fructose-6-phosphate enters glycolysis after being converted to glucose-1-6-phosphate by phosphofructokinase (PFK) [73-74]. Glycolysis is regulated by PFK, which experiences negative feedback when there is an excess of ATP and citrate [72]. Citrate is an intermediate used to synthesize fatty acids [72].

Fructose is mostly converted to fatty acids in the liver [71,75]. Consumption of a high fructose diet can lead to the presence of glucose, lactate and uric acid in the blood [72,75-76]. Fructose is phosphorylated by KHK to fructose-1-phosphate, which is catabolized by aldolase-B to form DHAP and glyceraldehyde [72-73,75]. This pathway is not regulated by a feedback mechanism, resulting in a large decrease in ATP levels and increase in AMP [72,75]. AMP gets converted to uric acid, which enters the systemic circulation and induces ROS production in tissues [75]. DHAP and glyceraldehyde are used to synthesize free fatty acids, lactate, and glucose [75]. Fatty acids combine with glycerol to form triglycerides, which circulate in the blood as very-low-density lipoprotein (VLDL) and are taken up by adipocytes [72,75].

1.13. Measurement of Intestinal Permeability

Intestinal permeability can be assessed by a variety of methods. Histochemical staining of mucins in fixed gut tissue allows for an assessment of the thickness of the mucus layer [77]. Acidic mucins can be stained with Alcian blue and neutral mucins can be stained with Periodic Acid - Schiff's (PAS). Real-time quantitative PCR (qPCR) can be used to examine the mRNA expression of mucins, tight junction proteins, and defensins in gut tissue [77]. Immunohistochemical staining and Western blot can be conducted for mucins and tight junction proteins [77-78]. Immunohistochemical staining is used to examine the distribution of the proteins and a Western blot is used to examine the protein expression [77-78]. Intestinal permeability can be indirectly measured by quantifying the level of LPS in the blood [79]. A high LPS level in the serum suggests an increase in the movement of bacterial components across the epithelial barrier [79].

Functional assessments of intestinal permeability include the oral administration of fluorescein isothiocyanate-conjugated (FITC)-dextran [80]. The concentration of FITC-dextran in the serum is measured 1 hour after administration to assess small intestinal permeability, or after 4 hours for permeability in the colon [81]. Another functional assessment involves the oral administration of a sugar probe with sucrose, sucralose, lactulose and mannitol after a 4 hour fast [82]. The concentration of the sugars is measured using High-Performance Liquid Chromatography (HPLC). The concentration of sucralose provides a measure of both gastric and intestinal permeability [83]. Urinary sucrose excretion is used to assess gastroduodenal permeability since sucrose is catabolized by sucrase-isomaltase in the jejunum [83]. The lactulose/mannitol ratio (LacMan ratio) is a measure of small intestinal permeability since both sugars are catabolized in the cecum [79,83]. A high LacMan ratio indicates increased small intestinal permeability. Compared to mannitol, lactulose does not easily move across the intestinal epithelium due to its large size [79,83].

An ex-vivo measurement of intestinal permeability involves the mounting of a freshly excised gut tissue onto an Ussing chamber [82]. The mucosal and serosal sides of the tissue are bathed in buffer. The paracellular pathway is examined by adding different sized tracers to the mucosal surface and measuring the transepithelial potential difference [82-84]. For example, mannitol is used to observe the flux of small solutes and inulin is used to study large solutes [84].

Cell cultures can be used to study the effect of different factors on intestinal permeability. A monolayer of intestinal epithelial cells such as Caco-2 is grown on a transwell [85]. Substances can be added to the apical or basolateral compartments. Transepithelial electrical resistance (TER) is measured using a voltohmmeter to assess tight junction integrity. Paracellular tracers or FITC-dextran can also be added to the apical side, and the flux can be measured to examine the tight junction pore pathway [85].

1.14. The Effect of Sugars on Intestinal Permeability

Do et al. (2018) have shown that both high glucose and high fructose diets are associated with greater intestinal permeability [86]. Wild type mice were given high glucose, high fructose or normal diet for 12 weeks. Permeability was measured by orally administering the paracellular tracer FITC-dextran and measuring the concentration in the plasma. Mice fed a high glucose diet and a high fructose diet had higher levels of FITC-dextran in the plasma and greater levels of endotoxin in the serum, compared to normal diet-fed mice. The mice also had a decreased expression of ZO-1 and occludin in the colon and greater presence of pro-inflammatory cytokines such as TNF-α and IL-1β in the colon and liver. Both diets lead to microbial changes, such as an increase in *Proteobacteria*, a decrease in *Bacteroidetes*, and a decrease in microbial diversity. Do et al. (2018) suggest that the microbiota changes caused by high glucose and high fructose diets contribute to the greater intestinal permeability and inflammation seen [86].

Both the *Bacteroidetes* and *Proteobacteria* phyla consist of gram-negative bacteria and are sources of LPS [87]. Although *Bacteroidetes* are the main source of LPS in the gut, LPS derived from *Bacteroidetes* does not elicit a pro-inflammatory response [87-88]. In contrast, LPS derived from *Proteobacteria* such as *E.coli* produce large amounts of TNF-α, IL-1β and IL-6. The structural differences in the lipid A domain of LPS from *Bacteroidetes* and *Proteobacteria* contribute to the differences in immunogenicity. The lipid A from *Proteobacteria* but not *Bacteroidetes* is able to stimulate TLR4 and the NF-κβ signaling pathway [87-88].

Turner et al. (1997) have shown that activation of SGLT1 is associated with an increase in intestinal permeability [89]. A monolayer of SGLT1-expressing Caco-2 intestinal epithelial cells was used. Intestinal permeability was assessed with transepithelial resistance (TER), and the movement of mannitol and inulin across the monolayer. Activation of SGLT1 caused a decrease in TER, corresponding to an increase in tight junction permeability. Incubation with the

SGLT1 inhibitor phloridzin caused an increase in TER. Activation of SGLT1 was associated with an increase in the transepithelial flux of mannitol but not the larger sized inulin. The increased permeability of small-sized molecules is suggested to involve phosphorylation of myosin regulatory light chain (MLC). Inhibitors of myosin regulatory light chain kinase (MLCK) prevented the increased permeability seen with SGLT1 activation. Phosphorylation of MLC causes contraction of the perijunctional actomyosin ring (PAMR), which is a component of tight junctions. PAMR contraction leads to distortions in the structure of tight junctions and subsequently greater intestinal permeability [89].

Johnson et al. (2014) demonstrated that fructose metabolism in the intestines by KHK may be associated with increased intestinal permeability [90]. Wild type mice were given 15% fructose solution or tap water with a standard diet for 3 weeks. Mice given the fructose solution had lower expression of occludin and ZO-1, and greater expression of KHK-C in the duodenum. KHK exists in the form of KHK-A and KHK-C, but KHK-C is the main isoform involved in fructose metabolism in the intestines and liver. When mice lacking both KHK-A and KHK-C were given a 30% fructose solution for 3 weeks, the expression of occludin and ZO-1 did not change. Exposure of Caco-2 cells to fructose was found to cause a decrease in the expression of claudin-4 [90]. These findings suggest that metabolites produced from fructose metabolism may induce changes in the expression of tight junction proteins and increase intestinal permeability.

1.15. Dextran Sodium Sulfate (DSS) Colitis Model

There are various mouse models that resemble human UC and are used to study the effect of treatments on colitis [91]. Chemically-induced colitis models involve the oral or intrarectal administration of substances such as dextran sodium sulfate (DSS), acetic acid, or 2,4,6-trinitrobenzenesulfonic acid (TNBS) [91]. Colitis may be induced with bacteria such as *Salmonella typhimurium*, adherent-invasive *Escherichia coli* (AIEC), or *Citrobacter rodentium* [91-92]. There are genetically engineered mice that spontaneously develop colitis due to impaired intestinal barrier integrity or immune response, such as IL-10-deficient mice or MUC2-deficient mice [93].

Dextran sodium sulfate (DSS) is a chemical that is administered *ad libitum* through drinking water to induce colitis in mice [94]. Administration of DSS with a molecular weight of 40-50 kDa leads to colitis. Acute or chronic colitis can be induced by varying the concentration

and the amount of time mice are exposed to DSS. DSS increases gut permeability by damaging the epithelial barrier and causing a decrease in the tight junction protein ZO-1 [94-95]. Immune cells in the lamina propria become exposed to lumenal contents and bacteria, and initiate an inflammatory response [94]. DSS-induced colitis is similar to human UC and is characterized by superficial inflammation, shorter colon length, larger spleen, and mesenteric lymph nodes, diminished mucus layer and basal crypts, a decrease in the number of Goblet cells and submucosal edema [94-98]. There is an infiltration of neutrophils, macrophages, T and B cells into the colon and an increase in pro-inflammatory cytokines such as TNF-α and IL-1β [97-98]. The disease activity index (DAI) score is a measure of colitis severity and is determined by assessing the consistency of stool, presence of blood in stool and body weight loss [94]. When DSS is removed, there is a gradual improvement in mouse weights and colon lengths [97]. The epithelial barrier repairs itself and there is a decrease in the amount of pro-inflammatory cytokines and infiltration of immune cells in the colon [97].

The DSS-induced colitis model was used for this thesis because DSS can be easily administered through drinking water, colitis is induced quickly, disease severity can be easily assessed, the results are reproducible if homogenous groups of mice are used, and both the development and recovery from acute colitis can be studied [91, 94, 99-100]. There are limitations to the DSS-induced colitis model, including the influence of biological factors such as the age and gender of mice [94]. Colitis appears to be delayed in younger mice, and more severe in males compared to females. The severity of the colitis is influenced not just by the dosage, but also the lot number of the DSS or manufacturer [94]. The development of DSS-induced colitis may not resemble the development of human IBD since it is initiated by chemical damage and involves both innate and adaptive immune responses [94, 100]. Human IBD appears to be driven by an adaptive Th1/Th17 or Th2 immune response [100].

1.16. Hypothesis and Aims

The main questions addressed by this thesis are:

1. Do high sugar diets increase susceptibility to DSS-induced colitis due to the high sugar content, or altered fiber content?
2. If the increased susceptibility is caused by the high sugar content, are the effects due to glucose or fructose?

This thesis will test the following hypotheses:

1. Short-term exposure to high sucrose, high glucose and/or high fructose will lead to increased susceptibility and lack of epithelial barrier repair in DSS-induced colitis mice.
2. High sugar diets increase susceptibility to DSS-induced colitis by reducing SCFA levels.

The primary objectives of this thesis are:

1. To examine the effects of short-term exposure to high glucose and high fructose solutions on caloric intake from water and food, gastroduodenal and intestinal permeability, and short-chain fatty acid concentrations (Chapter 2).
2. To examine the effects of a short-term (two-day) exposure to high glucose, high fructose and high sucrose diet in a DSS-induced mouse colitis model (Chapter 3).
3. To investigate potential mechanism(s) responsible for the observed effects of high sugar diets on DSS-induced colitis (Chapter 3).

Chapter 2: The Impact of High Sugar Water Treatments on Caloric Intake, Intestinal Permeability and Short-Chain Fatty Acids

2.1. Introduction

A Western-style diet contains a high amount of added sugar which comes from the consumption of soft drinks, sweets and processed foods [101]. A 2011-2014 National Health and Nutrition Examination Survey showed sugar-sweetened beverages contributed to 6.5% of the calories consumed daily by adults living in the United States [102]. Soft drinks are sweetened with high fructose corn syrup (HFCS), and most commonly the HFCS-55 form, which contains 55% free fructose and 45% free glucose [103]. HFCS is preferred by manufacturers over sucrose, which is a disaccharide consisting of equal amounts of glucose and fructose [104]. The increase in the use of HFCS over sucrose for processed foods appears to be associated with an increase in chronic diseases such as diabetes and obesity [104]. A recent European population-based cohort study found an association with high consumption of sugar-sweetened beverages and mortality caused by digestive disease [105].

The consumption of sugar-sweetened beverages may be contributing to the rise in chronic diseases by increasing intestinal permeability which can increase interactions between the host immune system and gut microbes and/or microbial products [106-109]. However, studies in mice and humans show contradictory results. Bergheim et al. (2008) conducted a study in which C57BL/J6 mice were given either 30% glucose water, 30% fructose water, 30% sucrose water or control water for 8 weeks [106]. Mice that consumed the 30% fructose water had greater portal endotoxin levels, suggesting that the treatment had increased intestinal permeability [106]. Mastrocola et al. (2018) found that C57BL/J6 mice given 60% high fructose diet or 60% fructose syrup had reduced mRNA expression of tight junction proteins, such as occludin and zonula occludens-1 (ZO-1), in the ileum [107]. Mice on the high fructose diet or syrup also had lower levels of fecal acetic acid, propionic acid, and butyric acid, compared to mice on a control diet [107]. In contrast, no differences in measures of intestinal permeability were observed with the consumption of glucose, fructose or HFCS-sweetened beverages for 8 days by human participants [108].

High sugar ingestion may impact intestinal permeability through interaction with transporters on enterocytes, metabolism by enterocytes, or alterations gut metabolites, including

SCFA levels. Enterocytes absorb glucose present in the lumen via the sodium-glucose co-transporter SGLT1 [64-66]. Turner et al. (1997) have shown that activation of SGLT1 on Caco-2 intestinal epithelial cells increased tight junctional permeability [89]. Fructose metabolism by ketohexokinase (KHK) has been found to impact the expression of occludin and ZO-1 in the duodenum [90]. The consumption of a 15% fructose solution by mice for 3 weeks caused a decrease in the expression of occludin and ZO-1, but not in mice lacking isoforms of KHK [90]. Alterations in SCFAs, specifically butyrate levels, can impact gut barrier integrity since butyrate can stimulate the expression of tight junction proteins and MUC-2 by intestinal epithelial cells [18-20].

The short-term consumption of a high sugar diet was previously found to decrease cecal acetate concentrations and increase susceptibility to DSS-induced colitis [63]. However, it was not clear if the increased susceptibility to colitis was due to a direct effect of increasing sugar content or indirectly by the subsequent reduction and change in fiber content of the high sugar diet. The objective of this initial study was to develop an appropriate animal model to answer this question. In this pilot study, glucose and fructose were added to water while the composition and amount of fiber in the food remained the same. This model resembled the consumption of sugar-sweetened beverages by humans [102]. Around 35.0 to 37.5 grams of sugar is found in a 12-ounce soft drink [109]. The caloric intake from food and water were monitored as differences in water intake would make this model inappropriate for use with DSS-induced colitis. The impact of the sugar water treatments on intestinal permeability and short-chain fatty acid (SCFA) concentrations were assessed. It was hypothesized that if the high sugar content of the diet was responsible for the changes in gut physiology observed in the earlier study, we would observe decreased fecal SCFA concentrations and increased small intestinal permeability.

2.2 Methods

2.2.1 Experimental Design

Wild type mice of the 129S1/SvimJ strain were raised and housed under conventional conditions. Twelve female mice were randomized and separated into three treatment groups (n = 4 per group) at 35-39 weeks of age. For a period of nine days, mice were given purified water (CW) (Millipore: Milli-Q), purified water containing 15% (w/v) glucose (HGW) (ThermoFisher Scientific: Cat. No. D16) or purified water containing 15% (w/v) fructose solution (HFW) (ThermoFisher Scientific: Cat. No. L96). A duration of 9 days was chosen to resemble a dextran sulfate sodium (DSS) study involving a 2 day diet pre-treatment period, followed by 5 or more days of DSS treatment. All mice were fed a regular chow diet *ad libitum* (LabDiet 5001). The mice were housed as pairs in each cage. Mouse weights, food intake and water intake were measured on days 0, 1, 2, 3, 4, 7, 8 and 9. Food and water intake were measured as an average of 2 mice within a cage. Glucose and fructose solutions were made on the days that measurements were taken. The freshly-voided stool was collected on days 0 and 9, snap-frozen in liquid nitrogen and frozen at -80°C until SCFA analysis.

2.2.2 In Vivo Measurement of Gut Permeability

On day 9, food and water were removed from the cages and mice were left to fast for 4 hours. Mice were gavaged with 200 µL of a sugar probe containing 500 mg/mL of sucrose, 60 mg/mL of lactulose, and 40 mg/mL of mannitol. Mice were placed individually into metabolic cages for 22 hours. Urine was collected into collection tubes containing 100 µL of paraffin oil and 30 µL of 10% Thymol. Urine samples were frozen at -20°C until further analysis by High-Performance Liquid Chromatography (HPLC). Mice were returned to conventional mouse cages with regular chow diet and the water treatments.

1000 µL of the urine was combined with 200 µL of the internal standard (cellobiose). The urine was filtered through a 0.2 µm filter and centrifuged at 3.5 g at 4°C for 10 minutes. The concentrations of sugars were measured using HPLC by Jenny Hyun (research assistant). The lactulose/mannitol ratio and sucrose excretion (mg/mL) were reported.

2.2.3 Measurement of Lipopolysaccharide (LPS) Level in Plasma

Blood was immediately collected after euthanasia by retro-orbital bleeding into lithium heparin tubes (BD Microtainer). The tubes were centrifuged at 1 500 g for 10 minutes and the plasma was removed and stored in 1.5 mL microcentrifuge tubes. The plasma was frozen at -80°C until lipopolysaccharide (LPS) analysis.

The concentration of LPS in the plasma was determined using an Endotoxin (ET) Enzyme-Linked Immunosorbent Assay (ELISA) Kit (Abbexa Ltd., Cambridge, UK: Cat. No. abx514093). The plasma was diluted 1:20 using the sample diluent provided by the kit, and the manufacturer's protocol was followed.

2.2.4 Measurement of Fecal and Cecal Short-Chain Fatty Acids (SCFAs)

Mice were euthanized on day 11 and cecal contents were collected, snap-frozen in liquid nitrogen and frozen at -80°C until SCFA analysis. 20 mg of the stool samples collected on day 0 and 9, and cecal content collected on day 11 were aliquoted. 320 µL of 0.1 N hydrochloric acid (v/v) and 80 µL of 25% (v/v) phosphoric acid were added to the aliquots. The samples were centrifuged at 15 000 g for 10-30 minutes. 250 µL of the supernatant from each sample was transferred into new tubes and combined with 50 µL of internal standard (23.752 µmol/mL of 4-methyl-valeric acid). The remaining stool pellets were left to dry and were weighed after one week. 200 µL of the combined supernatant and internal standard were transferred to glass chromatography tubes. The concentrations of SCFAs were measured with gas chromatography at the Agriculture, Food and Nutritional Science (AFNS) Chromatography Facility. SCFA concentrations were normalized to dry stool weight.

2.2.5 Statistical Analysis

All data are presented as mean ± standard error of the mean (SEM). Statistical analyses were performed using GraphPad Prism 8. One-way ANOVA with Dunn's multiple comparison test was used when comparing the group means with one independent variable. Two-way ANOVA with Tukey's or Bonferroni's multiple comparison test was used when comparing the group means involving two independent variables, including time. Significance was defined as $p<0.05$.

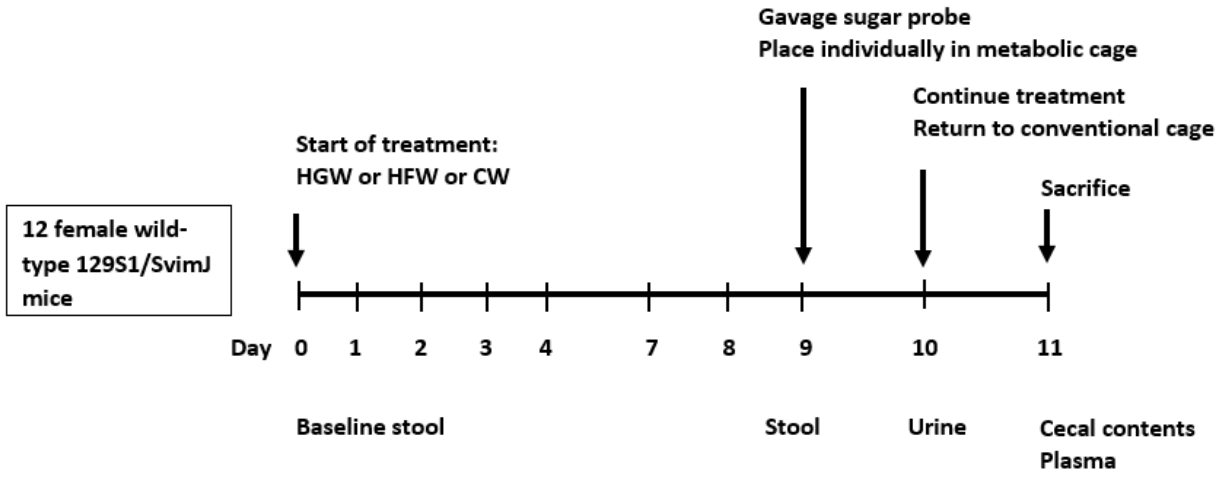

Figure 2.1. Experimental design and sample collection. 12 female wild-type mice (129S1/SvimJ) were separated into 3 treatment groups with n=4 each: 1) 15% (w/v) glucose water (HGW), 2) 15% (w/v) fructose water (HFW), 3) Control water (CW). Mouse weights, food intake and water intake were measured on days 0, 1, 2, 3, 4, 7, 8, and 9. On day 9, mice were given a sugar probe to measure permeability. Mice were housed individually in metabolic cages for 22 hours. On day 10, mice were returned to their conventional cage with their respective treatments. Mice were sacrificed on day 11.

2.3 Results

2.3.1 Effect of sugar water treatments on body weight, food intake, and water intake

Figure 2.2 shows changes in body weight (percentage of the initial weight on day 0), food intake (grams/mouse/day), and water intake (grams/mouse/day) measured throughout the study. Mice were given high glucose water (HGW, n=4) had a significant weight gain after 9 days on the treatment ($p<0.0001$) (Figure 2.2A). Mice were given high fructose water (HFW, n=4) or control water (CW, n=4) had no significant change in weight after 9 days. The HGW-fed mice gained significantly more weight than mice fed CW after 9 days ($p=0.0319$) (HGW: 1.328 ± 0.227; HFW: 0.128 ± 0.434; CW: -0.378 ± 0.317). The average weight change experienced by HFW-fed mice was not significantly different from that of HGW or CW-fed mice.

Food intake and water intake were measured as an average of 2 mice within a cage (n=2 for HGW, HFW, and CW). Mice on the HGW and HFW significantly decreased their food intake over time (Figure 2.2B). In addition, mice given HGW had increased water intake after 9 days compared to CW-fed mice (Figure 2.2C). Mice given HFW decreased their food intake after 9 days compared to CW-fed mice, but they did not change their water intake.

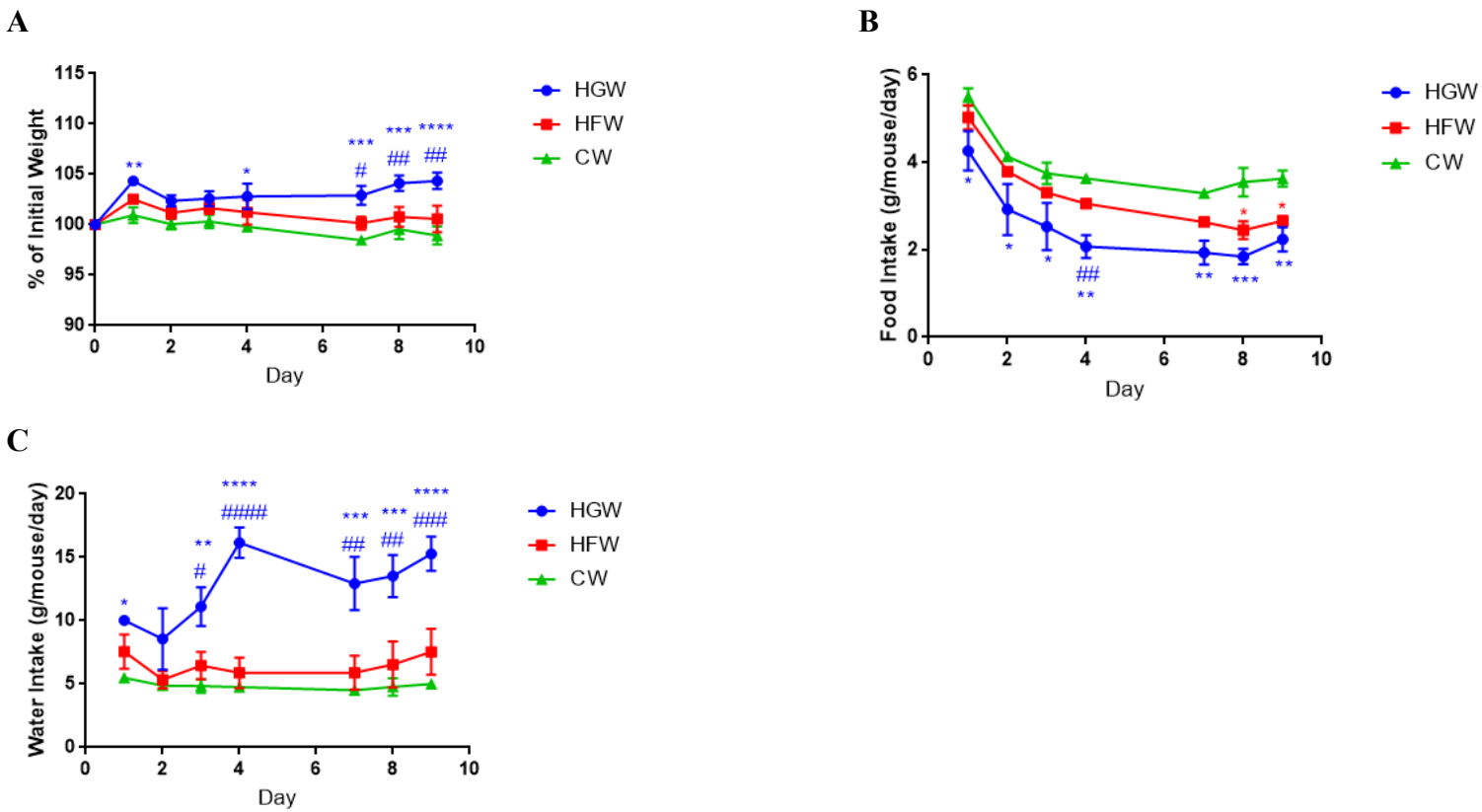

Figure 2.2. Effect of sugar water treatments on (A) change in weight, (B) food intake and (C) water intake. Blue = high glucose water (HGW). Red = high fructose water (HFW). Green = control water (CW). n=4 for HGW, HFW and CW for (A). For (B) and (C), the intakes were calculated as an average of 2 mice within a cage (n=2 for HGW, HFW, and CW). Data are presented as mean ± SEM. Statistical significance was determined between treatment groups for each time point. Two-way ANOVA with repeated measures and Tukey's multiple comparisons test was used. Blue asterisks compare HGW with CW, blue hashtags compare HGW with HFW, and red asterisks compare HFW with CW. * $p<0.05$, ** $p<0.01$, *** $p<0.001$, **** $p<0.0001$. # $p<0.05$, ## $p<0.01$, ### $p<0.001$, #### $p<0.0001$.

2.3.2 Effect of sugar water treatments on total caloric intake

Total caloric intake was measured as an average of 2 mice within a cage (n=2 for HGW, HFW, and CW). Mice on all treatments significantly decreased their total caloric intake (kcal/mouse) over time (Figure 2.3A) (HGW day 0 and day 9: $p=0.0012$, HFW day 0 and day 0: $p<0.0001$, CW day 0 and day 9: $p<0.0001$). Mice were given HGW had the smallest reduction in total caloric intake between D1 and D9 compared to the other treatments (HGW: -3.658 ± 1.246; HFW: -7.960 ± 0.919; CW: -6.275 ± 0.042).

Mice were given HGW had a higher total caloric intake after 9 days of treatment compared to mice given HFW and CW (n=2 for HGW, HFW, CW; HGW: 16.680 ± 0.122; HFW: 13.460 ± 0.788; CW: 12.190 ± 0.630) (Figure 2.3B). HGW-fed mice had higher caloric intake from water (HGW: 9.170 ± 0.810; HFW: 4.520 ± 1.090) and lower caloric intake from food (HGW: 7.520 ± 0.930; HFW: 8.940 ± 0.300; CW: 12.190 ± 0.630).

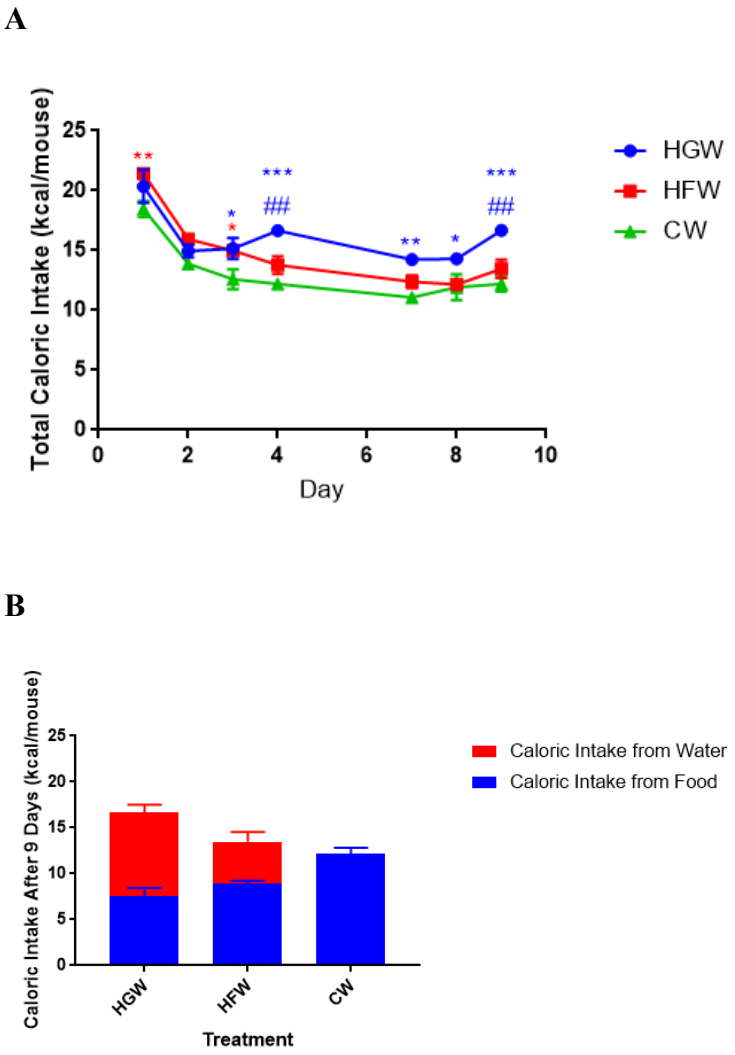

Figure 2.3. Effect of sugar water treatments on (A) total caloric intake throughout the study and (B) caloric intake on day 9. Blue = high glucose water (HGW). Red = high fructose water (HFW). Green = control water (CW). The caloric intake was calculated as an average within a cage (n=2 for HGW, HFW and CW). Data are presented as mean ± SEM. Statistical significance was determined for (A) between treatment groups by two-way ANOVA with repeated measures and Tukey's multiple comparisons test. Blue asterisks compare HGW with CW, blue hashtags compare HGW with HFW, and red asterisks compare HFW with CW.
* $p<0.05$, ** $p<0.01$. # $p<0.05$, ## $p<0.01$.

2.3.4 Effect of sugar water treatments on gastrointestinal permeability

Sucrose excretion (mg/mL) was significantly higher in mice given HGW compared to mice given CW ($p=0.0243$) ($n=4$ for HGW, HFW, and CW; HGW: 0.854 ± 0.156; HFW: 0.387 ± 0.158; CW: 0.130 ± 0.043) (Figure 2.4A). The average lactulose/mannitol ratios were not significantly different between treatment groups (Figure 2.4B).

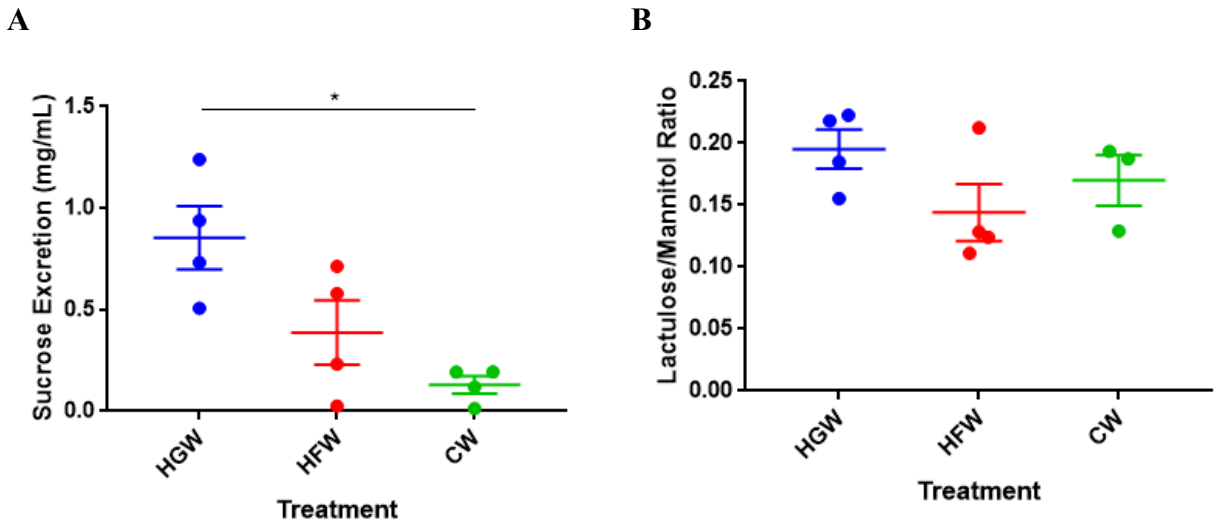

Figure 2.4. Effect of sugar water treatments on (A) gastroduodenal permeability and (B) small intestinal permeability. Blue = high glucose water (HGW). Red = high fructose water (HFW). Green = control water (CW). $n=4$ for HGW, HFW and CW for (A). $n=4$ for HGW, HFW, and $n=3$ for CW. Each data point represents a single measurement. Data are presented as mean ± SEM. Statistical significance was determined between groups by one-way ANOVA (Kruskal-Wallis) and Dunn's multiple comparisons test. * $p<0.05$.

2.3.5 Effect of sugar water treatments on plasma lipopolysaccharide (LPS) concentration

There were no significant differences in the mean LPS concentration between the treatment groups (HGW: 4.973 ± 0.805; HFW: 4.750 ± 0.480; CW: 4.995 ± 0.836) (Figure 2.5).

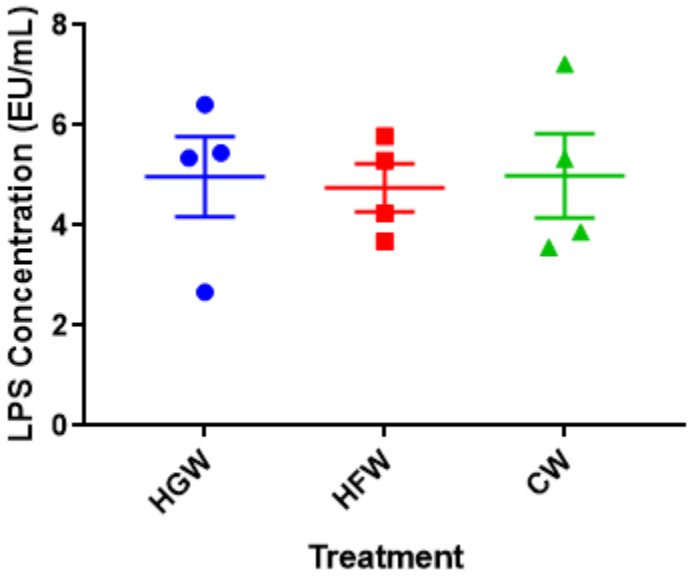

Figure 2.5. Effect of sugar water treatments on plasma lipopolysaccharide (LPS) concentration. Blue = high glucose water (HGW). Red = high fructose water (HFW). Green = control water (CW). n=4 for HGW, HFW, and CW. Each data point represents a single measurement. Data are presented as mean ± SEM. Statistical significance was determined between groups by one-way ANOVA and Dunn's multiple comparisons test.

2.3.6 Effect of sugar water treatments on SCFA concentrations in stool and cecum

The total concentration of SCFAs (μmol/g of sample) was determined with the concentration of acetic acid, propionic acid, butyric acid, and isovaleric acid. The total concentration of SCFAs in the stool was not significantly different between day 0 and day 9 for the same treatment group, or between treatment groups (Figure 2.6A) (HGW day 0: 64.337 ± 11.972; HGW day 9: 64.393 ± 13.535; HFW day 0: 58.489 ± 4.275; HFW day 9: 54.316 ± 3.610; CW day 0: 49.610 ± 2.370; CW day 9: 57.661 ± 5.842). There were no significant differences in the total concentration of SCFAs in the cecum between treatments (Figure 2.6B) (HGW 88.870 ± 5.048; HFW 125.300 ± 31.280; CW 108.500 ± 3.489).

There were no significant differences in the concentration (μmol/g of sample) of acetic acid, propionic acid, butyric acid or isovaleric acid in the stool between day 0 and day 9, or between treatments (Figure 2.7). There were no significant differences in the concentration of the SCFAs between treatments in the cecum (Figure 2.8).

A

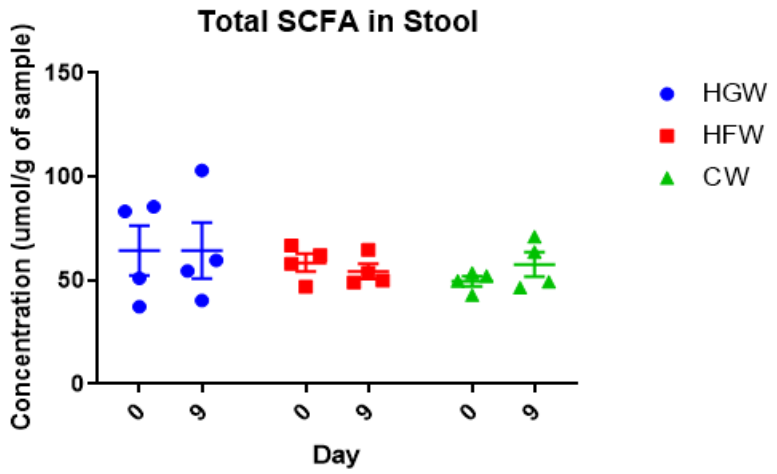

B

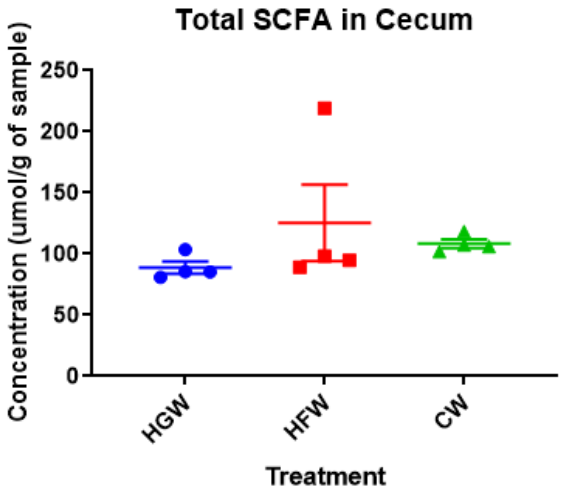

Figure 2.6. Effect of sugar water treatments on total SCFA concentration in (A) stool and (B) cecum. Total SCFA was determined using acetic acid, propionic acid, butyric acid and isovaleric acid concentrations. Blue = high glucose water (HGW). Red = high fructose water (HFW). Green = control water (CW). n=4 for HGW, HFW, and CW. Each data point represents a single measurement. Data are presented as mean ± SEM. Statistical significance was determined for (A) between the day 0 and 9 time points and between groups by two-way ANOVA with repeated measures. Tukey's multiple comparisons test was used to test

significance between groups at each time point. Bonferroni's multiple comparisons test was used to test significance between time points within a treatment group. Statistical significance was determined for (B) between groups by one-way ANOVA (Kruskal-Wallis) and Dunn's multiple comparisons test.

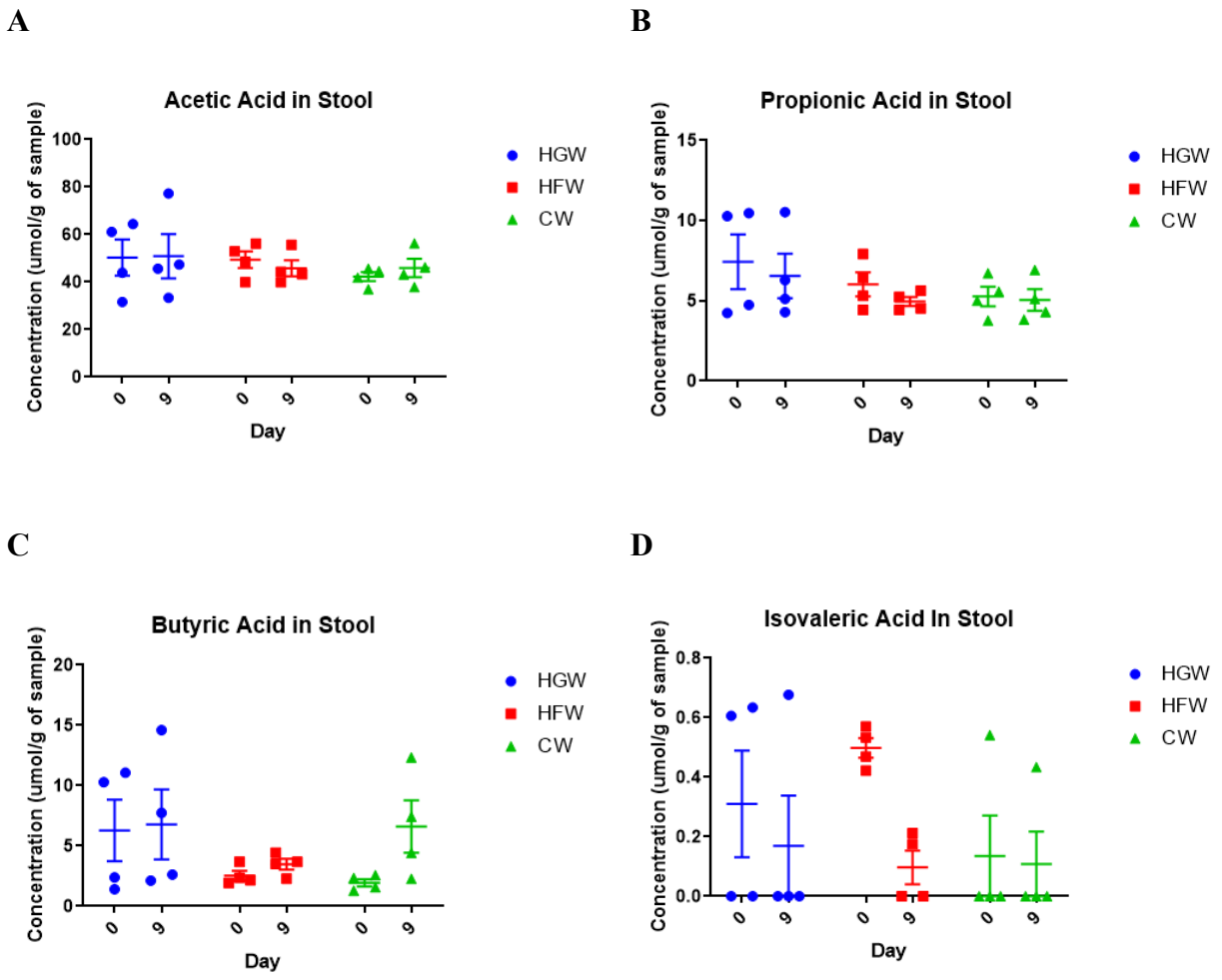

Figure 2.7. Effect of sugar water treatments on the concentration of acetic acid, propionic acid or butyric acid in the stool. Blue = high glucose water (HGW). Red = high fructose water (HFW). Green = control water (CW). n=4 for HGW, HFW, and CW. Each data point represents a single measurement. Data are presented as mean ± SEM. Statistical significance was determined between the day 0 and 9 time points and between groups by two-way ANOVA with repeated measures. Tukey's multiple comparisons test was used to test significance between

groups at each time point. Bonferroni's multiple comparisons test was used to test significance between time points within a treatment group.

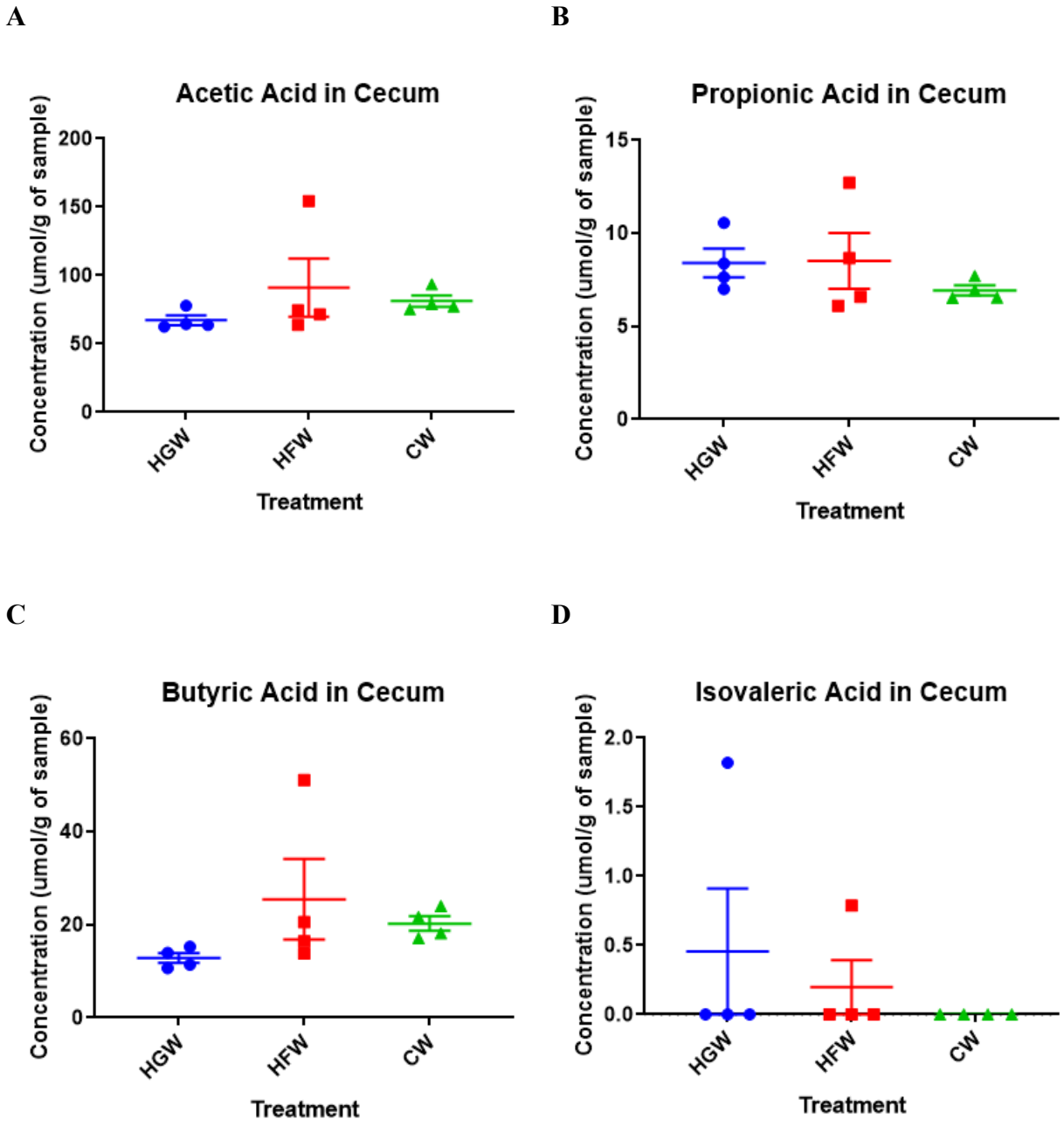

Figure 2.8. Effect of sugar water treatments on the concentration of acetic acid, propionic acid or butyric acid in the cecum. Blue = high glucose water (HGW). Red = high fructose water (HFW). Green = control water (CW). n=4 for HGW, HFW, and CW. Each data point represents a single measurement. Data are presented as mean ± SEM. Statistical significance was

determined for (B) between groups by one-way ANOVA (Kruskal-Wallis) and Dunn's multiple comparisons test.

There were no significant differences in the proportion of acetic acid, propionic acid or isovaleric present in the stool on day 0 and day 9, or between treatments (Figure 2.9A). The proportion of butyric acid present in the stool significantly increased after 9 days in mice given CW ($p=0.0295$) (day 0: $3.886\% \pm 0.508$, day 9: $10.979\% \pm 3.075$). No changes were observed in the butyric acid percentage for HGW or HFW-fed mice after 9 days.

There were no significant differences in the proportion of acetic acid, propionic acid, butyric acid, or isovaleric acid in the cecum between treatments (Figure 2.9B).

A

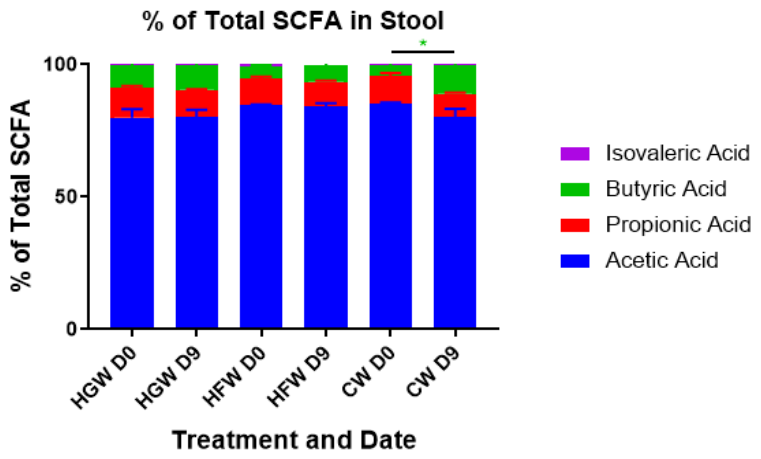

B

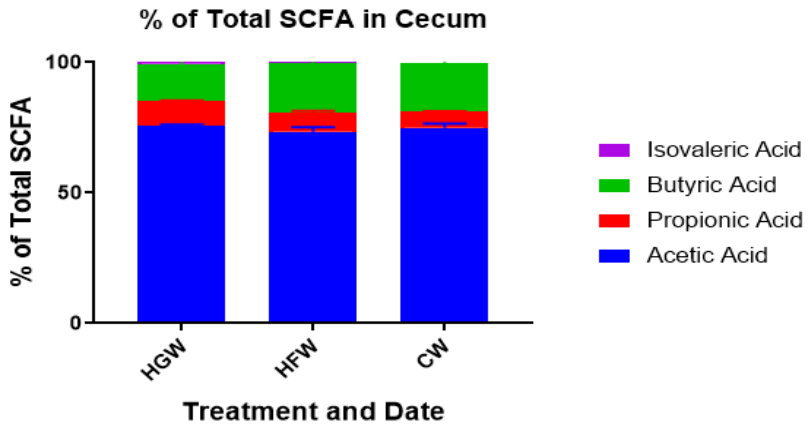

Figure 2.9. Effect of sugar water treatments on the proportion of acetic acid, propionic acid or butyric acid in (A) stool and (B) cecum. Blue = high glucose water (HGW). Red = high fructose water (HFW). Green = control water (CW). n=4 for HGW, HFW, and CW. Data are presented as mean ± SEM. Statistical significance was determined for (A) between day 0 (D0) and day 9 (D9) time points and between groups by two-way ANOVA with repeated measures. Tukey's multiple comparisons test was used to test significance between groups at each time point. Bonferroni's multiple comparisons test was used to test significance between time points within a treatment group. Statistical significance was determined for (B) between groups by one-way ANOVA (Kruskal-Wallis) and Dunn's multiple comparisons test. * $p<0.05$.

2.4. Discussion

The objective of this study was to determine whether a model involving high glucose water and high fructose water would be appropriate to use in a DSS-induced colitis study. Mice given HGW and HFW had reduced food intake compared to CW-fed mice after 9 days. However, HGW-fed mice had increased water intake and total caloric intake and gained weight as a result. There was no increase in the total caloric intake for HFW-fed mice, suggesting that they may have reduced their food intake to compensate for the increased caloric intake from water. HGW-fed mice gained weight despite having a lower caloric intake on the treatment compared to day 0. This may have been due to the conversion of readily available sugars from the water to fatty acids, and an increase in abdominal fat. These findings are supported by other studies [106,110]. Bergheim et al. (2008) found that C57BL/J6 mice given 30% glucose water for 8 weeks had higher total caloric intake compared to controls and mice given 30% fructose water [106]. The 30% glucose water-fed mice also had greater plasma triglyceride levels, abdominal fat and weight gain compared to control mice. Both the 30% glucose water and 30% fructose water-fed mice had lower food intake compared to controls, but the high glucose water-fed mice had greater water intake [106]. A similar finding was seen in rats given 23% glucose, fructose or sucrose water for 2 weeks [110]. The rats on the high sugar treatments had reduced food intake, but the rats on high glucose water had a higher water intake than rats on high fructose water. All rats on high sugar water treatments had increased total caloric intake and weight gain after 2 weeks [110]. Van der Borght et al. (2011) conducted a similar study in which rats were given 23% glucose, 23% fructose, 23% sucrose or control water for 4 weeks [111]. All rats given high sugar water treatments had significantly reduced food intake and greater water intake compared to control water-fed rats. They experienced no weight change despite having a greater caloric intake compared to controls [111]. These results contradict the finding of weight gain seen in the HGW-fed mice. The previously mentioned studies are similar in that they show that rodents fed sugar through drinking water have decreased food intake and increased water intake compared to controls but are contradictory in terms of weight changes. The contradictory results among studies may be due to differences in study design, such as treatment duration and diets consumed with the sugar water treatments [112].

HGW-fed mice, and to a smaller extent, HFW-fed mice may have decreased food intake due to an increase in gut hormones such as cholecystokinin (CCK). Satiety hormones such as CCK and GLP-1 are released by enteroendocrine cells in the small intestine and lead to a reduction in food intake [113]. Both glucose and fructose have been found to increase the secretion of GLP-1 and CCK [114-116]. Kong et al. (1999) found that a glucose load caused a greater increase in plasma GLP-1 than a fructose load in humans [114]. However, both oral glucose and fructose loads caused similar levels of food intake [114]. The finding suggests that GLP-1 may not be the satiety hormone involved in the reduced food intake seen with HGW and HFW-fed mice.

The higher caloric intake found with HGW-fed mice was associated with higher water intake. The greater preference for glucose water compared to fructose water is supported by conditioning studies, in which a flavour was associated with a glucose or fructose solution [117-119]. The glucose and fructose solutions were infused into the stomach with a catheter. In these studies, mice showed a preference for the flavour associated with glucose compared with the flavour associated with fructose [117-119]. Zukerman et al. (2013) suggested that the preference for glucose is due to the activation of intestinal glucose transporters SGLT1, SGLT3 and GLUT2 [118]. They conducted a conditional study in which glucose solutions were infused into the stomach with antagonists for the receptors. The mice did not show a preference for the glucose-associated flavour. Since fructose does not bind to SGLT1 or SGLT3, this provides a possible explanation for the preference for glucose water over fructose water [118].

Significantly higher sucrose excretion in the urine was observed with HGW-fed mice compared to CW-fed mice. The amount of urinary sucrose excretion for HFW-fed mice was an intermediate between the values for HGW and CW-fed mice. Sucrose excretion was used as a measure of gastroduodenal permeability [120]. One possible explanation for the increased sucrose excretion involves an increase in the expression of SGLT1 with HGW. In Caco-2 cells, activation of SGLT1 led to an increase in tight junctional permeability [89]. In mice, the expression of SGLT1 mRNA is the greatest in the jejunum, followed by the duodenum and ileum [121]. When various sections of the intestine of rats were infused with 250 mM of D-glucose, SGLT1 protein expression increased the most in the duodenum and proximal jejunum [122]. The infusion of 250 mM of fructose was also found to increase SGLT1 protein expression, despite

fructose not being transported by the protein [122]. However, this finding is contradicted by another study in which 30% glucose water did not change the expression of SGLT1 mRNA in the duodenum of mice [123].

Another possible explanation for increased sucrose excretion by HGW-fed mice is delayed gastric emptying. The entry of glucose into the duodenum leads to the release of GLP-1 by L cells, which slows gastric emptying [124]. Compared to fructose, glucose causes a greater increase in GLP-1 and slows gastric emptying to a greater extent [114, 125]. By slowing gastric emptying, the glucose solution would cause sucrose to remain in the duodenum longer [126]. The sucrose excretion may overestimate the extent of gastroduodenal permeability. Permeability measurements involving the ratio of two probes, such as lactulose and mannitol, are less affected by factors such as gastric emptying and transit time [127].

No difference was observed in the lactulose/mannitol ratio or plasma LPS levels between groups. The finding suggests that HGW and HFW do not cause a change in overall small intestinal permeability. The result is supported by a study that found no difference in the lactulose/mannitol ratio when high fructose or glucose beverages were consumed by human participants for 8 days [108]. Volynets et al. (2017) also found no increase in the lactulose/mannitol ratio when female mice were given a control diet with 30% fructose water for 12 weeks [128]. However, increased permeability was shown through other methods. They found that the high fructose water-fed mice had increased portal endotoxin levels compared to controls. There was a decrease in the expression of mRNA for occludin and α-defensin 1 in the ileum, and MUC2 and claudin-5 in the colon. The lack of an increase in plasma endotoxin levels may be due to clearance by the liver [129]. There may be a difference in portal LPS levels between treatment groups, though this was not measured in our study. Alternatively, LPS might enter the lamina propria and induce a response in the colonic mucosa without entering the portal blood [129].

No difference was observed in the concentration of SCFAs in the cecum or stool after 9 days on the HGW or HFW. When the SCFAs were compared in the percentage of total SCFAs in the stool, an increase in the proportion of butyric acid was observed after 9 days in control mice. Other studies have shown significant changes in the concentration of SCFAs with mice on a control diet. The studies are not consistent in terms of the specific SCFA that is increased with

time. In a study by Zhang et al. (2016), mice randomized to the control group showed a significant increase in fecal propionic acid concentration after 10 days [130]. In a different study by Hu et al. (2012), mice in the control group experienced an increase in fecal acetic acid concentration after 20 days [131]. The increase in butyric acid proportion may have occurred due to changes in the gut microbiota community caused by randomization and coprophagy.

2.5. Significance of Findings and Future Directions

The increased water intake seen with HGW needs to be considered when conducting DSS-induced colitis experiments. DSS is administered through drinking water, but the presence of glucose in the water may cause the mice to consume more DSS than mice in other treatment groups. The mice in the high glucose water treatment may experience more severe colitis due to higher consumption of DSS, rather than due to the treatment.

Short-term exposure to high sugar diets has been previously found to reduce fecal acetate and butyrate levels and increase susceptibility to DSS-induced colitis [63]. We found no change in fecal or cecal SCFA concentrations despite the decreased food intake and consequently lower fiber intake, by mice consuming HGW or HFW. There might not have been enough of a dietary change to reduce SCFA concentrations. The composition of the diet, including the fiber content, was the same for all treatment groups. Another possibility is that the 15% sugar concentration was not high enough to induce a change. A higher concentration or longer time period may be needed to see a change in permeability or SCFA concentrations.

Sucrose excretion was greater in HGW-fed mice, but the lactulose/mannitol ratio showed no difference. The finding suggests that permeability may be increased in only in the upper regions of the small intestine in HGW-fed mice. Future studies might involve taking permeability measurements of specific areas of the small intestine, such as the jejunum or ileum. There might be an increase in permeability in the jejunum since it has the highest concentration of sugar transporters such as SGLT1 [122]. Portal LPS levels and the expression of proteins involved in barrier function can be measured, such as tight junction proteins, mucins and defensins. Higher sugar concentrations can be tested to see if they impact intestinal permeability.

2.6. Conclusions

The addition of glucose or fructose to drinking water altered water intake. Future work looking at the effects of high sugar treatments on DSS-induced colitis should not involve sugar water treatments. It may be more appropriate to incorporate sugars into the diet rather than drinking water for DSS-induced colitis studies. No differences were observed in the lactulose/mannitol ratio or plasma LPS concentrations between treatments, but a difference was observed with sucrose excretion. Future studies may involve looking at permeability in specific areas of the small intestine, such as the jejunum. There was no change in fecal or cecal SCFA concentrations, suggesting that sufficient fiber was present in all treatment groups to drive SCFA production. This would suggest that the reduced acetate and butyrate concentrations seen previously with high sugar diets may be due to altered fiber content rather than a direct effect of sugar, but further studies would be required to conclusively demonstrate this.

Chapter 3: Impact of High Sugar Diets on DSS-Induced Colitis

3.1. Introduction

Western diets have been associated with a higher risk of IBD [132-133]. A Western diet involves a low consumption of vegetables and high consumption of processed meats, fats, starches and soft drinks [132-133]. Specifically, low vegetable intake and high sugar and soft drink intake were found to be associated with an increased risk of UC [38]. An increased risk with UC or CD was not found with only sugar intake, suggesting that fiber intake plays an important role in IBD risk [134]. However, a recent study in a population-based cohort of over 400 000 participants found a positive association between increased consumption of sweetened soft drinks and digestive disease deaths [105].

In a previous study, mice were given a Western diet high in sugar and fat and low in fiber for 18 weeks had greater susceptibility to DSS-induced colitis [39]. The diversity and richness of the microbiota in the proximal colon was reduced, and the microbial community differed from that in conventional diet-fed mice. The Western diet-fed mice had greater *Proteobacteria* and higher fecal lipocalin-2, suggesting possible intestinal inflammation. Fecal acetic acid, propionic acid, and butyric acid were reduced, which Agus et al. (2016) suggested to be due to the reduced fiber content of the diet. Mice on the Western diet had more severe DSS-induced colitis compared to conventional diet-fed mice, and a higher concentration of pro-inflammatory cytokines such as IL-6 and IL-1β in the colon [39].

The fiber content of diets has been found to impact DSS-induced colitis susceptibility without the presence of sugar. Macia et al. (2015) gave mice a zero-fiber diet, a diet with 2.3% fiber or a diet with 35% fiber for 7 days, followed by 2% DSS for 6 days [135]. Mice on the zero-fiber diet had greater weight loss, worse clinical and histological scores, and shorter colon lengths than mice on the 2.3% or 35% fiber diets. DSS-induced colitis was least severe in mice on the 35% fiber diet. Mice deficient in GPR43 and GPR109A, the receptors for SCFAs, did not experience an improvement in DSS-induced colitis with a higher fiber diet. The results suggest that the SCFA produced from the fermentation of fiber act on GPR43 and GPR109A, and protect against colitis [135].

Microbial and intestinal permeability changes have been found with high glucose and high fructose diets. The consumption of high glucose and high fructose diets by mice for 12 weeks resulted in decreased *Bacteroidetes* and increased *Akkermansia* and *Desuflovibrio vulgaris* [86]. The mice also had increased intestinal permeability as evidenced by enhanced levels of serum LPS, altered tight junction proteins, and increased passage of FITC-dextran into the blood. The mice also increased levels of TNF-α and IL-1β in the colon suggesting a more inflammatory environment [86].

In a study by Laffin et al. (2019), mice were given high sucrose diets for 2 days, followed by 5 days of DSS and an additional 5 days of regular drinking water [63]. After 2 days on the high sucrose diets, mice had greater intestinal permeability as determined with intestinal loops and serum LPS levels. There was also a decrease in total cecal SCFAs and acetate levels. The high sucrose diet-fed mice had more severe DSS-induced colitis compared to chow-fed mice, and a higher concentration of pro-inflammatory cytokines such as TNF-α and IL-1β in the colon. Supplementation of high sugar diets with acetate prevented an increase in intestinal permeability and reduced the severity of DSS-induced colitis. The short-term consumption of high sucrose diets decreased cecal acetate levels, and this was associated with increased disease severity [63].

The objective of this study was to examine the impact of a short-term (two-day) exposure to high glucose, fructose or sucrose diets in comparison with a standard chow diet on DSS-induced colitis. The amount of fiber was kept constant in the four diets (~5.0-5.1%) but the fibers came from different sources. The fiber from high sugar diets came from cellulose, whereas the control diet also contained hemicellulose, pectin and lignins [136]. In addition, the fiber content in the control chow diet came from ground corn, ground oats, alfalfa meal, wheat germ, soybean meal and beet pulp [136]. The effects of these different high sugar diets on disease severity, cytokines and chemokines, SCFAs, and microbiota composition were assessed.

It was hypothesized that the consumption of high glucose, high fructose, and high sucrose diets would increase susceptibility to DSS-induced colitis compared to the chow diet due to the altered fiber content. The study described in Chapter 1 found no difference in permeability or SCFA levels with increased glucose, fructose or sucrose intake. The fiber content did not vary among the treatments. The finding suggests that the reduced total cecal SCFA levels seen by Laffin et al. (2019) may be associated with the altered fiber content of the high sucrose diets

rather than the high sucrose content. The lack of diverse and easily fermentable fibers in the high sugar diets would promote a gut microbiota that was low in SCFA-producing bacteria. The mice would have reduced fecal SCFA, leading to increased susceptibility to DSS-induced colitis and delayed repair after the removal of DSS.

3.2. Methods

3.2.1 Experimental Design

Wild type mice of the 129S1/SvimJ strain were raised and housed under conventional conditions. Twenty-seven female mice were randomized and separated into four treatment groups at 8-11 weeks of age. The mice were given regular chow diet (C, n = 7) (LabDiet, St. Louis, MO: Laboratory Rodent Diet 5001), high glucose diet (HG, n = 7) (50% Glucose; Harlan Teklad AIN76A), high fructose diet (HF, n = 7) (50% Fructose; Harlan Teklad AIN76A), or high sucrose diet (HS, n = 6) (50% Sucrose; Harlan Teklad AIN76A). Mice were housed as 2-3 per cage and were all fed the treatment diet and regular drinking water *ad libitum* for a period of 2 days (day -2 to day 0). On day 0, the regular drinking water was replaced with 1.5% (w/v) dextran sodium sulfate (DSS; MW 36 000 - 50 000; MP Biomedicals). New DSS water was made on days 2 and 4. DSS water was replaced with regular drinking water on day 5 and mice were euthanized on day 9.

Table 3.1. Composition of experimental diets.

	Chow (C)	**High glucose diet (HG)**	**High fructose diet (HF)**	**High sucrose diet (HS)**
Carbohydrate (% of kcal)	57.996	67.776	67.776	67.776
% of Carbohydrate or Nitrogen-Free Extract (NFE)*				
Starch	31.90	22.60	22.60	22.60
Glucose	0.22	74.57	0.00	0.00
Fructose	0.30	0.00	74.57	0.00
Sucrose	3.70	2.83	2.83	77.40
Fiber (% of total g)	5.1	5.0	5.0	5.0
Protein (% of kcal)	28.507	20.726	20.726	20.726
Fat (% of kcal)	13.496	11.498	11.498	11.498
Total kcal/g	3.36	3.92	3.92	3.92

***** The percentage of Nitrogen-Free Extract (NFE) composed of starch, glucose, fructose, and sucrose was obtained for the chow diet (C) (LabDiet 5001).

Mouse weights, food intake and water consumption were measured on day -2 and daily between days 0 and 9. The freshly-voided stool was collected on days -2, 0, and 5, snap-frozen in liquid nitrogen and frozen at -80°C until SCFA analysis. Between days 0 and 9, the percentage weight loss from the initial weight at day 0, stool consistency and the presence of blood in the stool (hemoccult) were determined daily. Hemoccult was assessed using the Beckman Coulter test. The percentage weight loss, stool consistency, and hemoccult were each given a score on the scale of 0-4 (Table 1) and combined to provide a Disease Activity Index (DAI) score with a range of 0-12.

Table 3.2. Measurement of the Disease Activity Index (DAI).

Scale 0-4	Weight Loss From Initial Weight at D0 (%)	Stool Consistency	Blood in Stool
0	0-0.99	Normal	Negative
1	1-5.99	Soft, formed pellet	Specks of blue
2	6-10.99	Soft, unformed pellet	Solid light blue
3	11-15.99	Diarrhea, mostly solids	Solid dark blue
4	>15.99	Diarrhea, mostly liquid	Solid very dark blue

The liver was excised from mice, collected into 1.5 mL microcentrifuge tubes, snap-frozen in liquid nitrogen and frozen at -80°C until analysis. The colon and a 10 cm long section of the terminal ileum was excised from the point of attachment to the cecum. The terminal ileum and colon were flushed with 1X phosphate-buffered saline (PBS) (GE Healthcare Life Sciences: Cat. No. SH30256.01) containing 100 µL of gentamicin (50 mg/mL; ThermoFisher Scientific: Cat. No. 15750-060) per 100 mL of PBS. The weight and length of the terminal ileum and colon were measured and the weight-to-length ratio was recorded. The terminal ileum and colon were cut longitudinally and 1.5 cm long sections were cut 1 cm from the cecum. The sections were collected into 1.5 mL microcentrifuge tubes, snap-frozen in liquid nitrogen and frozen at -80°C until tissue cytokine analysis. 2 cm long sections of the small intestine and colon were cut 2.5 cm from the cecum, cut further by half and placed into a histology cassette. The cassettes were stored in 10% buffered formalin phosphate until histological analysis. The cecum was excised and the contents were collected into 1.5 mL microcentrifuge tubes. The tubes were frozen in liquid nitrogen and frozen at -80°C until microbiome analysis. The cecum was flushed with 1X PBS with gentamicin and weighed.

3.2.2 Histological Analysis

Ileal and colonic tissue were processed using standard paraffin-embedding methods and stained with hematoxylin and eosin (H&E). A score was provided in a blinded way by a pathologist (Dr. Aducio Thiesen) to the following: enterocyte injury (0 to 3), epithelial hyperplasia (0 to 3), the presence of lymphocytes in the lamina propria, (0 to 2), and presence of neutrophils in the lamina propria (0 to 2). A total histologic score was determined as a sum of the previously mentioned variables and with a range of 0 to 10.

3.2.3 Measurement of Lipopolysaccharide (LPS) Level in Plasma

Blood was immediately collected after euthanasia by retro-orbital bleeding into lithium heparin tubes (BD Microtainer). The tubes were centrifuged at 1 500 g for 10 minutes. Plasma was collected into 1.5 mL microcentrifuge tubes and frozen at -80°C.

The LPS concentration was determined using an Endotoxin (ET) Enzyme-Linked Immunosorbent Assay (ELISA) Kit (Abbexa Ltd., Cambridge, UK: Cat. No. abx514093). The plasma was diluted 1:20 using the sample diluent provided by the kit, and the manufacturer's protocol was followed.

3.2.4 Measurement of Macrophage Receptor with Collagenous Structure (MARCO) Expression in Liver

Exposure to Gram-negative and Gram-positive bacteria induce the expression of macrophage receptor with collagenous structure (MARCO) on liver Kupffer cells [137]. An increase in MARCO expression may suggest an increase in endotoxins in the portal blood and increased permeability [138].

Total RNA extraction from liver, complementary DNA (cDNA) synthesis and real-time quantitative PCR (real time-qPCR) were conducted by Wei Jen Ma (research assistant). The liver samples were cut in half with clean scissors and ground with a tissue grinding pestle. 700 µL of TRIzol reagent (ThermoFisher Scientific: Cat. No. 15596026) was added to each liver sample and then left to sit for 5 minutes. 200 µL of chloroform was added, samples were vortexed then left to incubate on ice for 2-3 minutes. The samples were centrifuged at 14 000 rpm at 4°C for 15

minutes. Approximately 550 µL of the clear phase was pipetted into RNase-, DNase- and pyrogen-free microtubes (ThermoFisher Scientific: Cat. No. MCT175C) kept on ice.

The RNeasy Mini Kit (Qiagen: Cat. No. 74104) was used to purify the RNA. 1 volume of 50% ethanol was added to the samples and mixed with pipetting. 700 µL of each sample was transferred to a spin column and put into a 2 mL collection tube. The tubes were centrifuged at 8 000 g for 15 seconds and the flowthrough was discarded. 700 µL of Buffer RW1 was added, tubes were centrifuged at 8 000 g for 15 seconds, and the flowthrough was discarded. 500 µL of Buffer RPE was added, tubes were centrifuged at 8 000 g for 15 seconds, and the flowthrough was discarded. 500 µL of Buffer RPE was added again, tubes were centrifuged at 10 000 g for 2 min, and the flowthrough was discarded. Each spin column was placed into a new 2 mL collection tube and centrifuged for 1 minute at full speed. The spin columns were placed into new 1.5 mL collection tubes and 18 µL of Molecular Biology Grade water (GE Healthcare Life Sciences: Cat. No. SH30538.02) was added. The tubes were centrifuged at 10 000 g for 1 minute and the RNA was quantified using the NanoDrop ND-1000 Spectrophotometer (ThermoFisher Scientific).

The RNA was diluted to approximately 50 ng/µL and cDNA was synthesized using the High Capacity cDNA Reverse Transcription Kit (Applied Biosystems: Cat. No. 4368814). A 2X RT Master-mix was prepared with 2 µL of 10X RT Buffer, 0.8 µL of 25X dNTP mix, 2 µL of 10X Random Primers, 1 µL of MultiScribe Reverse Transcriptase and 4.2 µL Molecular Biology Grade water per reaction. 10 µL of the 2X RT Master-mix and 10 µL of the diluted RNA were pipetted into each PCR tube. The tubes were tapped to mix the contents and briefly centrifuged. They were placed into a Veriti 96 Well Thermal Cycler (Applied Biosystems) set at 25°C for 10 minutes (Step 1), 37°C for 120 min (Step 2), 85°C at 5 minutes (Step 3), and held at 4°C (Step 4).

Primers were synthesized by Integrated DNA Technologies (IDT) for macrophage receptor with collagenous structure (MARCO) mRNA and 18S rRNA. The sequences were 5'-GAAGACTTCTTGGGCAGCAC-3' for the MARCO forward primer, 5'-CTTCTTGGGCACTGGATCAT-3' for the MARCO reverse primer, 5'-GGGGAGTATGGTTGCAAAGC-3' for the 18S rRNA forward primer, and 5'-CGCTCCACCAACTAAGAACG-3' for the 18S rRNA reverse primer. 10 µL of the primers

were reconstituted with 90 µL of Molecular Biology Grade water to obtain a 10X working stock. 500 µL of the Fast SYBR Green Master Mix (ThermoFisher Scientific: Cat. No. 4385612) was combined with 50 µL of the forward primer and 50 µL of the reverse primer. 7 µL of the Molecular Biology Grade water, 12 µL of the mixture of SYBR Green Master Mix and primers, and 2 µL of the cDNA were added to a MicroAmp Fast Optical 96-well reaction plate (Applied Biosystems: Cat. No. 4346906). The reaction plate was sealed with optical adhesive film and put into the 7900HT Fast real-time PCR System (Applied Biosystems). The annealing temperature was set to 57°C. Gene expression results were obtained using the Sequence Detection Systems (SDS) 2.4 software (Applied Biosystems). MARCO gene expression was normalized to 18S rRNA and the log2 fold change was visualized with Prism 8.

3.2.5 Measurement of Cytokines in Ileal and Colonic Tissue

Ileal and colonic tissue was homogenized using 1X PBS with 0.05% Tween 20 (PBST) (ThermoFisher Scientific: Cat. No. BP337), 1 µL/mL of Protease Inhibitor Cocktail (Sigma-Aldrich: Cat. No. P8340), and 10% Bovine Serum Albumin (BSA) (Sigma-Aldrich: Cat. No. A3059). An amount of PBST with protease inhibitors and BSA equivalent to 7.5 times the tissue weight was added to the ileal and colonic tissues. The tissues were cut and homogenized by sonication for 5 seconds. The samples were centrifuged at 10 000 g for 10 minutes at 4°C. The supernatant was collected and the concentration of cytokines was measured using the Mouse Proinflammatory 7-Plex Tissue Culture Kit (Meso Scale Diagnostics, Rockville, MD: Cat. No. K15012B-2). The following cytokines were measured: IL-1β, IL-12 p70, IFN-γ, IL-6, Keratinocyte Chemoattractant (KC), IL-10, TNF-α. Concentrations were normalized to tissue weight.

3.2.6 Microbiome Analysis of Stool and Cecum Contents

Microbiome analysis was conducted on stool samples collected on days -2, 0 and 5, and on cecum contents collected on day 9. Stool and cecum contents were added to screw-top 1.5 mL tubes containing 200 µL of AquaStool (MultiTarget Pharmaceuticals LLC: Cat. No. 7030) and 100 mg of beads. The samples were homogenized with a bead beater set at 6 meters/second for 40 seconds. 100 µL of AquaRemove (MultiTarget Pharmaceuticals LLC: Cat. No. 1208) was

added to the samples. Samples were centrifuged at 14 000 g for 5 minutes at room temperature. The supernatant was transferred to new tubes and isopropanol was added with a volume equivalent to 0.8 times the volume of the supernatant. After 1 minute, the tubes were inverted 10 times and left on ice for 10 minutes. The tubes were centrifuged at 14 000 g for 5 minutes. The liquid was decanted and the pellet was cleaned twice with 70% ethanol precipitation. Residual ethanol was removed and DNA pellets were left to dry for 10 minutes. 100 µL of Buffer EB (Qiagen: Cat. No. 19086) was added and DNA was left to solubilize overnight at 4°C. The following day, the pellets were centrifuged at 14 000 g for 10 minutes. The supernatant was transferred to a new tube. 10 µL of 5M NaCl was added and the tubes were inverted 3-5 times. 100 µL of ice-cold 100% ethanol was added and tubes were inverted 10 times. Samples were incubated for 30 minutes at -20°C. Samples were then centrifuged at 10 000 g at room temperature for 15 minutes. The liquid was decanted and 70% ethanol was added to the tubes. The tubes were vortexed for 20 seconds, then centrifuged at 10 000 g for 5 minutes. The liquid was decanted again and the tubes were centrifuged at 10 000 g for 20 seconds. Residual ethanol was removed and DNA pellets were left to dry for 10 minutes. 50 µL of Buffer EB (Qiagen: Cat. No. 19086) was added to the pellets and DNA was left to solubilize overnight at 4°C. The DNA was diluted to a concentration of 25-60 ng/µL and sequenced using the Illumina MiSeq PE250 platform at the McGill University and Genome Quebec Innovation Centre.

The 341F-805R primer pair was used to target the V3 and V4 regions of the 16S rRNA genes. Microbiome analysis was conducted using the QIIME2 2019.4 pipeline (https://qiime2.org/) [139]. The DADA2 plugin was used to denoise, quality filter and cluster the sequences into amplicon sequence variants (ASVs) [140]. ASVs in stool and cecum samples were analyzed separately. The feature table for cecum samples was rarefied to a sampling depth of 5500 and features with a total frequency of less than 42 were removed. For stool samples, the feature table was rarefied to a sampling depth of 4500 and features with a total frequency of less than 68 were removed. The following alpha diversity metrics were calculated: Pielou's Evenness, Faith's Phylogenetic Diversity (PD), Observed OTUs, and Shannon's diversity index. Beta diversity was measured using Jaccard distance, Bray-Curtis distance, unweighted UniFrac distance, and weighted UniFrac distance. Taxonomy was assigned to the ASVs using the Greengenes 13_8 99% OTUs full-length sequences classifier.

3.2.7 Measurement of Fecal Short-Chain Fatty Acids (SCFAs)

The concentration of SCFAs was measured in stool samples collected on day -2, 0 and 5. 20 mg of the stool samples were aliquoted and 320 µL of 0.1 N hydrochloric acid (v/v) and 80 µL of 25% (v/v) phosphoric acid were added. The samples were centrifuged at 15 000 g for 10-30 minutes. For each sample, 250 µL of the supernatant was collected into a new tube and 50 µL of internal standard (23.752 µmol/mL of 4-methyl-valeric acid) was added. 200 µL was transferred to a glass chromatography tube. The concentrations of SCFAs were measured with gas chromatography at the Agriculture, Food and Nutritional Science (AFNS) Chromatography Facility. The stool pellets were left to dry for one week and weighed. SCFA concentrations were normalized to dry stool weight.

3.2.8 Statistical Analysis

All data are presented as mean ± standard error of the mean (SEM). Statistical analyses were performed using GraphPad Prism 8. Beta diversity principle coordinates analysis (PCoA) plots were created using R Studio. Statistical analyses were performed on beta diversity metrics with PERMANOVA using the q2-diversity plugin in QIIME2. One-way ANOVA with Dunn's multiple comparison test was used when comparing the group means with one independent variable. Two-way ANOVA with Tukey's or Bonferroni's multiple comparison test was used when comparing the group means involving two independent variables, including time, unless mentioned otherwise. A mixed model with Tukey's multiple comparison test was used for food and water intake. Statistical significance was determined for bacteria in cecum contents using two-way ANOVA with the original FDR method of Benjamini and Hochberg. Significance was defined as $p<0.05$.

Linear discriminant analysis effect size (LEfSe) (https://huttenhower.sph.harvard.edu/galaxy/) was used to identify differentially abundant bacteria in cecum and stool samples [141]. The following criteria were selected: alpha value for the Kruskal Wallis test between treatment groups needed to be less than 0.05, and the logarithmic linear discriminant analysis (LDA) score needed to be greater than 2.0. The less strict (one-against-all) multi-class analysis strategy was chosen.

Metaboanalyst 4.0 (https://www.metaboanalyst.ca/) was used to generate a heatmap, and Spearman rank correlations and p-values of DAI, SCFA, microbial relative abundance, and cytokines and chemokines information [142]. The Pearson distance measure, Ward clustering algorithm, and top 25 significant features were used to create the heatmap.

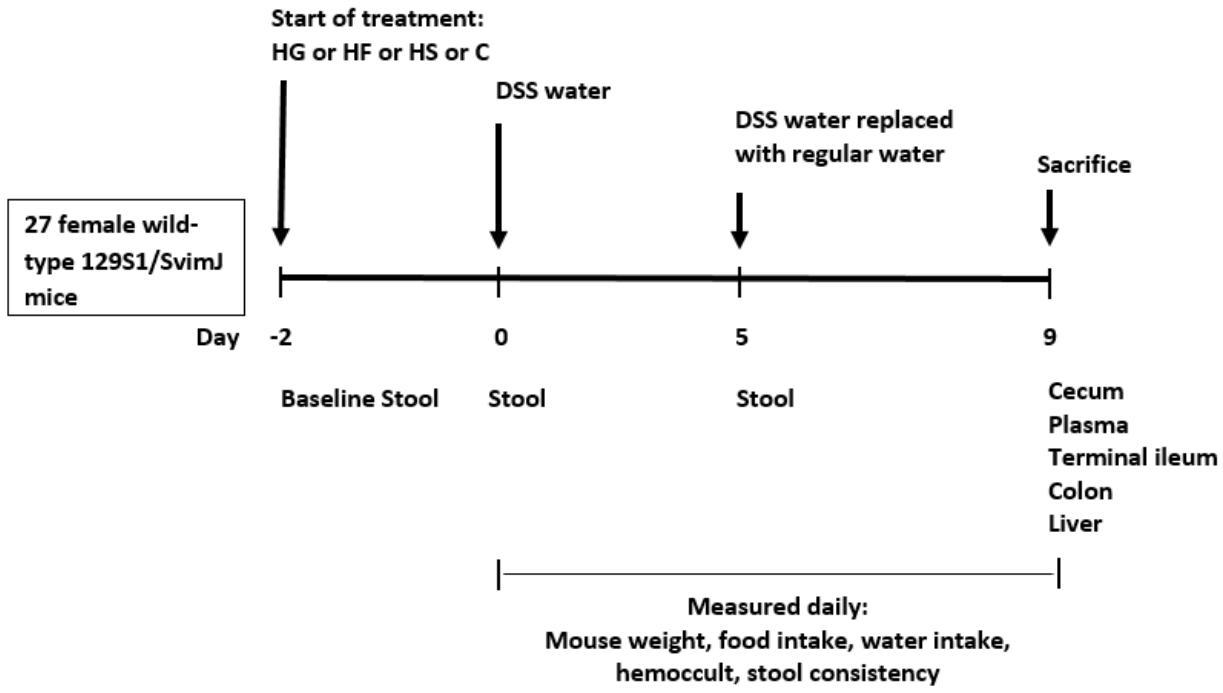

Figure 3.1. Experimental design and sample collection. 27 female wild-type mice of the 129S1/SvimJ strain were separated into 4 treatment groups: 1) 50% high glucose diet (HG), 2) 50% high fructose diet (HF), 3) 50% high sucrose diet (HS), 4) conventional diet (C). The HG, HF and C groups had n=7 and the HS group had n=6 mice. After 2 days on the diets, 1.5% (w/v) DSS was administered with the drinking water (day 0). The DSS water was replaced with regular drinking water after 5 days (day 5), and the mice were euthanized after 9 days (day 9). Mice continued to consume their respective diets throughout the study. Mouse weights, food intake, water intake, hemoccult and stool consistency were measured daily between days 0 and 9.

3.3. Results

3.3.1. Effect of high sugar diets on food and water intake

Food intake (Table 3.3) and water intake (Table 3.4) were measured as grams/mouse/day for four time periods: days -2 to 0 (pre-treatment), days 0 to 5 (DSS treatment), days 5 to 7 (recovery from DSS), and days 7 to 9 (recovery from DSS). There were no significant differences between the groups during the time periods between days -2 and 7. From day 7 to day 9, HG-fed mice had a significantly lower food intake ($p=0.035$) and water intake ($p=0.041$) compared to control mice.

HG-fed mice had significantly higher food intake during the diet pre-treatment period compared to the DSS recovery periods (Days 5 to 7: $p=0.0134$, Days 7 to 9: $p=0.0070$). Food intake was also higher during the DSS treatment period than the DSS recovery periods (Days 5 to 7: $p=0.0449$, Days 7 to 9: $p=0.0129$). For HF-fed mice, the food intake was greater during the diet pre-treatment ($p=0.0306$) and DSS treatment periods ($p=0.0231$) compared to the DSS recovery period between days 7 and 9. There were no significant differences between food intake within the HS and chow groups.

Compared to the diet pre-treatment period, water intake was significantly greater for HG-fed mice during the DSS treatment period ($p=0.0014$) and lower during the DSS recovery period between days 7 and 9 ($p=0.0244$). Water intake was also greater during DSS treatment compared to either of the DSS recovery periods (Days 5 to 7: $p=0.0111$, Days 7 to 9: $p=0.0066$). Within the DSS recovery periods, water intake was significantly greater between days 5 and 7 than between days 7 and 9 ($p=0.0069$). For HF-fed mice, water intake was significantly greater during the DSS treatment period than the DSS recovery period between days 5 and 7 ($p=0.0453$). There were no significant differences in water intake for HS-fed mice. For control mice, water intake was significantly greater during the DSS treatment period than the diet pre-treatment ($p=0.0296$) or the DSS recovery period between days 5 and 7 ($p=0.0304$).

Table 3.3. Effect of high sugar diets on food intake (grams/mouse/day).

	High glucose diet (HG)	**High fructose diet (HF)**	**High sucrose diet (HS)**	**Chow diet (C)**
D-2 to D0	2.882 ± 0.283	2.529 ± 0.190	2.851 ± 0.514	3.711 ± 0.298
D0 to D5	3.132 ± 0.099	2.9021 ± 0.133	2.810 ± 0.190	3.477 ± 0.087
D5 to D7	1.686 ± 0.346	2.029 ± 0.691	2.375 ± 0.302	3.032 ± 0.410
D7 to D9	**0.583 ± 0.393***	0.972 ± 0.400	1.189 ± 0.280	2.573 ± 0.290

Data are presented as mean ± SEM. n=4 for HG, HF, HS, and C for time periods D-2 to D0, D0 to D5, and D5 to D7. For time period D7 to D9, n=4 for HG, HF, and HS, and n=3 for C.
*p<0.05 compared with chow diet.

Table 3.4. Effect of high sugar diets on water intake (grams/mouse/day).

	High glucose diet (HG)	**High fructose diet (HF)**	**High sucrose diet (HS)**	**Chow diet (C)**
D-2 to D0	2.786 ± 0.291	4.386 ± 0.502	2.961 ± 0.427	3.776 ± 0.123
D0 to D5	4.090 ± 0.332	4.011 ± 0.313	3.709 ± 0.464	5.184 ± 0.134
D5 to D7	2.579 ± 0.204	3.085 ± 0.426	2.560 ± 0.315	3.403 ± 0.427
D7 to D9	**1.603 ± 0.138***	2.493 ± 0.531	1.838 ± 0.271	3.334 ± 0.293

Data are presented as mean ± SEM. n=4 for HG, HF, HS, and C for time periods D-2 to D0, D0 to D5, and D5 to D7. For time period D7 to D9, n=4 for HG, HF, and HS, and n=3 for C.
*p<0.05 compared with chow diet.

3.3.2. Effect of high sugar diets on susceptibility to DSS-induced colitis

Figure 3.2 shows the average weight change (percentage of initial weight on day 0), stool consistency, hemoccult, and the DAI scores measured throughout the DSS treatment and recovery periods. After 5 days of DSS and 4 days of recovery, HG-fed mice lost more weight than control mice ($p=0.0008$). Mice fed HG, HF, and HS diets had significantly higher stool consistency (HG: $p<0.0001$, HF: $p=0.0005$, HS: $p=0.0003$), hemoccult (HG: $p<0.0001$, HF: $p=0.0082$, HS: $p=0.0008$) and DAI scores (HG: $p<0.0001$, HF: $p=0.0002$, HS: $p<0.0001$) than control mice. HG-fed mice also had a higher DAI score than HF-fed mice after 4 days of recovery ($p=0.0110$).

The area under the curve (AUC) was calculated for the DAI scores for the DSS treatment period (day 0 to day 5), and the recovery period (day 5 to day 9) (Figure 3.3). The AUC values were not significantly different between treatment groups during the DSS treatment period ($n=7$ for HG, HF, C and $n=6$ for HS; HG: 11.790 ± 2.903, HF: 10.570 ± 2.650, HS: 10.670 ± 2.121, C: 6.071 ± 0.988). During the recovery period, HG, HF, and HS-fed mice had significantly higher AUC values than control mice (HG: 26.070 ± 4.255, $p<0.0001$; HF: 20.210 ± 3.894, $p=0.017$; HS: 24.250 ± 2.622, $p=0.001$; C: 8.071 ± 2.030).

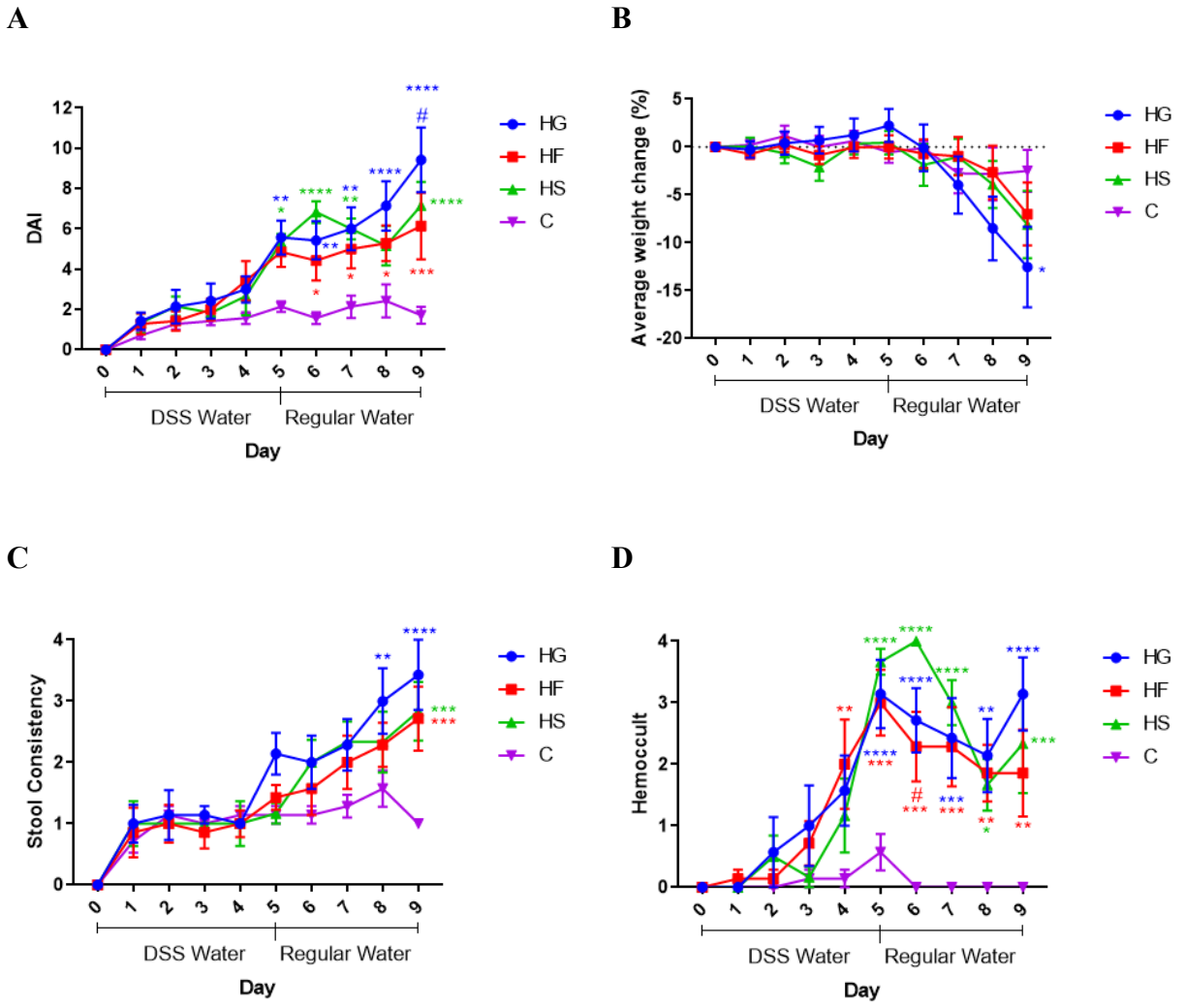

Figure 3.2. Effect of high sugar diets on DSS-induced colitis. (A) Disease Activity Index was calculated using (B) average weight change, (C) stool consistency, and (D) hemoccult scores. Blue = high glucose diet (HG). Red = high fructose diet (HF). Green = high sucrose diet (HS). Purple = control diet (C). n=7 for HG, HF, C, and n=6 for HS. Data are presented as mean ± SEM. Statistical significance was determined between treatment groups for each time point. Two-way ANOVA with repeated measures and Tukey's multiple comparisons test was used. Blue asterisks compare HG with C, red asterisks compare HF and C, and green asterisks compare HS and C. Blue hashtags compare HG with HF. * $p<0.05$, ** $p<0.01$, *** $p<0.001$, **** $p<0.0001$. # $p<0.05$.

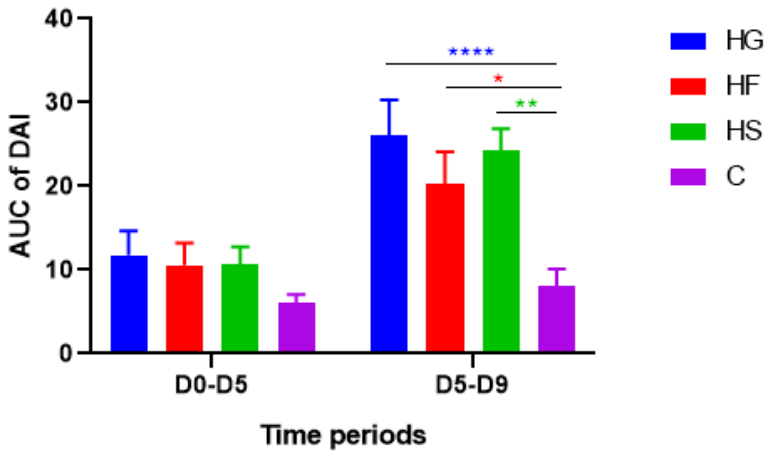

Figure 3.3. Effect of high sugar diets on the area under the curve (AUC) of Disease Activity Index (DAI) scores. AUC was calculated for DAI scores during the DSS treatment period (day 0 to day 5) and the recovery period (day 5 to day 9). Blue = high glucose diet (HG). Red = high fructose diet (HF). Green = high sucrose diet (HS). Purple = control diet (C). n=7 for HG, HF, C, and n=6 for HS. Data are presented as mean ± SEM. Statistical significance was determined between treatment groups for each time period with two-way ANOVA and Tukey's multiple comparisons test. * $p<0.05$, ** $p<0.01$, *** $p<0.001$, **** $p<0.0001$. # $p<0.05$.

3.3.3. Effect of high sugar diets on intestinal weight to length ratios and cecum weights

Figure 3.4 shows weight to length ratios (mg/cm) calculated for small intestine and colon, and cecum weights assessed on day 9. There were no significant differences in the small intestinal weight to length ratios between treatment groups (Figure 3.4A). HG-fed mice had a greater colonic weight to length ratio compared to control mice ($p=0.019$). The colon weights were not significantly different between treatments (HG: 0.200 ± 0.008, HF: 0.208 ± 0.013, HS: 0.187 ± 0.017, C: 0.220 ± 0.015). Colon lengths were significantly reduced in HG-fed mice compared to control mice ($p = 0.0064$) (HG: 5.300 ± 0.392, HF: 5.886 ± 0.363, HS: 5.550 ± 0.291, C: 7.643 ± 0.459). There were no significant differences in the cecum weights between treatment groups (Figure 3.4B) (HG: 0.124 ± 0.018, HF: 0.123 ± 0.015, HS: 0.131 ± 0.017, C: 0.180 ± 0.008).

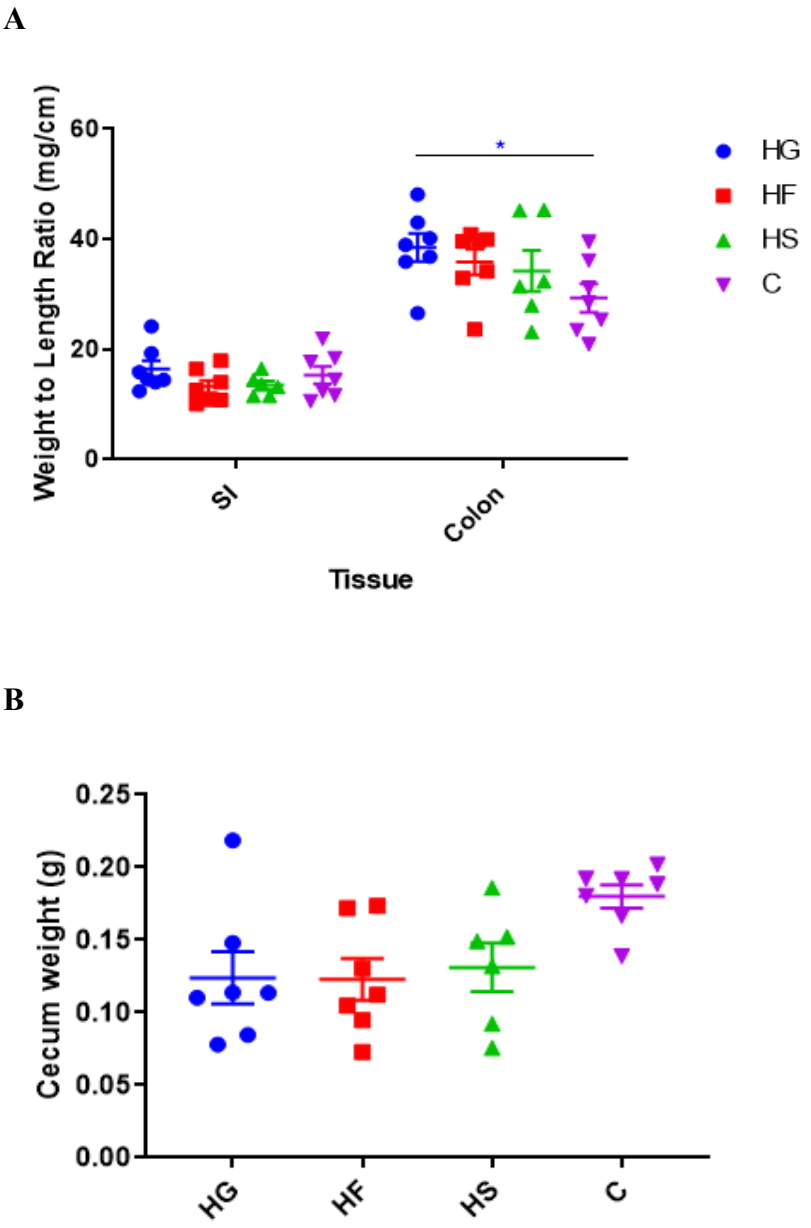

Figure 3.4. Effect of high sugar diets on (A) intestinal weight to length ratios and (B) cecum weights. Blue = high glucose diet (HG). Red = high fructose diet (HF). Green = high sucrose diet (HS). Purple = control diet (C). n=7 for HG, HF, C, and n=6 for HS. Each data point represents a single measurement. Data are presented as mean ± SEM. Statistical significance was determined between treatment groups. Two-way ANOVA and Tukey's multiple comparisons test was used for (A). One-way ANOVA (Kruskal-Wallis) with Dunn's multiple comparisons test was used for (B). * $p<0.05$.

3.3.4. Effect of high sugar diets on terminal ileum and colon histological scores

A histological score with a range from 0 to 10 was calculated for terminal ileum and colon segments from each mouse. The score was calculated as a sum of the scores for enterocyte injury (0 to 3), lamina propria infiltration by lymphocytes (0 to 2) and neutrophils (0 to 2), and epithelial hyperplasia (0 to 3). The epithelial hyperplasia scores were zero for the colon segments of all mice. The histological scores were zero for the terminal ileum segments of all mice. The average histological score (Figure 3.5A) was greater for HG and HS-fed mice compared to control mice ($p=0.015$ for both) (HG: 7 ± 0, HF: 6.833 ± 0.167, HS: 7 ± 0, C: 2.857 ± 1.184). HG and HS-fed mice also had higher average enterocyte injury scores compared to control mice (Figure 3.5B) ($p=0.014$ for both) (HG: 3 ± 0, HF: 2.833 ± 0.167, HS: 3 ± 0, C: 1.000 ± 0.5345). The score for the infiltration of lymphocytes and neutrophils into the lamina propria (Figure 3.5C and D) was greater for HG ($p=0.019$ and $p=0.011$ respectively), HF ($p=0.019$ and $p=0.011$ respectively), and HS-fed mice ($p=0.028$ and $p=0.011$ respectively) compared to controls. The average scores for both the infiltration of lymphocytes and neutrophils were 2 ± 0 for HG, HF and HS-fed mice. For controls, the average score was 1.000 ± 0.378 for the infiltration of lymphocytes, and 0.857 ± 0.340 for the infiltration of neutrophils.

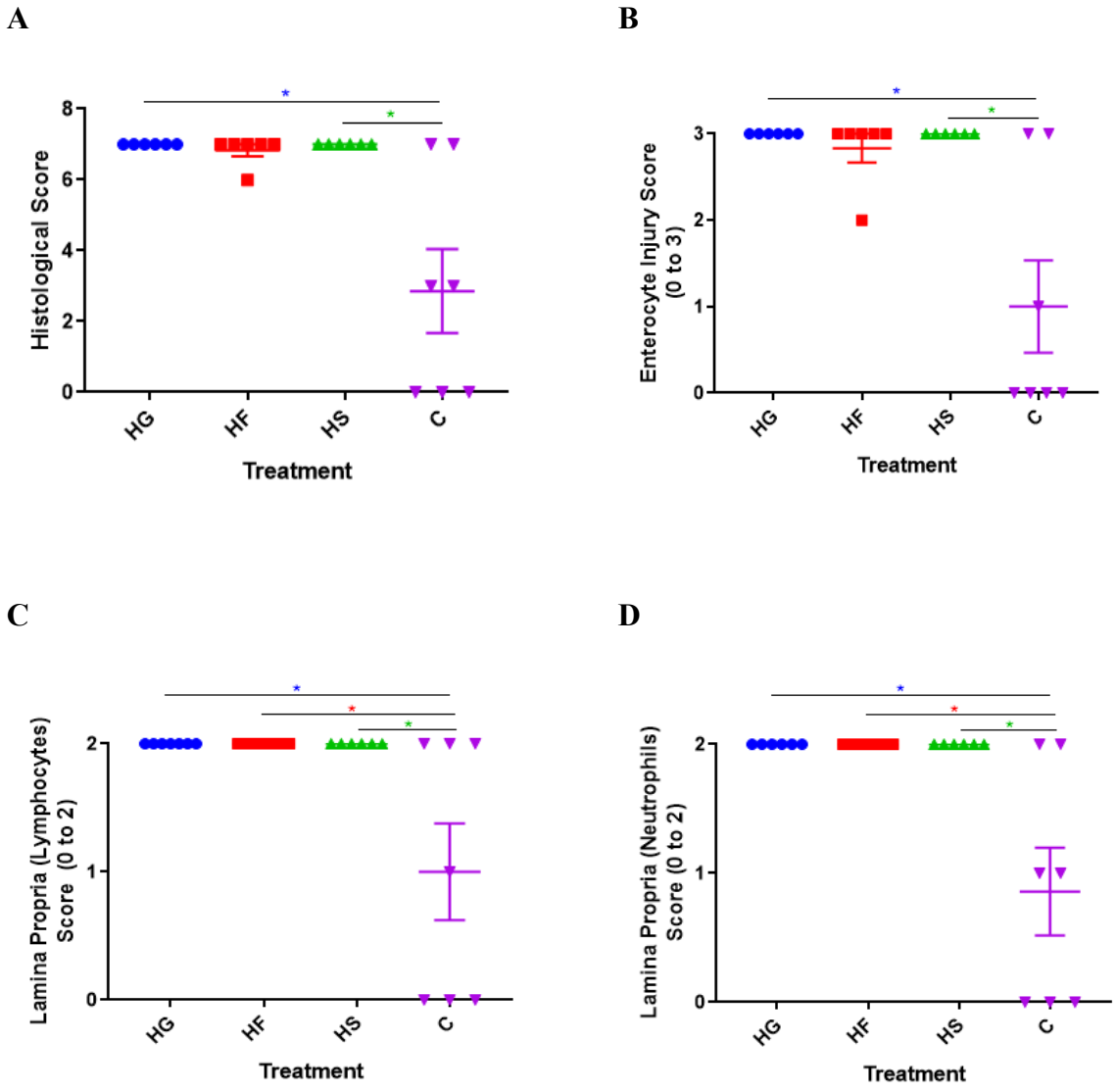

Figure 3.5. Effect of high sugar diets on colon histological scores. (A) Histological scores (0 to 10) were calculated using scores for (B) enterocyte injury (0 to 3), (C) infiltration of lymphocytes into the lamina propria (0 to 2), (D) infiltration of neutrophils into the lamina propria, and epithelial hyperplasia (0 to 3, not shown). Blue = high glucose diet (HG). Red = high fructose diet (HF). Green = high sucrose diet (HS). Purple = control diet (C). For (A), (B) and (D) n=6 for HG, HF, HS, and n=7 for C. For (C) n=7 for HG, HF, C and n=6 for HS. Each data point represents a single measurement. Data are presented as mean ± SEM. Statistical significance was determined between treatment groups using one-way ANOVA (Kruskal-Wallis) with Dunn's multiple comparisons test. * $p<0.05$.

3.3.5. Effect of high sugar diets on plasma lipopolysaccharide (LPS) concentration

There were no significant differences in the mean LPS concentration between the treatment groups (HG 0.786 ± 0.188, HF: 1.083 ± 0.257, HS: 1.183 ± 0.208, C: 0.560 ± 0.075) (Figure 3.6).

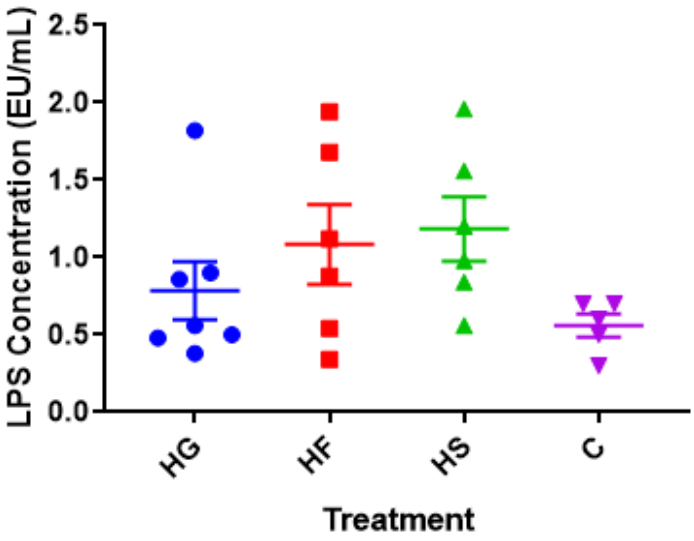

Figure 3.6. Effect of high sugar diets on plasma lipopolysaccharide (LPS) concentration. Blue = high glucose diet (HG). Red = high fructose diet (HF). Green = high sucrose diet (HS). Purple = control diet (C). n=7 for HG, n=6 for HF and HS, and n=5 for C. Each data point represents a single measurement. Data are presented as mean ± SEM. Statistical significance was determined between groups by one-way ANOVA (Kruskal-Wallis) and Dunn's multiple comparisons test.

3.3.6. Effect of high sugar diets on Macrophage Receptor with Collagenous Structure (MARCO) expression in the liver

The log2 fold change in macrophage receptor with collagenous structure (MARCO), normalized to 18S rRNA, was significantly greater in HG-fed mice compared to controls ($p=0.011$) (HG: 3.244 ± 0.157, HF: 1.966 ± 0.638, HS: 3.012 ± 0.727, C: $1 \times 10^{-6} \pm 0.756$). The difference between HS-fed mice and controls trended towards significance ($p=0.058$). There was no significant difference between the log2 fold change of HF-fed mice and controls ($p=0.692$).

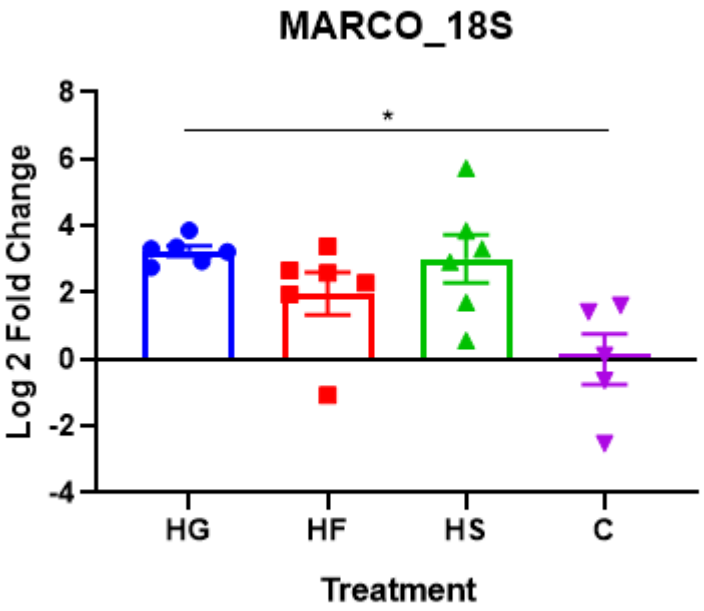

Figure 3.7. Effect of high sugar diets on the mRNA expression of macrophage receptor with collagenous structure (MARCO), normalized to 18S rRNA. n=6 for HG, HF, HS, and n=5 for C. Each data point represents a single measurement. Data are presented as mean ± SEM. Statistical significance was determined between groups by one-way ANOVA (Kruskal-Wallis) and Dunn's multiple comparisons test.

3.3.7 Effect of high sugar diets on the concentration of cytokines and chemokines in terminal ileum and colon segments

The concentration (pg/g of tissue) of IL-1β, IL-12p70, IFN-γ, IL-6, keratinocyte chemoattractant (KC), IL-10, and TNF-α were measured for terminal ileum (Figure 3.8) and colon segments (Figure 3.9). The concentration of TNF-α was zero in the terminal ileum. The concentration of KC was greater in the terminal ileum of HG, HF and HS-fed mice compared to control mice ($p=0.020$, 0.025, 0.044 respectively) (HG: 1006.00 ± 216.40, HF: 1236.00 ± 464.20, HS: 991.40 ± 204.60, C: 123.20 ± 11.21). There were no significant differences in the concentration of IL-1β, IL-12p70, IFN-γ, IL-6, IL-10 or TNF-α in the terminal ileum.

The colon of HG, HF and HS-fed mice had a higher concentration of IL-1β ($p=0.018$, 0.018, 0.007 respectively) and IL-6 ($p=0.007$, 0.018, 0.007) compared to controls. The average concentration of IL-1β in the colon were 7108.00 ± 2604.00 in HG-fed mice, 7806.00 ± 3128.00 in HF-fed mice, 10133.00 ± 3578.00 in HS-fed mice and 226.10 ± 65.75 in control mice. The average concentrations of IL-6 were 5788.00 ± 2954.00 in HG-fed mice, 6273.00 ± 2757.00 in HF-fed mice, 9956.00 ± 4560.00 in HS-fed mice and 19.43 ± 2.18 in control mice. The concentration of KC was greater in the colon of HG and HS-fed mice compared to controls ($p=0.015$ and 0.018 respectively) (HG: 6661.00 ± 2042.00, HF: 5096.00 ± 1990.00, HS: 6873.00 ± 2680.00, C: 193.10 ± 24.87). HG-fed mice had a higher concentration of IL-10 in the colon compared to control mice ($p=0.030$) (HG: 227.80 ± 67.57, HF: 132.90 ± 45.29, HS: 242.50 ± 113.30, C: 4.93 ± 2.51). There were no significant differences in the concentration of IL-12p70, IFN-γ or TNF-α between treatment groups.

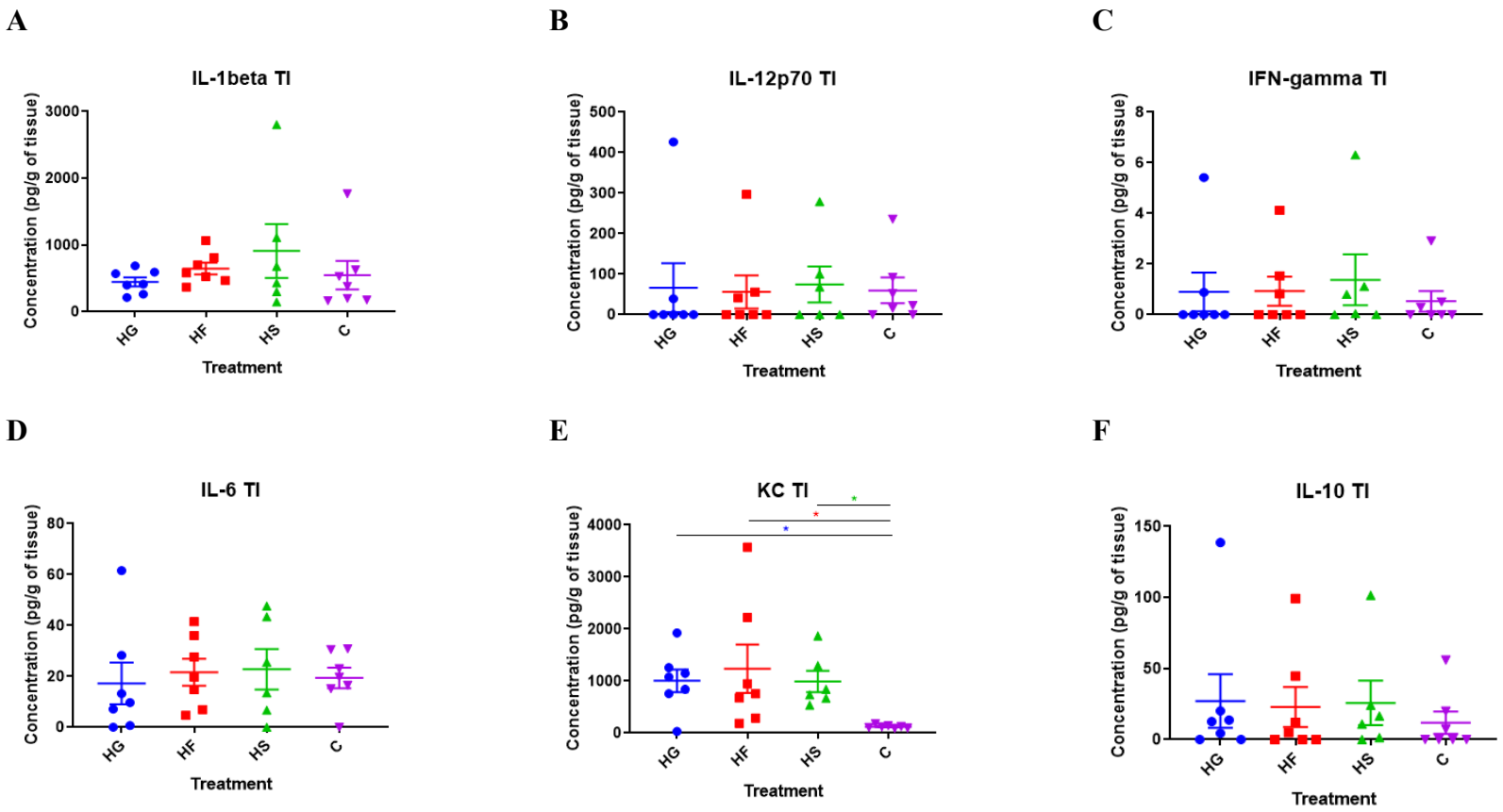

Figure 3.8. Effect of high sugar diets on the concentration of cytokines and chemokines in terminal ileum (TI) segments. The concentration (pg/g of tissue) of (A) IL-1β, (B) IL-12p70, (C) IFN-γ, (D) IL-6, (E) keratinocyte chemoattractant (KC), and (F) IL-10 were measured. Blue = high glucose diet (HG). Red = high fructose diet (HF). Green = high sucrose diet (HS). Purple = control diet (C). n=7 for HG, HF, and C, and n=6 for HS. Each data point represents a single measurement. Data are presented as mean ± SEM. Statistical significance was determined between groups by one-way ANOVA (Kruskal-Wallis) and Dunn's multiple comparisons test. * $p<0.05$.

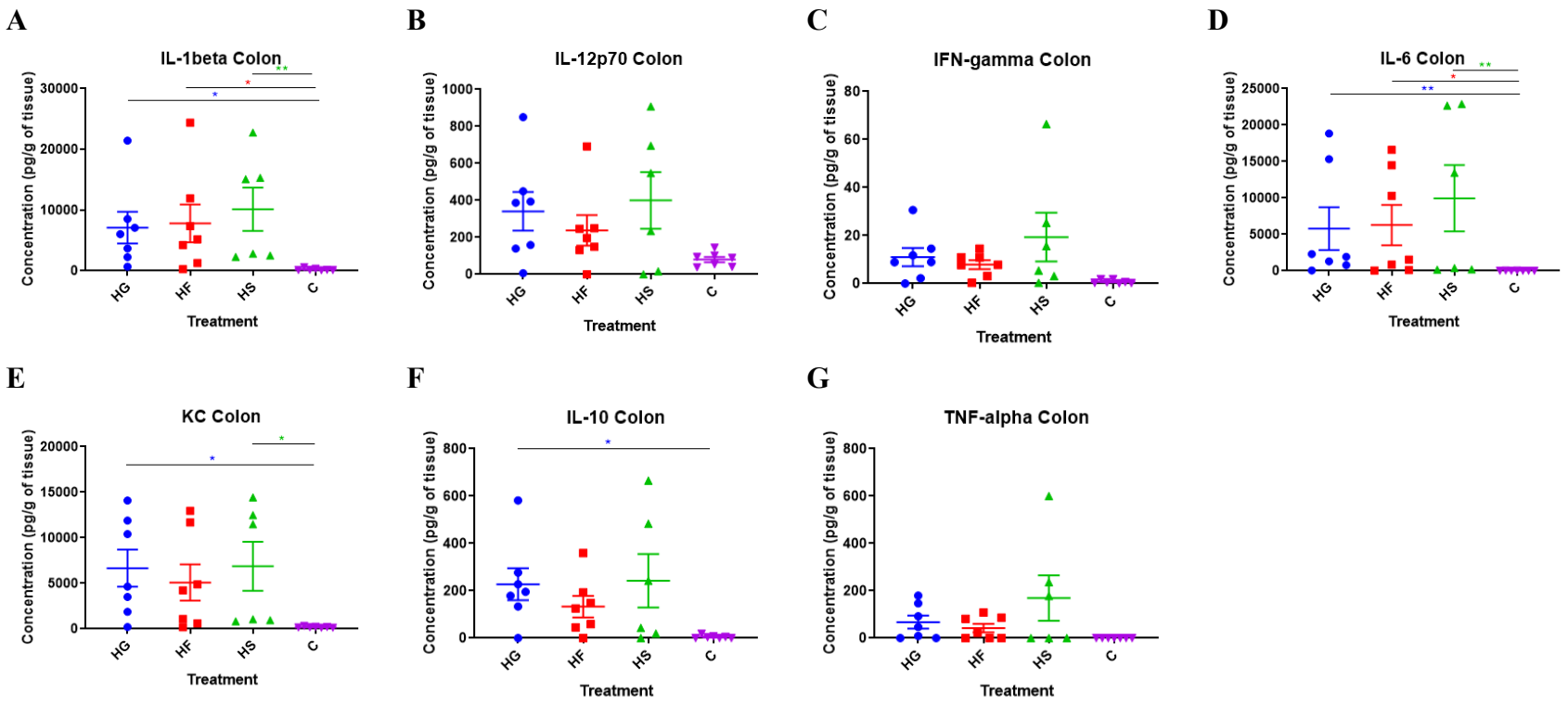

Figure 3.9. Effect of high sugar diets on the concentration of cytokines and chemokines in colon segments. The concentration (pg/g of tissue) of (A) IL-1β, (B) IL-12p70, (C) IFN-γ, (D) IL-6, (E) keratinocyte chemoattractant (KC), (F) IL-10, and (G) TNF-α were measured. Blue = high glucose diet (HG). Red = high fructose diet (HF). Green = high sucrose diet (HS). Purple = control diet (C). n=7 for HG, HF, and C, and n=6 for HS. Each data point represents a single measurement. Data are presented as mean ± SEM. Statistical significance was determined between groups by one-way ANOVA (Kruskal-Wallis) and Dunn's multiple comparisons test. * $p<0.05$, ** $p<0.01$.

3.3.8 Effect of high sugar diets on alpha and beta diversity of cecum contents and stool

The microbial composition of cecum contents and stool samples were analyzed. Alpha diversity was measured with metrics for evenness, Faith's phylogenetic diversity (PD), the number of observed OTUs and Shannon's diversity. There were no significant differences in the alpha diversity metrics for cecum contents (Figure 3.10). Stool samples collected from HG and HF-fed mice at day 0 had lower evenness compared to controls (Figure 3.11). Stool samples from HG and HS-fed mice had a lower number of observed OTUs compared to controls at day 0. The number of observed OTUs decreased at day 0 from baseline for HG and HF-fed mice and continued to remain low at day 5 for HG-fed mice. HG and HS-fed mice had a lower Shannon's diversity index compared to controls. The Shannon's diversity index decreased at day 0 for HG and HS-fed mice.

Beta diversity was measured for cecum contents (Figures 3.12 and 3.13) and stool samples (Figures 3.14 to 3.19) with Jaccard, Bray-Curtis, unweighted and weighted UniFrac distances. Significant differences were found with the Bray-Curtis ($p=0.012$), Jaccard ($p=0.026$) and unweighted UniFrac ($p=0.033$) distances for cecum contents. The Bray-Curtis, Jaccard and unweighted UniFrac distances were significantly different between controls, and HG ($p=0.026$, 0.035, and 0.016 respectively) and HS-fed mice ($p=0.010$, 0.009, and 0.013 respectively). The weighted UniFrac distances were significantly different between HS-fed mice and controls ($p=0.011$).

There were no significant differences in the beta diversity measurements for stool at day -2 (Figures 3.14 and 3.15). There were significant differences in the Bray-Curtis ($p=0.001$), Jaccard ($p=0.001$), unweighted and weighted UniFrac ($p=0.002$ for both) distances for stool samples at day 0 (Figures 3.16 and 3.17). The Bray-Curtis, Jaccard, unweighted UniFrac and weighted UniFrac distances were significantly different at day 0 between controls, and HG ($p=0.002$, 0.001, 0.010, 0.002 respectively) and HS-fed mice ($p=0.005$, 0.003, 0.004, 0.004). The Jaccard and unweighted UniFrac distances were significantly different between controls and HF-fed mice at day 0 ($p=0.006$ and 0.009 respectively). HG and HF-fed mice had significantly different Bray-Curtis, Jaccard, and weighted UniFrac distances at day 0 ($p=0.004$, 0.002, and 0.049 respectively). HF and HS-fed mice had significantly different Bray-Curtis, weighted and unweighted UniFrac distances at day 0 ($p=0.040$, 0.019, and 0.040 respectively).

Stool samples at day 5 had significantly different Jaccard (p=0.005) and unweighted UniFrac distances (p=0.001) (Figures 3.18 and 3.19). Control mice had significantly different Jaccard and unweighted UniFrac distances from HG (p=0.005 and 0.002 respectively), HF (p=0.002 for both), and HS-fed mice (p=0.018 and 0.003 respectively). The Bray-Curtis and weighted UniFrac distances for control and HG-fed mice trended towards significance (p=0.054 and 0.051). The Jaccard distances for HG and HF-fed mice, and unweighted UniFrac for HG and HS-fed mice also trended towards significance (p=0.055 and 0.051 respectively).

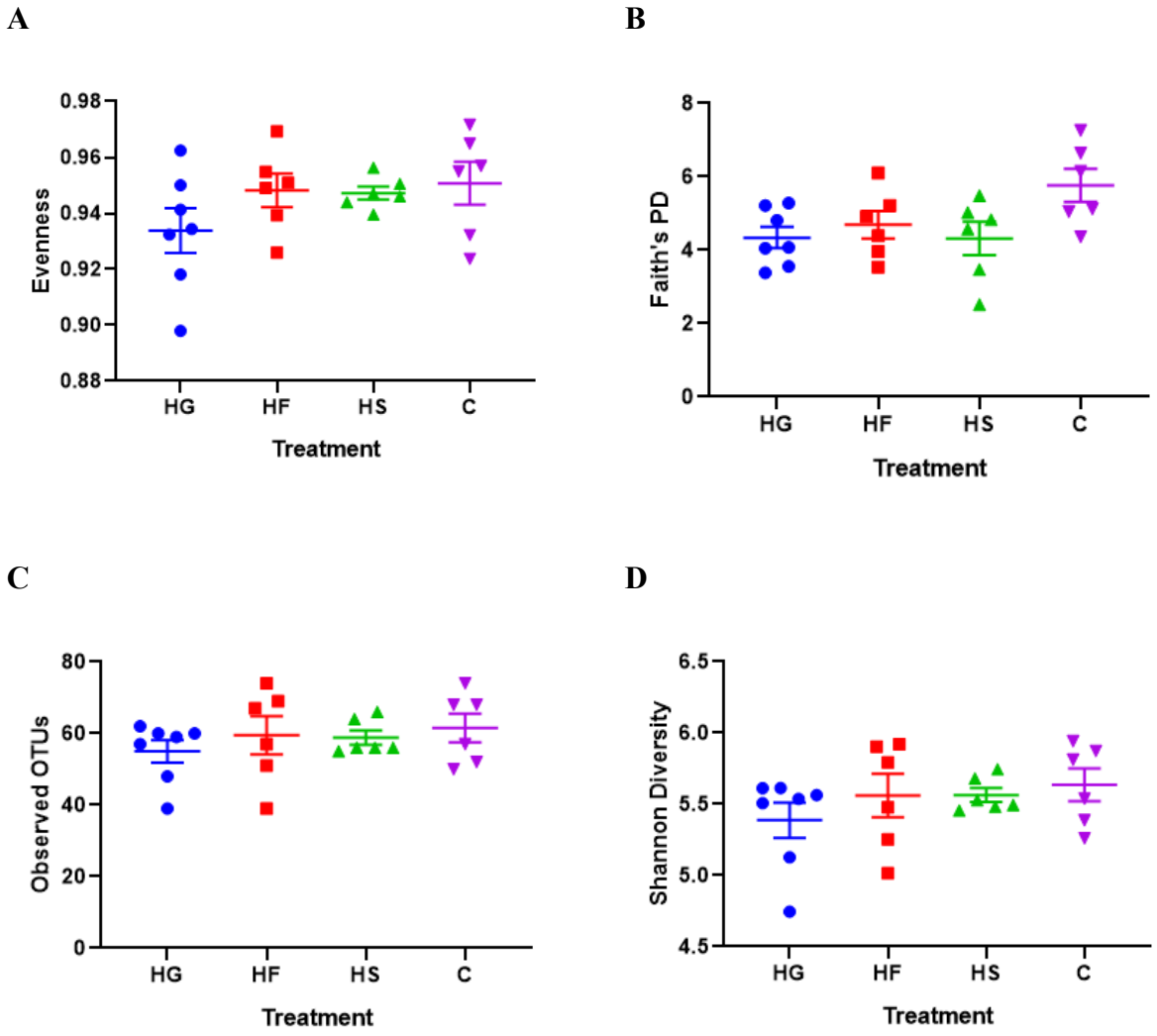

Figure 3.10. Alpha diversity metrics measured for cecum content. (A) Pielou's Evenness, (B) Faith's Phylogenetic Diversity (PD), (C) Observed OTUs, and (D) Shannon's diversity index. Blue = high glucose diet (HG). Red = high fructose diet (HF). Green = high sucrose diet (HS). Purple = control diet (C). n=7 for HG and n=6 for HF, HS, and C. Each data point represents a single measurement. Data are presented as mean ± SEM. Statistical significance was determined between groups by one-way ANOVA (Kruskal-Wallis) and Dunn's multiple comparisons test.

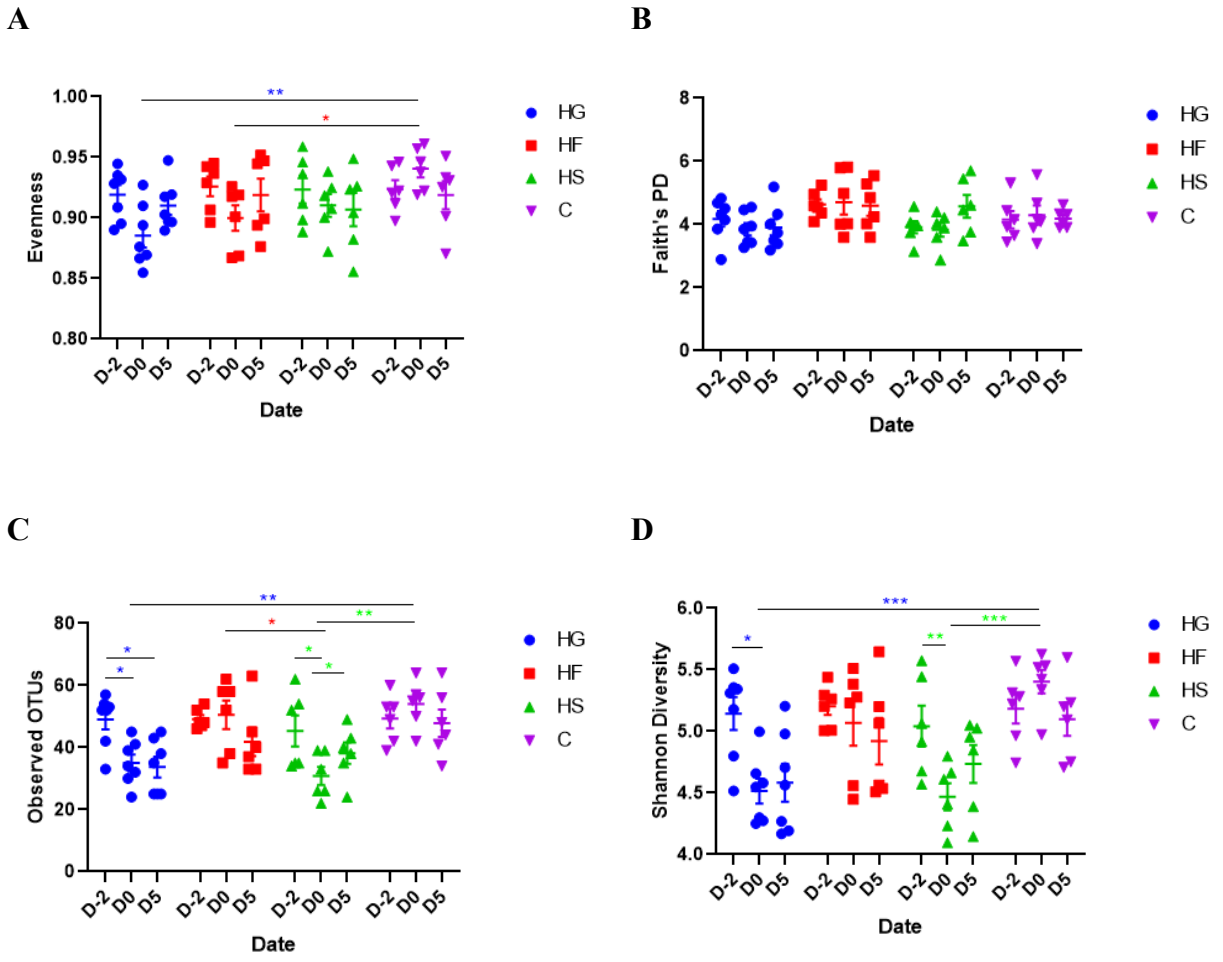

Figure 3.11. Alpha diversity metrics measured for stool. (A) Pielou's Evenness, (B) Faith's Phylogenetic Diversity (PD), (C) Observed OTUs, and (D) Shannon's diversity index. Blue = high glucose diet (HG). Red = high fructose diet (HF). Green = high sucrose diet (HS). Purple = control diet (C). n=7 for HG and n=6 for HF, HS, and C. Each data point represents a single measurement. Data are presented as mean ± SEM. Statistical significance was determined between groups by one-way ANOVA (Kruskal-Wallis) and Dunn's multiple comparisons test. * $p<0.05$, ** $p<0.01$, *** $p<0.001$.

A

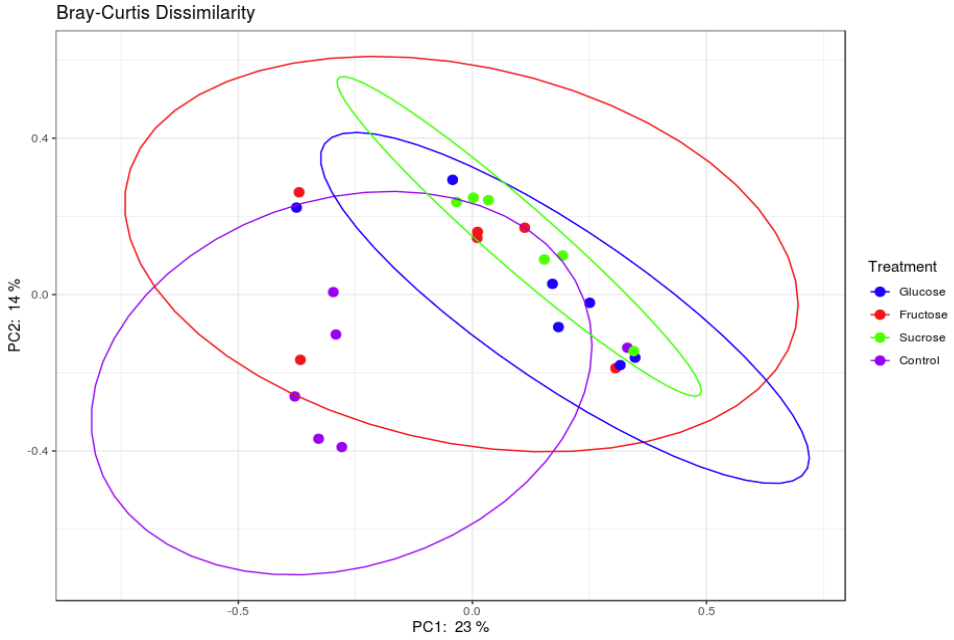

B

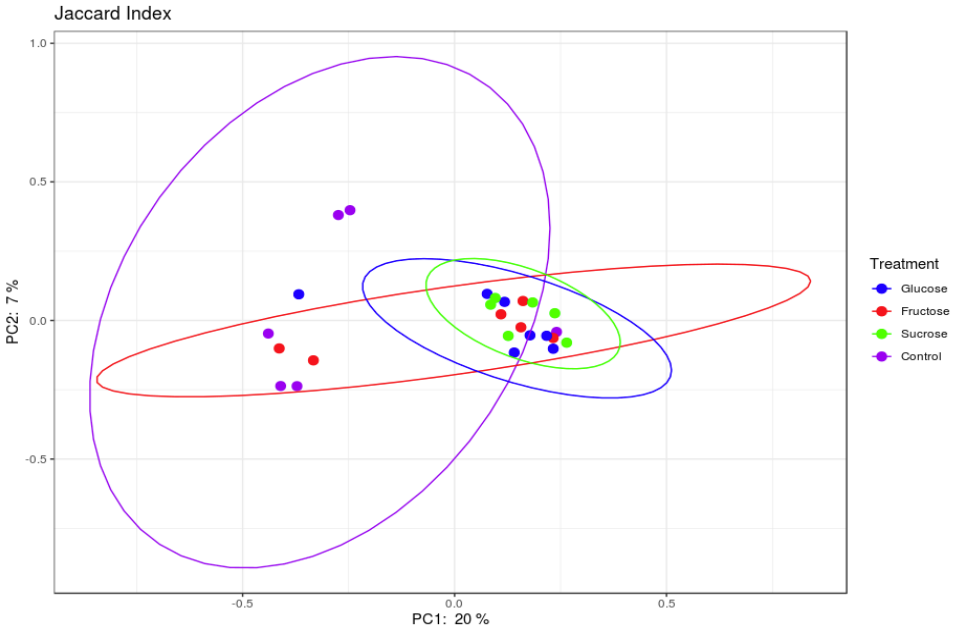

Figure 3.12. Principal Coordinates Analysis (PCoA) plot of the (A) Bray-Curtis and (B) Jaccard Indices of cecum contents. Each data point represents a single measurement. p=0.012 for (A) and p=0.026 for (B). The ellipse has a confidence interval of 95%.

A

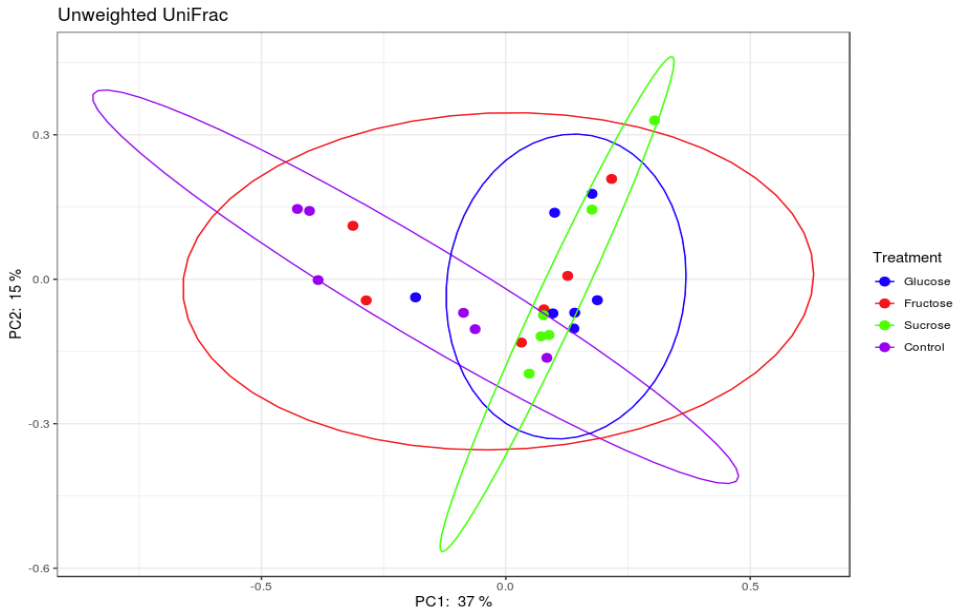

B

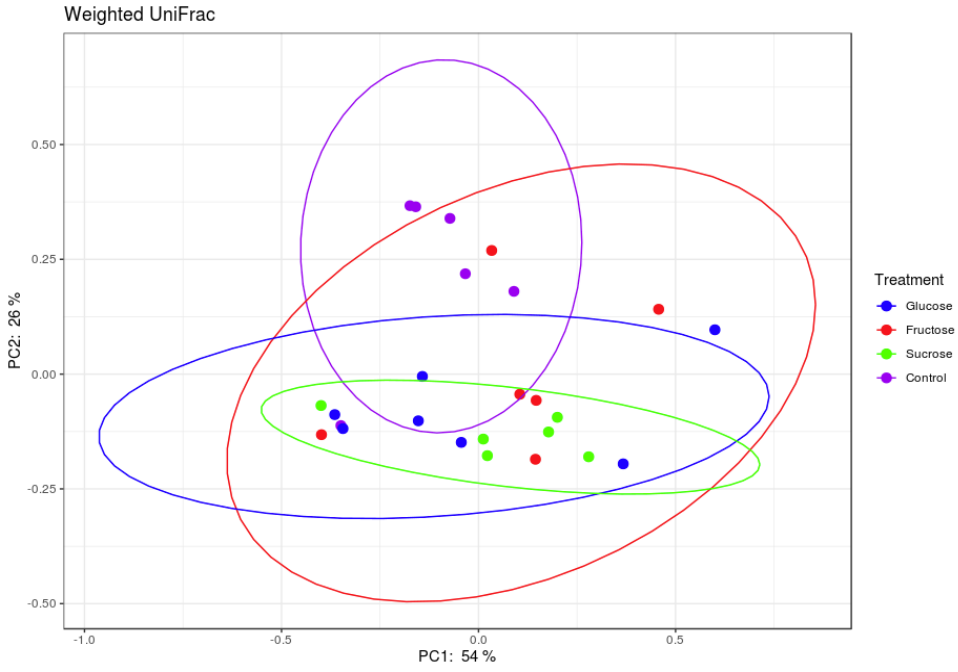

Figure 3.13. Principal Coordinates Analysis (PCoA) plot of the (A) unweighted and (B) weighted UniFrac of cecum contents. Each data point represents a single measurement. p=0.033 for (A) and p=0.094 for (B). The ellipse has a confidence interval of 95%.

A

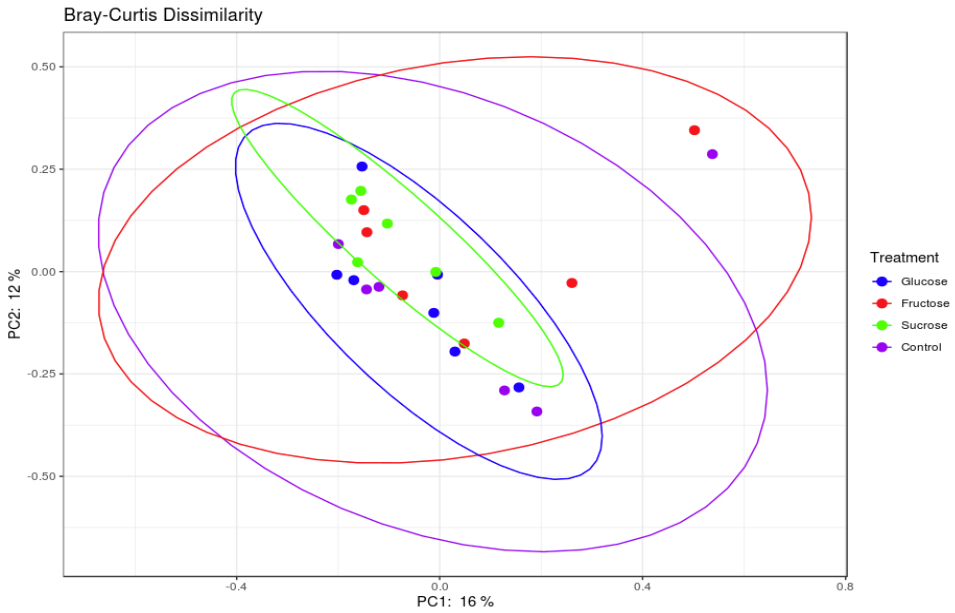

B

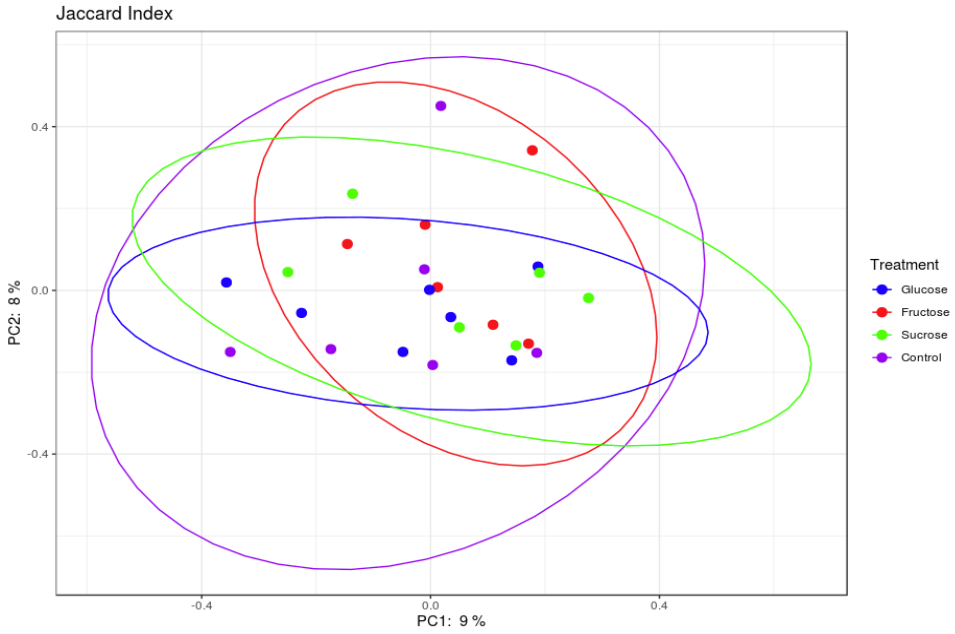

Figure 3.14. Principal Coordinates Analysis (PCoA) plot of the (A) Bray-Curtis and (B) Jaccard Indices of stool samples on day -2. Each data point represents a single measurement. p=0.595 for (A) and p=0.828 for (B).The ellipse has a confidence interval of 95%.

A

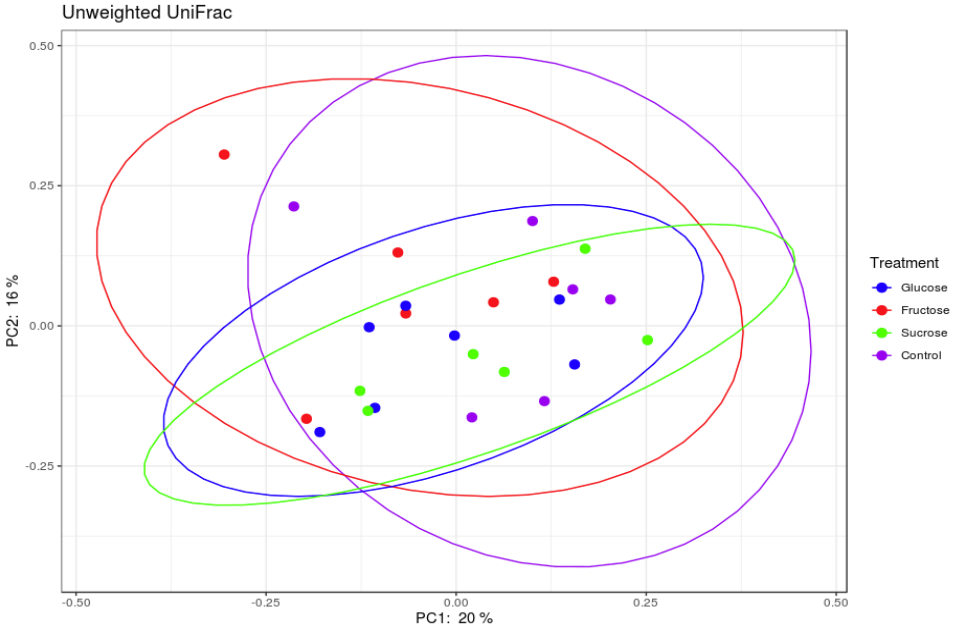

B

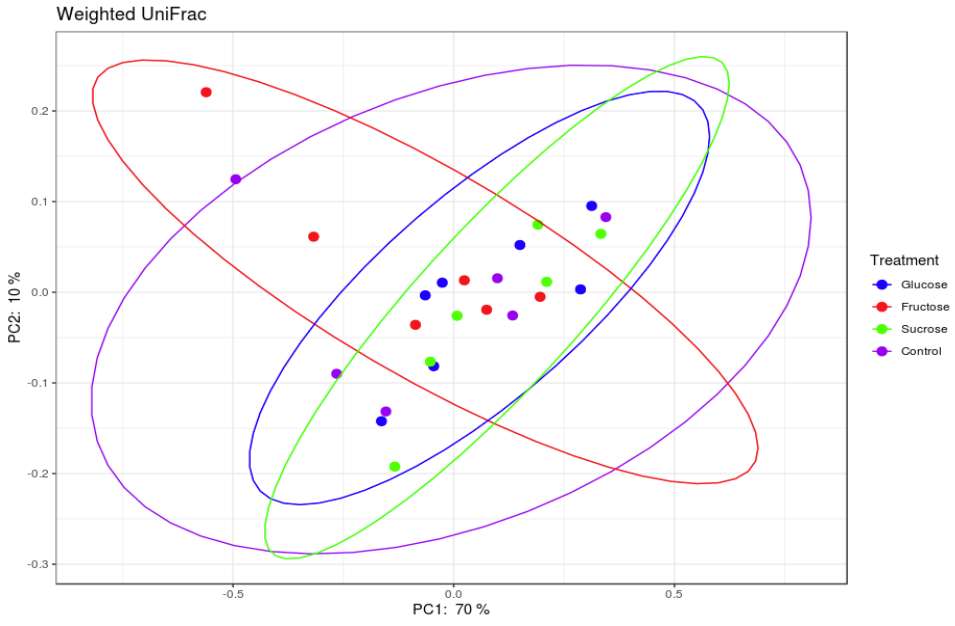

Figure 3.15. Principal Coordinates Analysis (PCoA) plot of the (A) unweighted and (B) weighted UniFrac of stool samples on day -2. Each data point represents a single measurement. p=0.881 for (A) and p=0.478 for (B). The ellipse has a confidence interval of 95%.

A

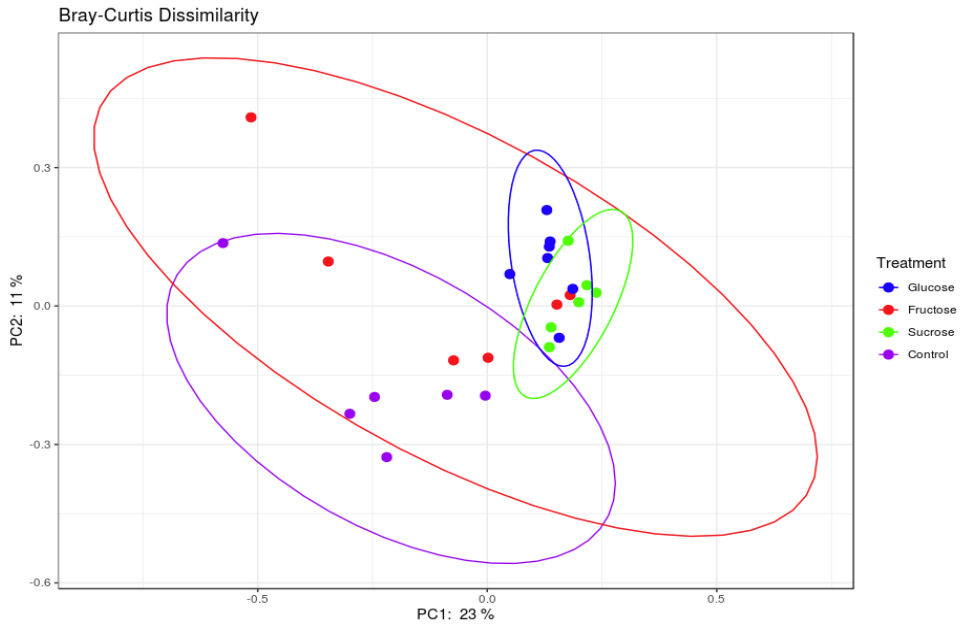

B

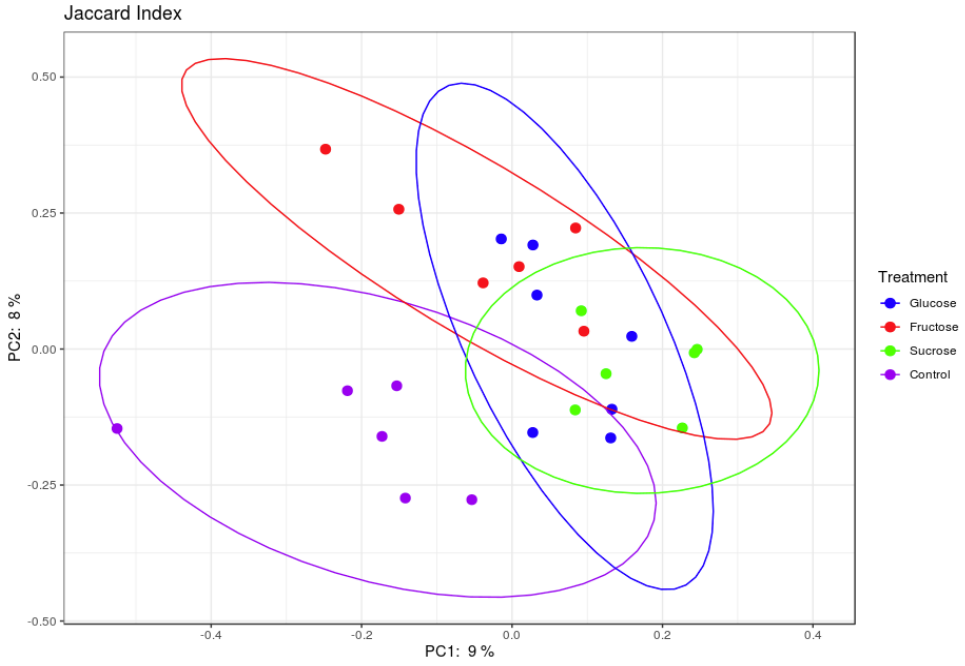

Figure 3.16. Principal Coordinates Analysis (PCoA) plot of the (A) Bray-Curtis and (B) Jaccard Indices of stool samples on day 0. Each data point represents a single measurement. p=0.001 for both (A) and (B). The ellipse has a confidence interval of 95%.

A

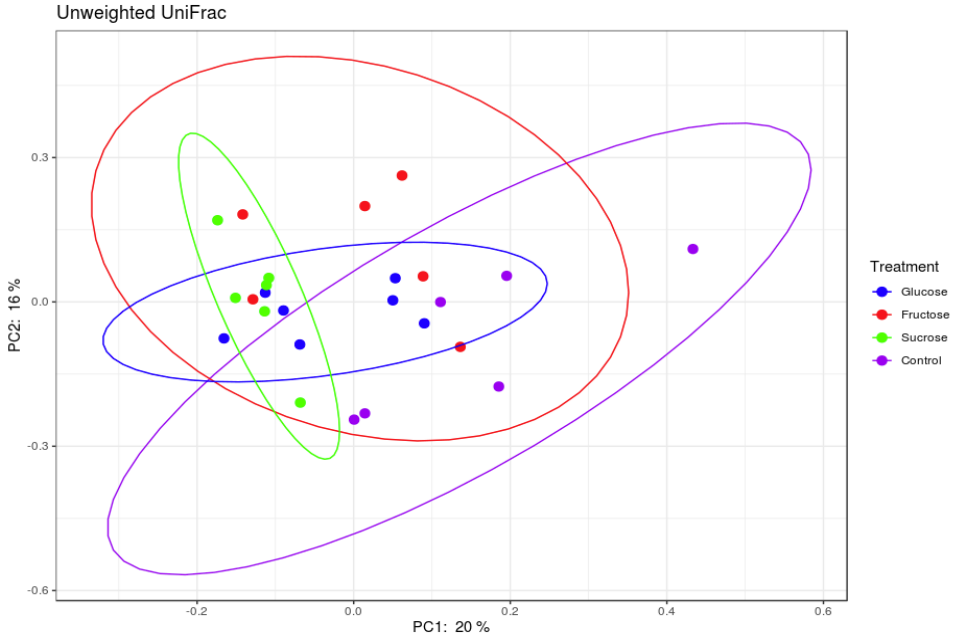

B

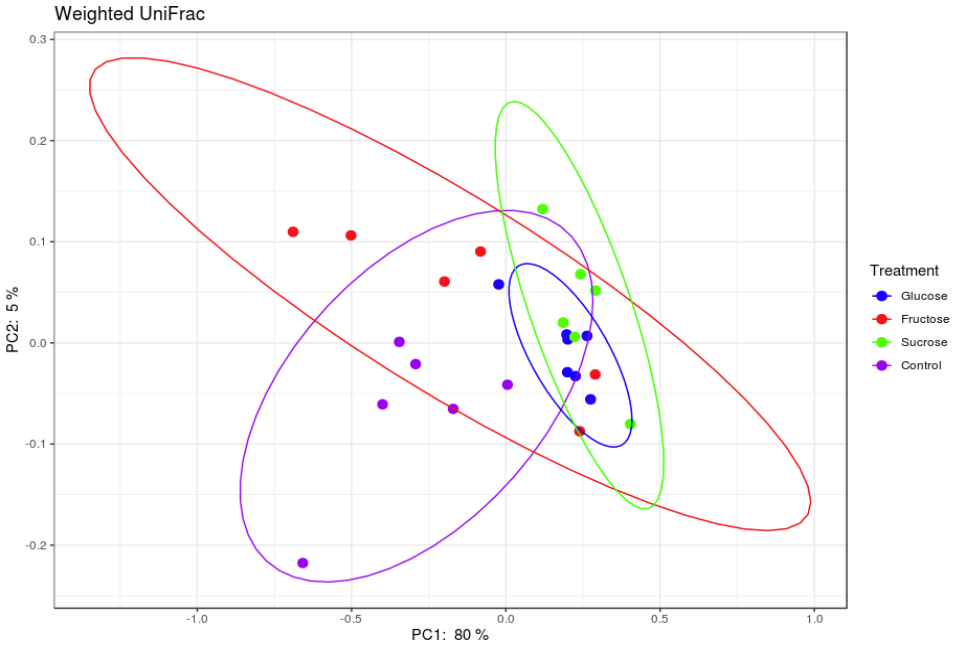

Figure 3.17. Principal Coordinates Analysis (PCoA) plot of the (A) unweighted and (B) weighted UniFrac of stool samples on day 0. Each data point represents a single measurement. p=0.002 for both (A) and (B). The ellipse has a confidence interval of 95%.

A

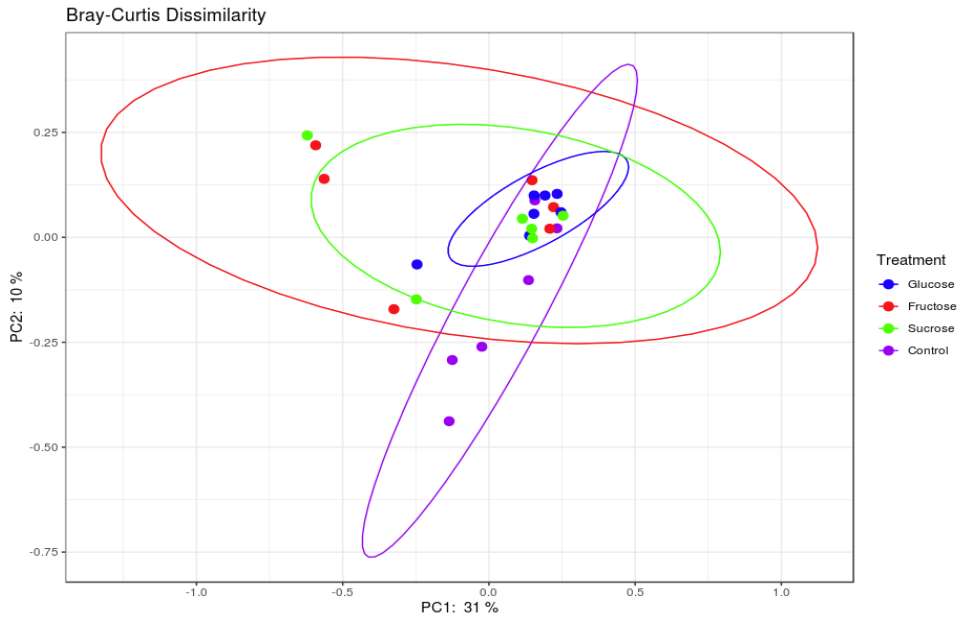

B

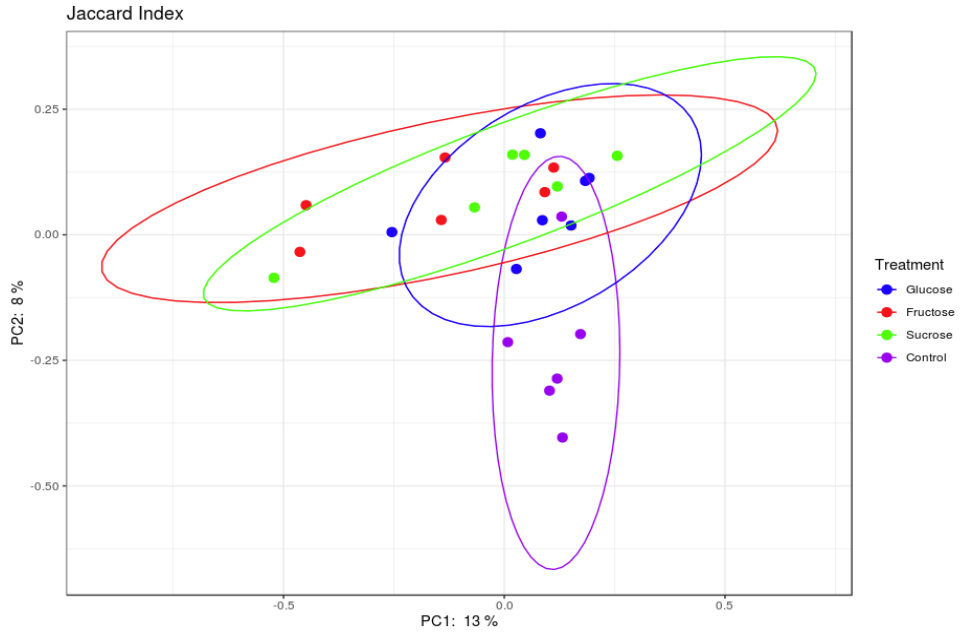

Figure 3.18. Principal Coordinates Analysis (PCoA) plot of the (A) Bray-Curtis and (B) Jaccard Indices of stool samples on day 5. Each data point represents a single measurement. p=0.182 for (A) and p=0.005 for (B). The ellipse has a confidence interval of 95%.

A

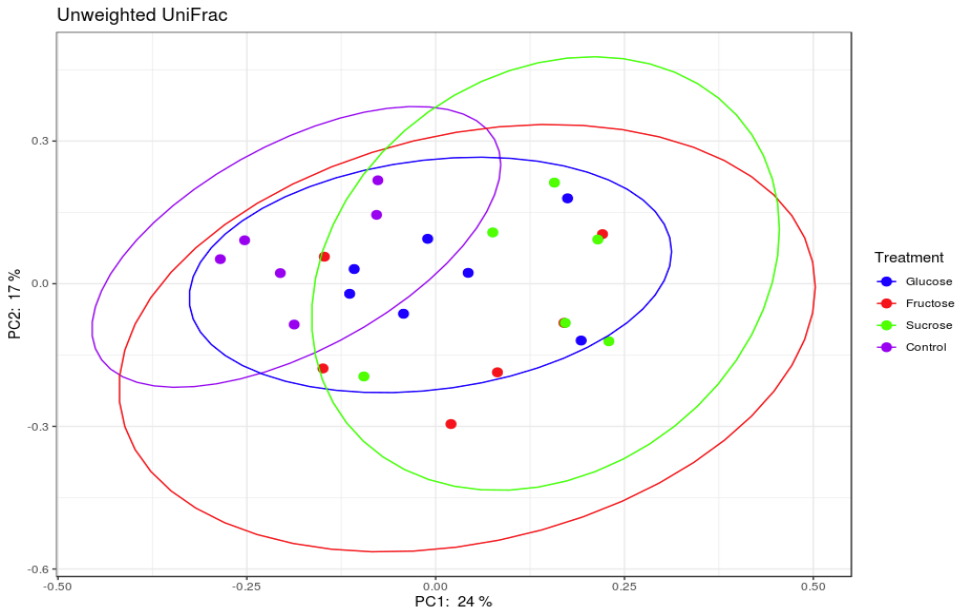

B

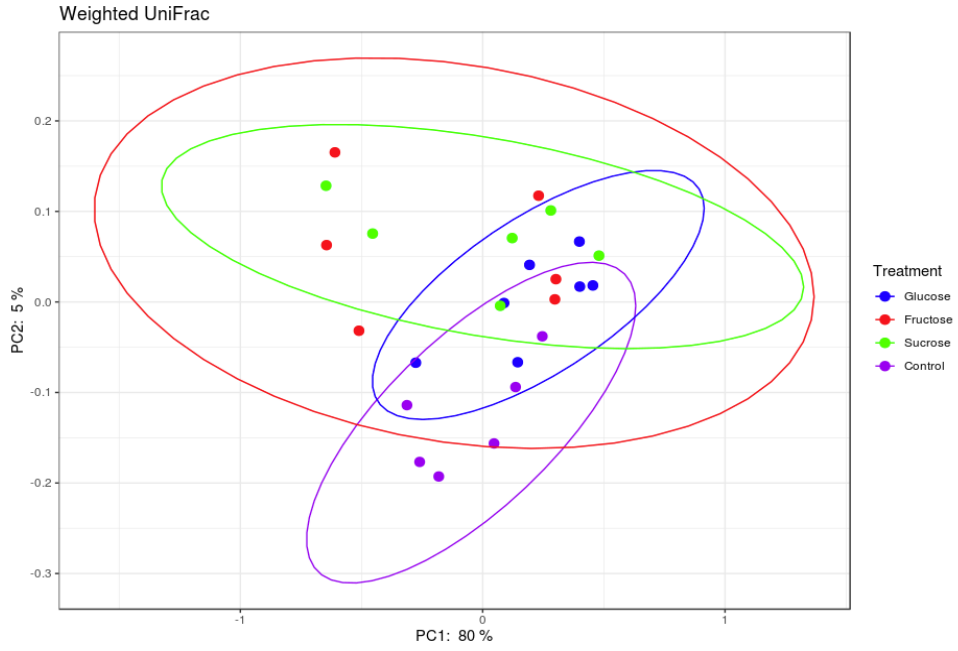

Figure 3.19. Principal Coordinates Analysis (PCoA) plot of the unweighted and weighted UniFrac of stool samples on day 5. Each data point represents a single measurement. p=0.001 for (A) and p=0.215 for (B). The ellipse has a confidence interval of 95%.

3.3.9 Effect of high sugar diets on the relative abundance of bacteria in cecum contents and stool

The microbial composition of cecum contents and stool samples is shown at the phylum level (Figure 3.20). In cecum contents, *Firmicutes* were significantly lower in HG, HF, and HS-fed mice compared to controls ($p=0.0006$, 0.036, and 0.0001 respectively) (Figure 3.20A). *Proteobacteria* were significantly increased in HG ($p=0.001$) and HS-fed mice ($p=0.044$) compared to controls. *Verrucomicrobia* were significantly increased in HF ($p=0.026$) and HS-fed mice ($p=0.020$) compared to controls.

In stool samples at baseline (day -2), *Firmicutes* were significantly lower in HG-fed mice compared to controls ($p=0.015$) (Figure 3.20B). HF-fed mice had lower *Verrucomicrobia* than HG ($p=0.021$) and HS-fed mice ($p=0.010$). In stool samples at day 0, *Bacteroidetes* were significantly decreased in HG ($p<0.0001$) and HS-fed mice ($p<0.0001$) compared to control mice. HF-fed mice had greater amounts of *Bacteroidetes* than HS-fed mice ($p=0.004$). HG-fed mice had lower amounts of *Firmicutes* compared to HF-fed mice ($p=0.008$) and control mice ($p=0.008$). *Verrucomicrobia* were greater in HG, HF, and HS-fed mice compared to control mice ($p<0.0001$, 0.0378, <0.0001). HG and HS-fed mice had greater amounts of *Verrucomicrobia* than HF-fed mice ($p<0.0001$ for both). In stool samples at day 5, *Verrucomicrobia* were increased in HG-fed mice relative to controls ($p=0.006$) and HF-fed mice ($p=0.0003$).

A

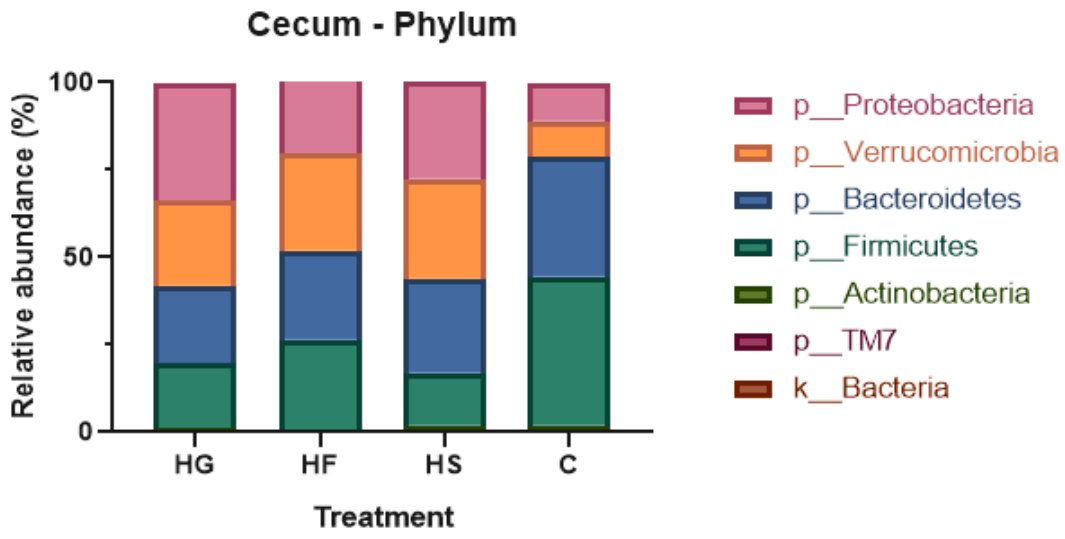

B

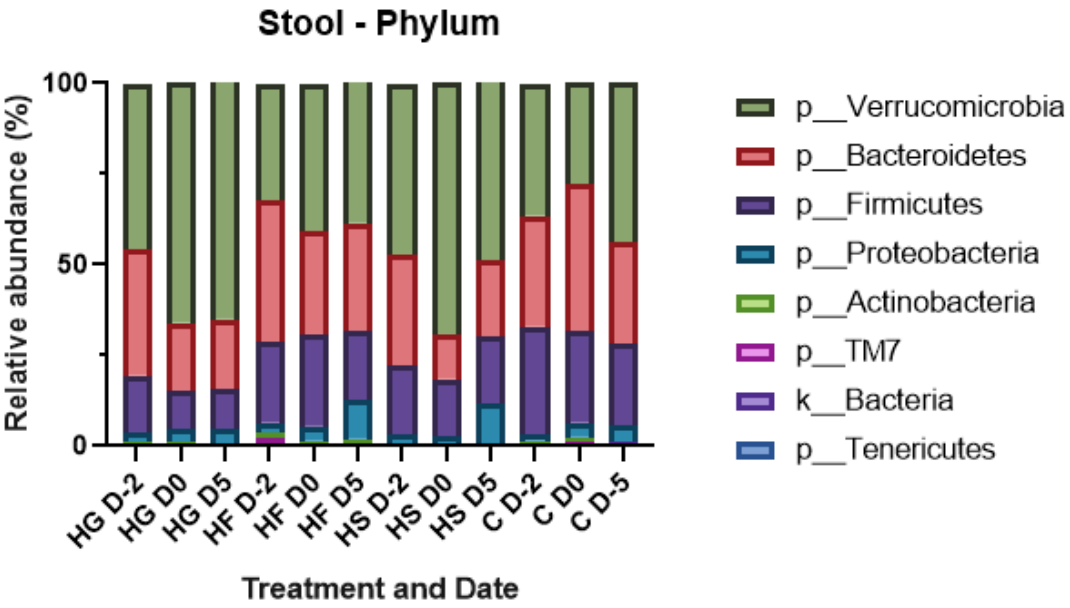

Figure 3.20. Average relative abundance of bacteria in the (A) cecum contents and (B) stool samples at the phylum level. HG = high glucose diet, HF = high fructose diet, HS = high sucrose diet, C = control diet. n=7 for HG and n=6 for HF, HS, and C.

Figure 3.21 shows significant changes in the relative abundance of groups of bacteria in cecum contents. There were no significant differences in the relative abundance of *Bacteroides* between the treatment groups. *S24-7* was decreased in HG, HF, and HS-fed mice relative to controls ($q<0.0001$, $p<0.0001$ for all). *Clostridiales* was reduced in HG ($q=0.0017$, $p=0.0006$), HF ($q=0.050$, $p=0.025$), and HS-fed mice ($q=0.001$, $p=0.0002$) compared to controls. *Lachnospiraceae* was decreased in HG ($q=0.028$, $p=0.009$) and HS-fed mice ($q=0.028$, $p=0.006$) relative to controls. *Enterobacteriaceae* was increased in HG ($q<0.0001$, $p<0.0001$), HF ($q=0.003$, $p=0.002$) and HS-fed mice ($q<0.0001$, $p<0.0001$) relative to controls. HF-fed mice had lower amounts of *Enterobacteriaceae* than HG ($q<0.0001$, $p<0.0001$) and HS-fed mice ($q=0.034$, $p=0.028$). *Akkermansia* was increased in HG, HF and HS-fed mice compared to controls ($q<0.0001$, $p<0.0001$ for all).

For stool samples, the log2 fold changes in the relative abundance of groups of bacteria were determined (Figure 3.22). The fold changes were determined for two time periods: the diet pre-treatment period between day -2 and day 0 (D-2D0), and the DSS treatment period between day 0 and day 5 (D0D5). During the diet pre-treatment period, *S24-7* was decreased in HG ($p=0.033$) and HS-fed mice ($p=0.009$), and *Enterobacteriaceae* was increased in HG, HF and HS mice ($p<0.0001$). During the DSS treatment period, *Bacteroides* increased in HS-fed mice during the DSS-treatment period ($p=0.009$), and to a larger extent than HF-fed mice ($p=0.046$). *Lachnospiraceae* decreased in all sugar diet-fed mice relative to the diet pre-treatment period and to controls during the DSS treatment period ($p<0.0001$ for all). There were no significant differences in the abundance of *Clostridiales* or *Akkermansia* between the treatments or time periods.

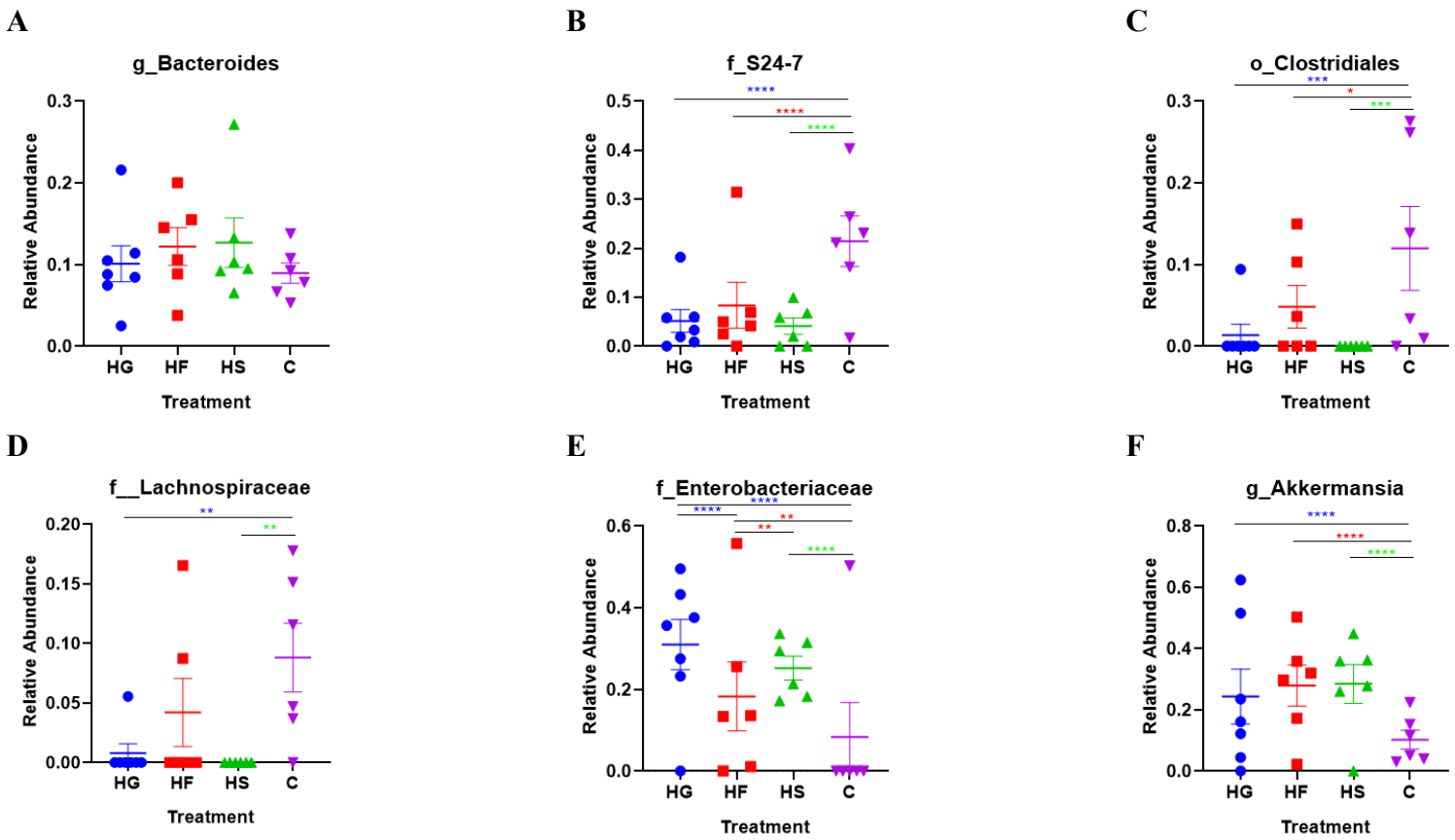

Figure 3.21. Relative abundance of bacteria in cecum contents. Blue = high glucose diet (HG). Red = high fructose diet (HF). Green = high sucrose diet (HS). Purple = control diet (C). n=7 for HG and n=6 for HF, HS, and C. Each data point represents a single measurement. Data are presented as mean ± SEM. Statistical significance was determined between treatment groups with two-way ANOVA and the original FDR method of Benjamini and Hochberg. * $p<0.05$, ** $p<0.01$, *** $p<0.001$, **** $p<0.0001$.

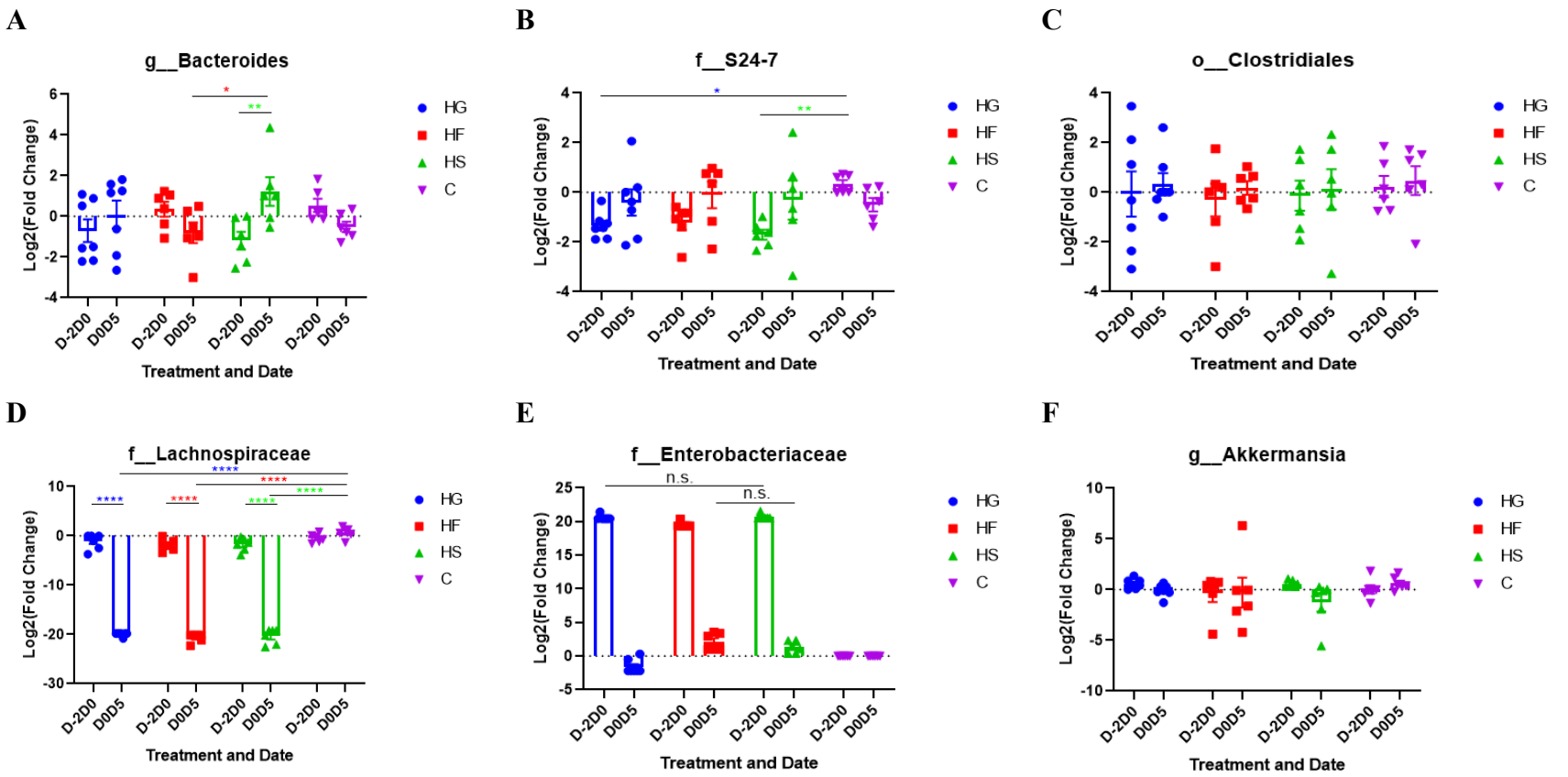

Figure 3.22. Log2 fold change in bacterial abundance of stool. Blue = high glucose diet (HG). Red = high fructose diet (HF). Green = high sucrose diet (HS). Purple = control diet (C). n=7 for HG and n=6 for HF, HS, and C. Log2 fold changes were determined between day -2 and day 0 (D-2D0), and between day 0 and day 5 (D0D5). Each data point represents a single measurement. Data are presented as mean ± SEM. Statistical significance was determined with two-way ANOVA and Tukey's multiple comparisons test between treatments at each time period. Bonferroni's multiple comparisons test was used to determine statistical significance between time periods within treatment groups. * $p<0.05$, ** $p<0.01$, *** $p<0.001$, **** $p<0.0001$.

3.3.10. Significant differential abundance of bacteria in cecum contents and stool

Linear discriminant analysis effect size (LEfSe) was used to identify bacteria that are differentially abundant within the HG, HF, HS and control treatment groups (Figure 3.23). Controls had greater amounts of the order *Clostridiales*, family *Ruminococcaceae* and *Lachnospiraceae*, and genus *Coprococcus* in the cecum contents (Figure 3.23A). There were no differentially abundant bacteria in the stool samples collected at day -2. Controls had greater amounts of the family *S24-7* and *Lachnospiraceae*, and genus *Coprococcus*, *Bacteroides* and *Sutterella* in stool samples collected at day 0 (Figure 3.23B). *Lachnospiraceae* was present in greater amounts in the stool samples of control mice at day 5 (Figure 3.23C).

A

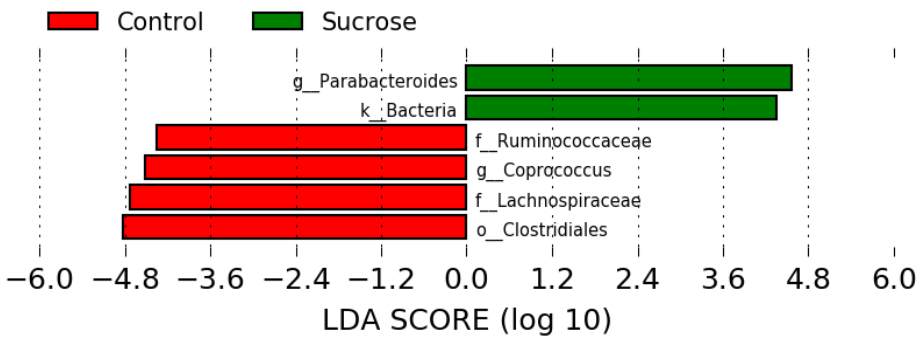

B

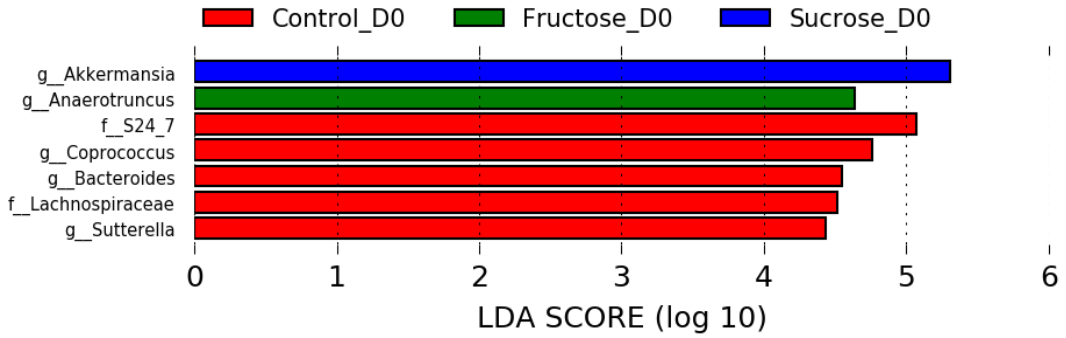

C

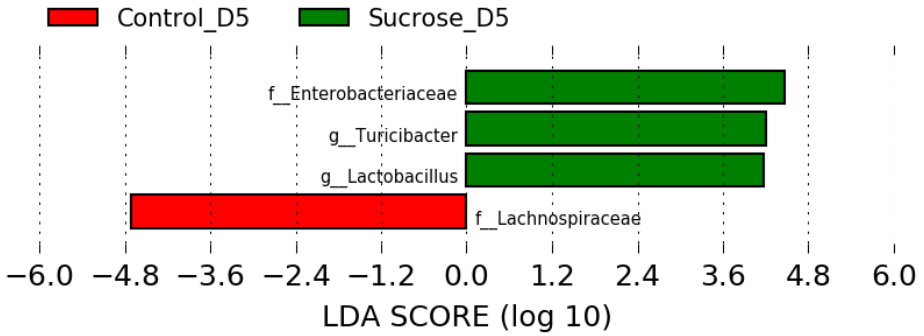

Figure 3.23. LEfSe plot of (A) cecum contents, (B) stool at day 0, (C) stool at day 5. Differentially abundant bacteria in the treatment groups were identified. The p-value from a Kruskal-Wallis test between treatment groups needed to be less than 0.05, and the logarithmic linear discriminant analysis (LDA) score needed to be greater than 2.0. The less strict (one-against-all) multi-class strategy was chosen.

3.3.11. Effect of high sugar diets on the concentration of short-chain fatty acids (SCFAs) in stool

Log2 fold changes in the concentration of SCFAs in the stool was determined during the diet pre-treatment period between day -2 and day 0 (D-2D0), and during the DSS treatment period between day 0 and 5 (D0D5) (Figure 3.24). During the diet pre-treatment period, acetic acid was significantly decreased in HG-fed mice relative to controls (HG: $p=0.024$, HF: $p=0.063$, HS: $p=0.050$). Propionic acid was not significantly different between treatment groups. Butyric acid was decreased in HG and HS-fed mice relative to controls (HG: $p=0.008$, HS: $p=0.013$, HF: $p=0.064$). Isovaleric acid was decreased in controls relative to the other treatments ($p<0.0001$ for all). Isovaleric acid was increased in HF-fed mice compared to the other treatment groups ($p<0.0001$ for all). During the DSS treatment period, acetic acid increased in the stool of HG ($p=0.017$) and HS-fed mice (0.016). Acetic acid increased in HS-fed mice relative to controls ($p=0.031$). Propionic acid increased in HS-fed mice relative to the diet pre-treatment period ($p=0.023$). Butyric acid increased in the stool of HG ($p=0.0001$), HF ($p=0.001$), and HS-fed mice ($p=0.0002$) relative to controls. Within treatment groups, there was an increase in butyric acid in HG ($p=0.012$) and HS-fed mice ($p=0.027$), and a decrease in control mice ($p=0.023$).

Figure 3.25 shows log2 fold changes in the proportion of SCFAs in stool during the D-2D0 and D0D5 time periods. There were no significant differences in the proportions of acetic acid or propionic acid between the treatment groups or time periods. During the D-2D0 period, the proportion of butyric acid was decreased in HG ($p=0.024$) and HS-fed mice ($p=0.020$) relative to controls. The proportion of isovaleric acid was decreased in the stool of control mice relative to HG, HF and HS-fed mice ($p<0.0001$ for all). The proportion of isovaleric acid was increased in HF-fed mice relative to the other treatment groups ($p<0.0001$ for all). During the D0D5 time period, the proportion of butyric acid increased in the stool of HG ($p=0.0006$), HF ($p=0.002$), and HS-fed mice ($p=0.002$) relative to controls. Within treatment groups, there was an increase in the proportion of butyric acid in HG ($p=0.044$) and decrease in control mice ($p=0.024$). There were no significant differences in the proportion of isovaleric acid during the D0D5 period.

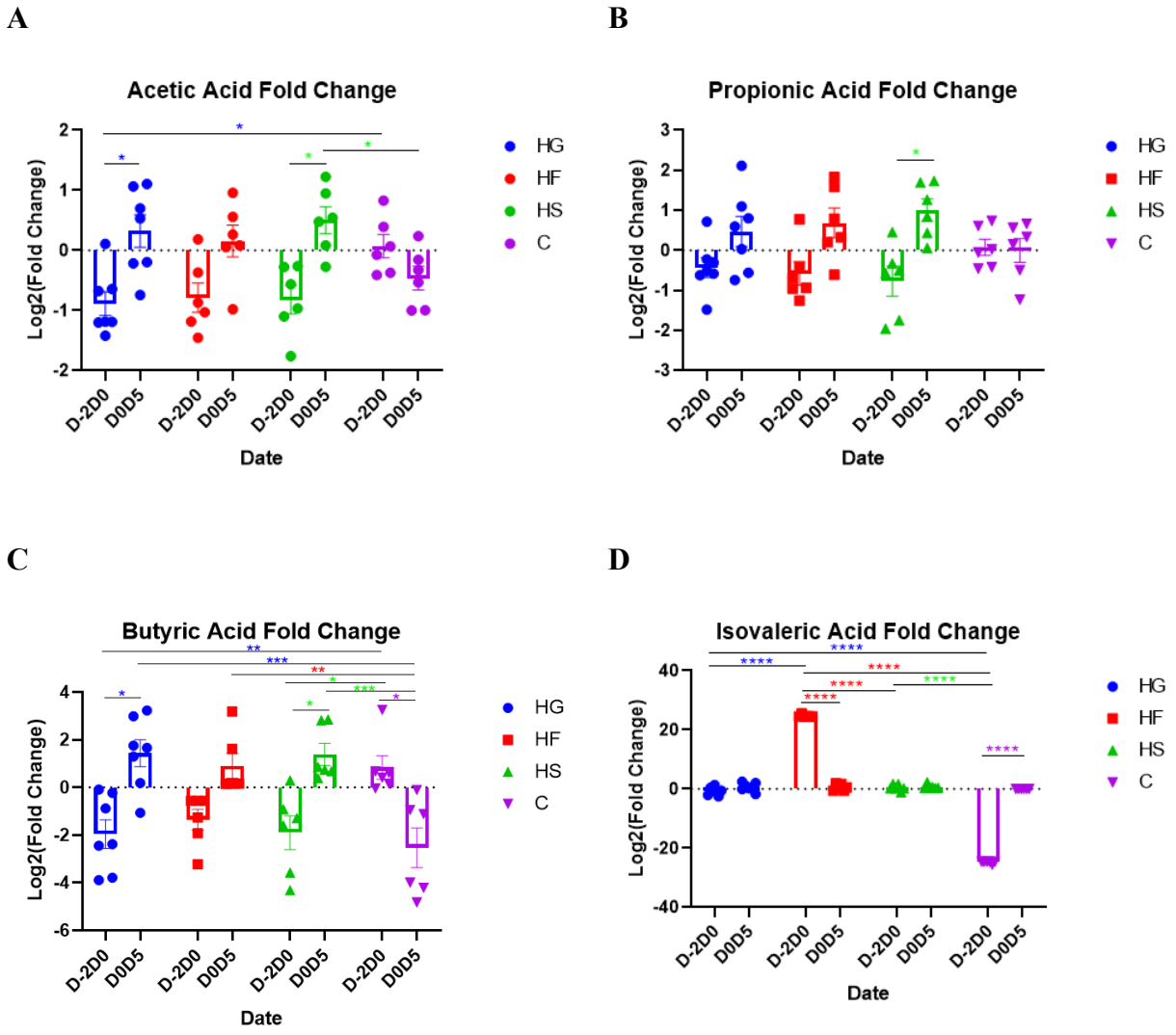

Figure 3.24. Effect of high sugar diets on the concentration of (A) acetic acid, (B) propionic acid, (C) butyric acid, and (D) isovaleric acid in stool. Blue = high glucose diet (HG). Red = high fructose diet (HF). Green = high sucrose diet (HS). Purple = control diet (C). n=7 for HG and n=6 for HF, HS, and C. Log2 fold changes were determined between day -2 and day 0 (D-2D0), and between day 0 and day 5 (D0D5). Each data point represents a single measurement. Data are presented as mean ± SEM. Statistical significance was determined with two-way ANOVA and Tukey's multiple comparisons test between treatments at each time period. Bonferroni's multiple comparisons test was used to determine statistical significance between time periods within treatment groups. * $p<0.05$, ** $p<0.01$, *** $p<0.001$, **** $p<0.0001$.

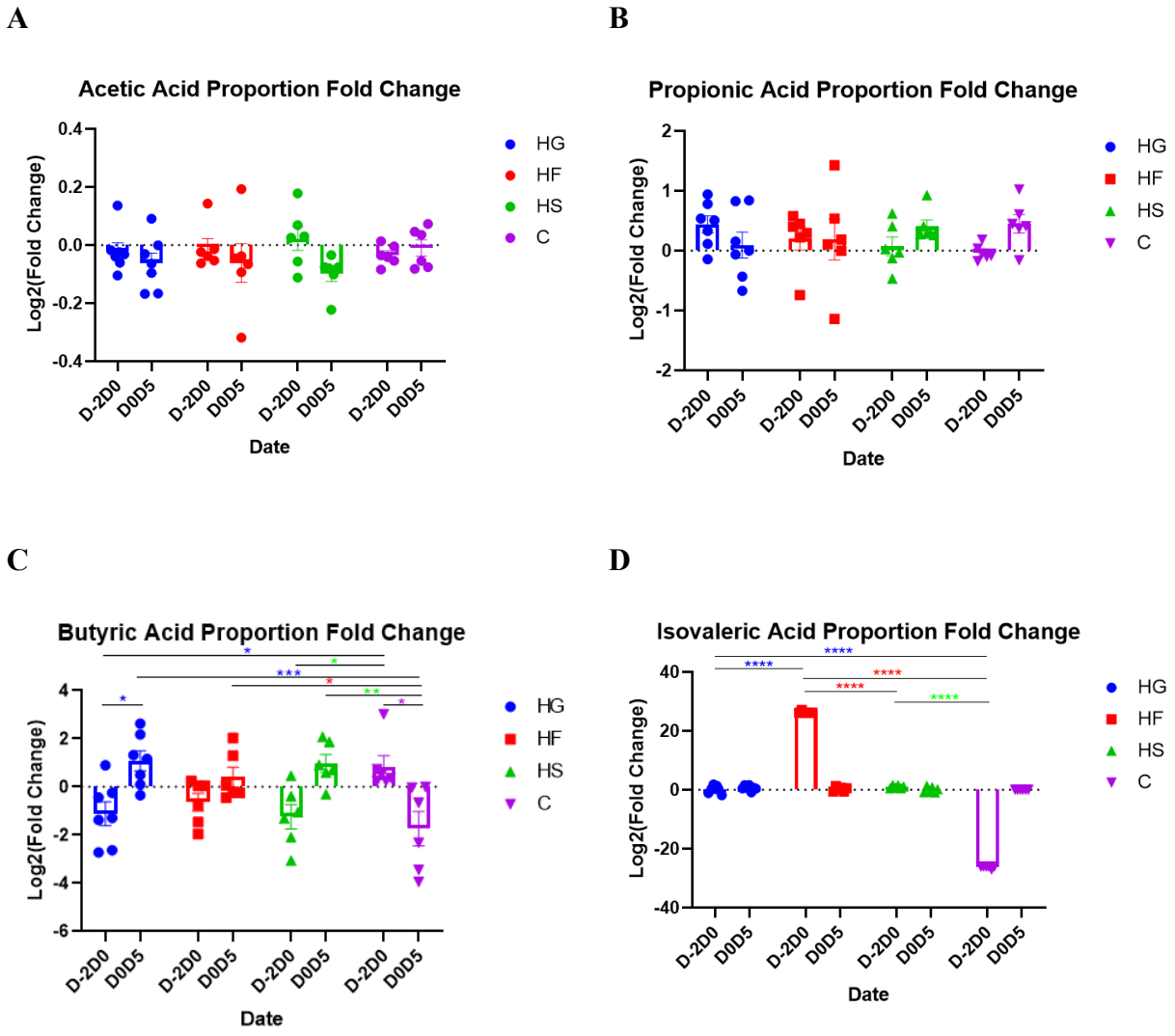

Figure 3.25. Effect of high sugar diets on the proportion of (A) acetic acid, (B) propionic acid, (C) butyric acid, and (D) isovaleric acid in stool. Blue = high glucose diet (HG). Red = high fructose diet (HF). Green = high sucrose diet (HS). Purple = control diet (C). n=7 for HG and n=6 for HF, HS, and C. Log2 fold changes were determined between day -2 and day 0 (D-2D0), and between day 0 and day 5 (D0D5). Each data point represents a single measurement. Data are presented as mean ± SEM. Statistical significance was determined with two-way ANOVA and Tukey's multiple comparisons test between treatments at each time period. Bonferroni's multiple comparisons test was used to determine statistical significance between time periods within treatment groups. * $p<0.05$, ** $p<0.01$, *** $p<0.001$, **** $p<0.0001$.

3.3.12. Associations between clinical parameters, SCFAs, and bacterial abundance

A heatmap was constructed using Metaboanalyst 4.0 with the AUC of DAI scores between days 0-5 and 5-9, log2 fold changes in the concentration and proportions of SCFAs, and log2 fold changes in the relative abundance of bacteria in cecum and stool samples. The top 25 significant features are shown in Figure 3.26. The DAI scores between days 0-5 and 5-9 were lower in controls than in the high sugar diet groups. During the diet pre-treatment period (day -2 to 0), controls had more positive fold changes in the abundance of *S24-7*, concentration of butyric acid, acetic acid, and propionic acid, and proportion of butyric acid and propionic acid. Controls had more negative fold changes in the abundance of *Enterobacteriaceae*, and concentration and the proportion of isovaleric acid. During the DSS treatment period, controls had more positive fold changes in the abundance of *Lachnospiraceae*. Control mice had more negative fold changes in the concentration of acetic acid, propionic acid and butyric acid, and proportion of butyric acid. Control mice also tended to have more negative fold changes in the abundance of *Enterobacteriaceae* and *Akkermansia* in cecum contents.

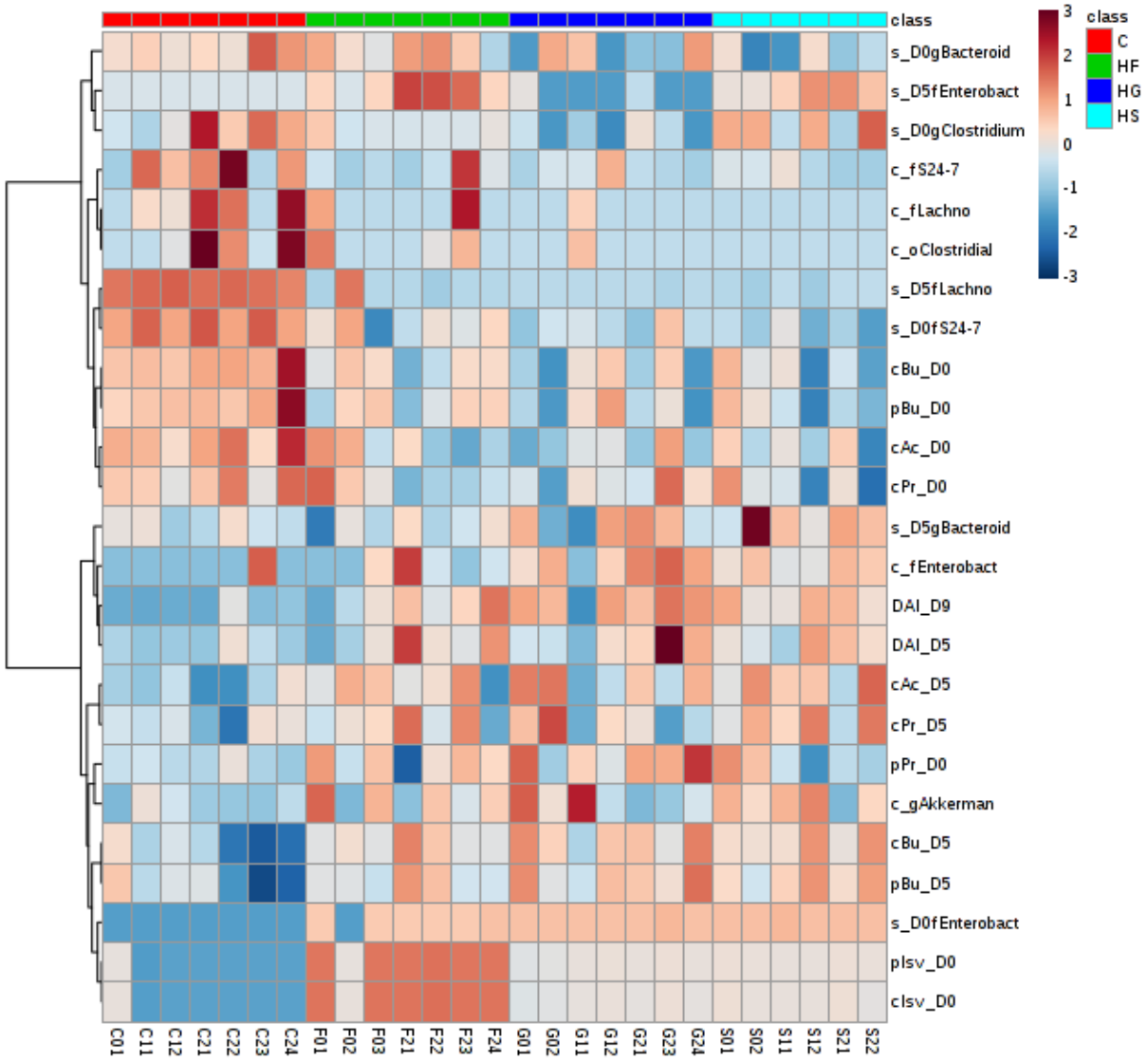

Figure 3.26. Heatmap containing Disease Activity Index (DAI) scores, log2 fold changes in SCFA concentrations and proportions, and log2 fold changes in the relative abundance of bacteria in cecum and stool. The top 25 significant features are shown. Pearson distance measure and Ward clustering algorithm were used. The heatmap was constructed using Metaboanalyst 4.0. DAI_D5 = AUC of DAI between days 0-5, DAI_D9 = AUC of DAI between days 5-9, prop = proportion, conc = concentration, D0 = day -2 to 0, D5 = day 0 to 5, Ac = acetic acid, Pr = propionic acid, Bu = butyric acid, Isv = isovaleric acid, c_ = cecum, s_ = stool, gBacteroid = genus *Bacteroides*, fEnterobact = family *Enterobacteriaceae*, fLachno = family *Lachnospiraceae*, f24-7 = family *S24-7*, oClostridial = order *Clostridiales*, gClostridium = genus *Clostridium*.

3.3.13. Correlations between fold changes in SCFAs, fold changes in relative abundance of bacteria, and susceptibility to DSS-induced colitis

Correlations between fold changes in SCFAs and the relative abundance of bacteria were determined between days -2 to 0 (Table 3.5) and between days 0 and 5 (Table 3.7). Correlations between the relative abundance of bacteria were also determined (Tables 3.6 and 3.8).

During the diet pre-treatment period (day -2 to 0), the fold change in *S24-7* abundance was positively correlated with fold changes in acetic acid concentration ($p=0.0001$), propionic acid concentration ($p=0.003$), butyric acid concentration ($p<0.0001$) and butyric acid proportion ($p=0.004$) (Table 3.5). Fold changes in *S24-7* abundance were negatively correlated with fold changes in isovaleric acid concentration ($p=0.046$) and proportion ($p=0.011$). *Lachnospiraceae* was negatively correlated with the proportion of isovaleric acid ($p=0.012$). *Clostridiales* had a positive correlation with acetic acid ($p=0.034$). *Enterobacteriaceae* was negatively correlated with acetic acid concentration ($p=0.028$), butyric acid concentration ($p=0.001$), and butyric acid proportion ($p=0.004$). *Enterobacteriaceae* was positively correlated with the proportion of isovaleric acid ($p=0.019$). *Akkermansia* had a negative correlation with the concentration of acetic acid ($p=0.007$), propionic acid ($p=0.014$) and butyric acid ($p=0.050$). *Enterobacteriaceae* was significantly negatively correlated with *Bacteroides* ($p=0.005$) and *S24-7* ($p=5.84 \times 10^{-5}$), and positively correlated with *Akkermansia* ($p=0.025$) (Table 3.6). *Akkermansia* was negatively correlated with *S24-7* ($p=0.004$), *Clostridiales* ($p=0.030$) and *Lachnospiraceae* ($p=0.013$).

During the DSS treatment period between day 0 and 5, *Lachnospiraceae* was negatively correlated with the concentration of butyric acid ($p=0.033$) (Table 3.7). *Akkermansia* was negatively correlated with the concentration and proportion of butyric acid ($p=0.007$ and 0.027 respectively). *Akkermansia* was negatively correlated with *Bacteroides* ($p=0.005$) and *S24-7* (5.92×10^{-6}) (Table 3.8).

Correlations were determined between the AUC of DAI scores between days 0-5 and fold changes in the concentration of SCFAs, proportions of SCFAs (Tables 3.9) and relative abundance of bacteria (Table 3.10) between day 0 and day 5. The DAI between days 0-5 was positively correlated with fold change in butyric acid concentration ($p=0.002$), butyric acid proportion ($p=0.009$), *S24-7* ($p=0.049$). The DAI between days 0-5 was negatively correlated with *Lachnospiraceae* ($p=0.016$), and *Akkermansia* ($p=0.0001$).

Table 3.5. Correlations between log2 fold changes in the concentration of SCFAs and log2 fold changes in the relative abundance of bacteria between days -2 and 0. Each cell contains the Spearman rank correlation and the p-value below. Significant correlations with a p-value of less than 0.05 are bolded.

	Log2 Fold Change in Concentration				Log2 Fold Change in Proportion			
	Acetic Acid	Propionic Acid	Butyric Acid	Isovaleric Acid	Acetic Acid	Propionic Acid	Butyric Acid	Isovaleric Acid
g_Bacteroides	0.122 0.545	0.096 0.633	0.063 0.754	-0.099 0.622	0.091 0.651	-0.282 0.993	0.002 0.993	-0.139 0.489
f_S24-7	**0.673** **0.0001**	**0.549** **0.003**	**0.745** **<0.0001**	**-0.387** **0.046**	-0.123 0.541	-0.240 0.227	**0.536** **0.004**	**-0.480** **0.011**
f_Lachnospiraceae	0.144 0.474	0.232 0.244	0.269 0.175	-0.370 0.057	-0.117 0.561	-0.063 0.754	0.234 0.241	**-0.475** **0.012**
o_Clostridiales	**0.409** **0.034**	0.173 0.388	0.264 0.184	0.129 0.521	0.036 0.857	-0.184 0.358	0.244 0.220	0.090 0.656
f_Enterobacteriaceae	**-0.423** **0.028**	-0.335 0.088	**-0.598** **0.001**	0.364 0.062	0.053 0.795	0.266 0.180	**-0.532** **0.004**	**0.448** **0.019**
g_Akkermansia	**-0.507** **0.007**	**-0.469** **0.014**	**-0.382** **0.050**	0.123 0.542	0.095 0.638	0.066 0.745	-0.212 0.288	0.198 0.322

Table 3.6. Correlations between the relative abundance of bacteria in stool between days -2 and 0. Each cell contains the Spearman rank correlation and the p-value below. Significant correlations with a p-value of less than 0.05 are bolded.

	g_Bacteroides	f_Enterobacteriaceae	g_Akkermansia	f_S24-7	o_Clostridiales	f_Lachnospiraceae
g_Bacteroides	1.000	**-0.526** **0.005**	-0.322 0.102	**0.408** **0.035**	-0.092 0.648	0.105 0.603
f_Enterobacteriaceae	**-0.526** **0.005**	1.000	**0.430** **0.025**	**-0.695** **5.84×10^{-5}**	-0.013 0.947	-0.358 0.067
g_Akkermansia	-0.322 0.102	**0.430** **0.025**	1.000	**-0.540** **0.004**	**-0.419** **0.030**	**-0.473** **0.013**
f_S24-7	**0.408** **0.035**	**-0.695** **5.84×10^{-5}**	**-0.540** **0.004**	1.000	0.180 0.369	0.255 0.200
o_Clostridiales	-0.092 0.648	-0.013 0.947	**-0.419** **0.030**	0.180 0.369	1.000	0.304 0.123
f_Lachnospiraceae	0.105 0.603	-0.358 0.067	**-0.473** **0.013**	0.255 0.200	0.304 0.123	1.000

Table 3.7. Correlations between log2 fold changes in the concentration of SCFAs and log2 fold changes in the relative abundance of bacteria between days 0 and 5. Each cell contains the Spearman rank correlation and the p-value below. Significant correlations with a p-value of less than 0.05 are bolded.

	Log2 Fold Change in Concentration				Log2 Fold Change in Proportion			
	Acetic Acid	Propionic Acid	Butyric Acid	Isovaleric Acid	Acetic Acid	Propionic Acid	Butyric Acid	Isovaleric Acid
g_Bacteroides	0.093 0.643	0.162 0.418	0.362 0.063	0.082 0.685	-0.114 0.572	-0.069 0.732	0.300 0.128	-0.229 0.252
f_S24-7	-0.082 0.685	-0.109 0.589	0.081 0.687	-0.095 0.638	0.136 0.499	-0.167 0.406	-0.024 0.904	-0.140 0.485
f_Lachnospiraceae	-0.357 0.068	-0.231 0.246	**-0.412** **0.033**	-0.302 0.126	0.090 0.656	0.172 0.392	-0.346 0.077	-0.209 0.295
o_Clostridiales	-0.126 0.104	-0.083 0.316	0.004 0.923	0.054 0.915	0.071 0.715	0.132 1.000	-0.052 0.696	0.107 0.115
f_Enterobacteriaceae	0.229 0.250	0.358 0.067	0.171 0.394	0.294 0.136	-0.306 0.120	0.149 0.459	0.173 0.387	-0.040 0.844
g_Akkermansia	-0.239 0.229	-0.159 0.429	**-0.508** **0.007**	-0.091 0.651	0.179 0.371	0.178 0.375	**-0.426** **0.027**	0.163 0.418

Table 3.8. Correlations between the relative abundance of bacteria in stool between days 0 and 5. Each cell contains the Spearman rank correlation and the p-value below. Significant correlations with a p-value of less than 0.05 are bolded.

	g_Bacteroides	f_Enterobacteriaceae	g_Akkermansia	f_S24-7	o_Clostridiales	f_Lachnospiraceae
g_Bacteroides	1.000	0.081 0.689	**-0.528** **0.005**	0.333 0.090	0.208 0.298	-0.022 0.914
f_Enterobacteriaceae	0.081 0.689	1.000	-0.357 0.067	0.103 0.609	-0.011 0.957	-0.378 0.052
g_Akkermansia	**-0.528** **0.005**	-0.357 0.067	1.000	**-0.753** **5.92×10^{-6}**	-0.183 0.361	0.288 0.145
f_S24-7	0.333 0.090	0.103 0.609	**-0.753** **5.92×10^{-6}**	1.000	0.163 0.415	-0.035 0.863
o_Clostridiales	0.208 0.298	-0.011 0.957	-0.183 0.361	0.163 0.415	1.000	0.332 0.091
f_Lachnospiraceae	-0.022 0.914	-0.378 0.052	0.288 0.145	-0.035 0.863	0.332 0.091	1.000

Table 3.9. Correlations between the area under the curve of disease activity index (DAI) scores between days 0-5, and log2 fold changes in the concentration or proportions of SCFAs between days 0-5.

	Log2 Fold Change in Concentration		Log2 Fold Change in Proportion	
	Spearman rank correlation	p-value	Spearman rank correlation	p-value
Acetic Acid	0.146	0.468	-0.099	0.622
Propionic Acid	0.084	0.678	-0.178	0.375
Butyric Acid	**0.560**	**0.002**	**0.493**	**0.009**
Isovaleric Acid	0.104	0.605	0.062	0.759

Table 3.10. Correlations between the area under the curve of disease activity index (DAI) scores between days 0-5, and log2 fold changes in the relative abundance of bacteria between days 0-5.

	Spearman rank correlation	p-value
g_Bacteroides	0.517	0.006
f_S24-7	**0.383**	**0.049**
f_Lachnospiraceae	**-0.459**	**0.016**
o_Clostridiales	-0.109	0.589
f_Enterobacteriaceae	0.216	0.280
g_Akkermansia	**-0.680**	**0.0001**

3.3.14. Correlations between relative abundance of bacteria in cecum, susceptibility to DSS-induced colitis, and colonic cytokines and chemokines

Table 3.11 shows correlations between AUC of DAI between days 5-9 and the relative abundance of bacteria in cecum contents. The DAI score was positively correlated with *Bacteroides* (p=0.021) and *Enterobacteriaceae* (p=0.0003), and negatively correlated with *Clostridiales* (p=0.001) and *Lachnospiraceae* (p= 0.001). *Bacteroides* and *Enterobacteriaceae* are significantly positively correlated with IFN-γ, IL-12, IL-10, IL-1β, IL-6 and KC in the colon (*Bacteroides*: p=0.017, 0.004, 0.012, 0.016, 0.027, 0.018; *Enterobacteriaceae*: p=0.009, 0.008, 0.004, 0.003, 0.002, 0.002) (Table 3.12). *Clostridiales* and *Lachnospiraceae* are significantly negatively correlated with IL-1β, IL-6 and KC (*Clostridiales*: p=0.002, 0.008, 0.002; *Lachnospiraceae*: 0.004, 0.009, 0.005). *Lachnospiraceae* are also negatively correlated with IFN-γ (p=0.042).

Enterobacteriaceae was significantly negatively correlated with *S24-7* (p=0.009), *Lachnospiraceae* ($p=7.53 \times 10^{-5}$) and *Clostridiales* (p=0.003) (Table 3.13).

Table 3.11. Correlations between the area under the curve of disease activity index (DAI) scores between days 5-9 and the relative abundance of bacteria in cecum contents.

	Spearman rank correlation	p-value
g_Bacteroides	**0.443**	**0.021**
f_S24-7	-0.238	0.233
f_Lachnospiraceae	**-0.592**	**0.001**
o_Clostridiales	**-0.614**	**0.001**
f_Enterobacteriaceae	**0.644**	**0.0003**
g_Akkermansia	0.039	0.848

Table 3.12. Correlations between colonic cytokines and chemokines, and the relative abundance of bacteria in cecum contents. Each cell contains the Spearman rank correlation and the p-value below. Significant correlations with a p-value of less than 0.05 are bolded.

	IFN-gamma	IL-12	IL-10	IL-1beta	IL-6	KC
g_Bacteroides	**0.454** **0.017**	**0.535** **0.004**	**0.475** **0.012**	**0.458** **0.016**	**0.424** **0.027**	**0.453** **0.018**
f_Enterobacteriaceae	**0.494** **0.009**	**0.500** **0.008**	**0.542** **0.004**	**0.548** **0.003**	**0.560** **0.002**	**0.565** **0.002**
g_Akkermansia	0.086 0.670	0.117 0.562	0.022 0.912	0.264 0.183	0.208 0.299	0.211 0.292
f_S24-7	-0.264 0.183	-0.303 0.125	-0.340 0.083	-0.294 0.136	-0.369 0.058	-0.323 0.100
o_Clostridiales	-0.379 0.051	-0.335 0.088	-0.360 0.065	**-0.572** **0.002**	**-0.501** **0.008**	**-0.560** **0.002**
f_Lachnospiraceae	**-0.395** **0.042**	-0.361 0.065	-0.374 0.054	**-0.533** **0.004**	**-0.493** **0.009**	**-0.529** **0.005**

Table 3.13. Correlations between the relative abundance of bacteria in cecum contents. Each cell contains the Spearman rank correlation and the p-value below. Significant correlations with a p-value of less than 0.05 are bolded.

	g_Bacteroides	f_Enterobacteriaceae	g_Akkermansia	f_S24-7	o_Clostridiales	f_Lachnospiraceae
g_Bacteroides	1.000	**0.569** **0.002**	-0.034 0.867	-0.076 0.706	-0.357 0.067	**-0.401** **0.038**
f_Enterobacteriaceae	**0.569** **0.002**	1.000	-0.173 0.387	**-0.495** **0.009**	**-0.553** **0.003**	**-0.687** **7.53×10^{-5}**
g_Akkermansia	-0.034 0.867	-0.173 0.387	1.000	0.188 0.349	0.036 0.857	0.037 0.854
f_S24-7	-0.076 0.706	**-0.495** **0.009**	0.188 0.349	1.000	**0.506** **0.007**	**0.669** **0.0001**
o_Clostridiales	-0.357 0.067	**-0.553** **0.003**	0.036 0.857	**0.506** **0.007**	1.000	**0.840** **4.22×10^{-8}**
f_Lachnospiraceae	**-0.401** **0.038**	**-0.687** **7.53×10^{-5}**	0.037 0.854	**0.669** **0.0001**	**0.840** **4.22×10^{-8}**	1.000

3.4. Discussion

Short-term consumption of high glucose, high fructose, and high sucrose diets increased susceptibility to DSS-induced colitis compared to chow diets. Disease severity did not differ between the high sugar diet treatments. After two days on the high sugar diets, mice experienced a reduction in microbial diversity, altered microbial composition involving a decrease in SCFA-producing bacteria and an increase in *Enterobacteriaceae*, and reduced butyrate levels. The reduced butyrate levels may have contributed to the increased colitis severity observed during the DSS treatment period. The inflammatory environment in the colon may have reduced the ability of colonocytes from high sugar diet-fed mice to utilize butyrate, and further exacerbated colitis. During recovery from colitis, the reduced butyrate levels may have impacted repair processes and led to higher histology scores, MARCO expression in the liver, and pro-inflammatory cytokines in the colon.

High sugar diet-fed mice had reduced microbial diversity during the diet pre-treatment period. The microbiota from HG and HF-fed mice had lower evenness, indicating that the microbial composition may be less evenly distributed compared to prior to the diet treatment. The Shannon diversity index takes into account both evenness and richness [143]. The decreased Shannon diversity seen with HG and HS seemed to be driven by the decrease in richness or number of unique species identified in the stool samples. Prior to changing the diet, all groups had similar microbial composition. However, after two days on the diet, *Lachnospiraceae* and *S24-7* were more abundant in control mice, and *Enterobacteriaceae* was increased in sugar diet groups. *Lachnospiraceae* is a family within the *Firmicutes* phylum that contains butyrate-producing members such as *Eubacterium rectale* and *Roseburia spp* [144]. Members of the *S24-7* family have not been cultured, but genomic analysis reveals that *S24-7* have enzymes to degrade complex carbohydrates such as hemicellulose and pectin [145].

The microbial changes may have contributed to the decrease in acetic acid seen in HG-fed mice and the decrease in butyric acid in HG and HS-fed mice. Despite consuming the same fiber content, the microbial composition may have varied among the HG, HF, and HS-fed mice due to the sugar content of the diets. Some of the sugars may have spilled over into the cecum or colon due to the high concentration present in the diet. The presence of glucose or fructose may have influenced the microbial composition, leading to the differences observed with SCFAs.

This would need to be investigated further by measuring the concentration of sugars in the cecal or gut contents.

Two-day exposure to high sucrose diets in mice was previously found to result in a decrease in total cecal SCFAs, and specifically acetate [63]. A decrease in the concentration of SCFA was also found with the consumption of a Western diet by mice for 18 weeks [39]. Agus et al. (2016) suggest that the reduced SCFA levels may have been due to the reduced fiber content of Western diets and might have contributed to the greater inflammatory response seen with DSS. A decrease in the expression of the receptor for SCFAs GPR43 was also observed by Agus et al. (2016). Administration of a GPR43 agonist lead to less severe colitis and a lower concentration of KC and IL-6 compared to mice not treated with an agonist. The reduced SCFA levels may have led to a lack of GPR43 activation and increased susceptibility to colitis [39].

In our study, the fiber percentage was not reduced but the source of fibers was altered. The control diets contained hemicellulose, cellulose, lignins and pectins [136], whereas the high sugar diets contained cellulose as the only source of fiber. The fiber consumed by the mice may have contributed to the changes in microbial composition and production of SCFAs. The decrease in S24-7 seen with the high sugar diets may have occurred due to a lack of hemicellulose and pectin [145]. The presence of fibers such as pectin in the control diet may have promoted higher SCFA production. Peng et al. (2013) found that mice had greater amounts of acetic acid and butyric acid in the intestinal contents after consumption of a 6% pectin diet compared to a 6% cellulose diet [146].

HG and HS-fed mice experienced a significant decrease in butyric acid levels, and this trended towards significance in HF-fed mice. Reduced butyric acid levels may have contributed to increased disease susceptibility as it is used as an energy source by enterocytes, promotes gut barrier integrity and an anti-inflammatory environment [18-21]. Butyrate promotes gut barrier integrity by upregulating the expression of tight junction proteins such as ZO-1 and claudin, and MUC2 [18-20]. Butyrate would also prevent an excessive inflammatory response by stimulating the production of IL-10 and regulatory T cells [18,21]. The control fed-mice may have had protection against DSS-induced colitis due to having higher butyrate levels. Reduced butyric acid levels may have also contributed to the increase in *Enterobacteriaceae* seen with high sugar diet-fed mice. In the controls, the higher levels of butyrate would have resulted in activation of

the peroxisome proliferator-activated receptor-γ (PPARγ) on enterocytes and increased consumption of oxygen [56-57,147]. The hypoxic environment would have limited the growth of the facultative anaerobic *Enterobacteriaceae* [147].

Control diet-fed mice experienced a decrease in isovaleric acid, but this was not observed in mice on high sugar diets. Isovaleric acid is produced from the fermentation of proteins by intestinal bacteria [148]. Other products of proteolytic fermentation, including ammonia and sulfides, are associated with UC. Increased exposure to sulfides is associated with impaired butyrate oxidation by colonocytes [149]. The reduced proteolytic fermentation experienced by controls may have been protective against DSS-induced colitis.

During the DSS treatment period, *Lachnospiraceae* was more abundant in controls but a decrease in butyric acid concentration was found. The decrease may have reflected increased butyrate utilization by controls during DSS-induced colitis. Colonic mucosal tissue from patients with UC has reduced the ability to oxidize butyrate [149]. There is a decrease in the expression of genes that participate in the uptake and oxidation of butyrate, such as MCT1 [16,150]. Inflammation has been found to decrease butyrate uptake by colonocytes [16,150]. When HT-29 human colon epithelial cells were exposed to IFN-γ and TNF-α, there was a downregulation in the mRNA for MCT1 [151]. The high sugar diet-fed mice may have experienced more inflammation, as suggested by the higher DAI score at day 5. Ahmad et al. (2000) saw changes in histology prior to impairment in butyrate oxidation, supporting the idea that inflammation contributes to impaired butyrate oxidation. The impaired butyrate oxidation could, in turn, exacerbate colitis further. Enterocytes would have to rely on the oxidation of glucose, which does not provide as much energy as butyrate [151]. The reduced utilization of butyrate would lead to loss of energy and impaired gut barrier integrity.

Having higher amounts of butyrate present during DSS-induced colitis may reduce the inflammation experienced and allow continued butyrate absorption. Vieira et al. (2012) provided mice with a 0.5% sodium butyrate diet or a control diet for 15 days [152]. Some mice were given the sodium butyrate diet or control diet for 7 days, and also 2.5% DSS through drinking water for an additional 7 days. Mice that consumed the 0.5% sodium butyrate diet without exposure to DSS had increased cecal butyrate levels. Mice that consumed a sodium butyrate diet with DSS had improved stool consistency, less histological damage and less neutrophil and eosinophil

infiltration in the colon compared to mice on a control diet with DSS. The cecal butyrate concentration was similar among mice given DSS while on a control diet, and mice given DSS while on the 0.5% sodium butyrate diet. Vieira et al. (2012) proposed that the butyrate might have been absorbed by colonocytes, leading to an improvement in DSS-induced colitis [152]. Studies in which a butyrate enema was administered with DSS showed improvement in clinical scores, smaller weight changes, longer colon lengths, lower histological scores, decreased pro-inflammatory cytokines in the colon, and decreased the infiltration of neutrophils in the colon [153-154]. In control mice, the presence of high levels of butyrate during DSS treatment may have reduced inflammation and promoted butyrate oxidation and protection against colitis. However, a recent study by Singh et al. (2019) found that high levels of butyrate exacerbated colitis [155]. Mice were fed diets containing cellulose, inulin or pectin and administered an antibody for an IL-10 receptor after 3 days. Inulin-fed mice experienced worse colitis compared to pectin-fed mice. The increased disease severity was associated with higher cecal butyrate levels and greater abundance of butyrate-producing bacteria. An improvement was seen with inulin-fed mice when butyrate production was inhibited with metronidazole or hops β-acids [155]. In cases of mucosal injury, intestinal epithelial stem cells may be exposed to butyrate due to the lack of uptake by colonocytes located towards lumen [156]. Butyrate was found to inhibit mucosal repair by preventing the proliferation of the intestinal epithelial stem cells [156]. Thus, it appears that butyrate levels need to be balanced as having either a surplus or a deficit may exacerbate colitis in mice.

The higher DAI scores, histological scores, MARCO expression in the liver, and concentration of cytokines and chemokines in the colon after 4 days of recovery from DSS indicates that the high sugar diet-fed mice have delayed the repair. Delayed repair may lead to greater intestinal permeability in high sugar diet-fed mice compared to controls. This is supported by the increased MARCO expression in the liver of HG-fed mice since MARCO expression has been found to be induced after exposure to bacteria or LPS [137-138]. IBD has been characterized as a Th17 response involving high concentrations of IL-1β and IL-6 [157]. Acute DSS-induced colitis is also primarily a Th1-Th17 response with an increase in IL-6, KC and IL-1β [158-159]. During the resolution of DSS-induced colitis, a reduction in all pro-inflammatory cytokines was expected [97], but this was not seen for mice on the high sugar diets. IL-10 is a cytokine that promotes barrier function, and thus, elevated levels may be an

indication of delayed repair processes taking place at day 9 with the high sugar diet-fed mice [160].

A significant reduction in food and water intake was observed during the recovery period for HG-fed mice. Reduced food and water intake are an indication of more severe disease and inflammation [161-162]. Moreau et al. (2003) gave rats a basal diet with 50 g/L of DSS in drinking water for 7 days [162]. Rats were then given basal diet, or a diet consisting of short-chain fructo-oligosaccharides (FOS) or type 3 resistant starch (RS) for an additional 7-14 days with a lower concentration of DSS (30 g/L). Rats that consumed the FOS diet had reduced food intake and greater weight loss compared to rats on the basal diet. On day 14, FOS had shorter colon length, greater colon weight and higher colitis severity score [162]. Similarly, we found significantly greater colon weight to length ratio with HG-fed mice compared to controls, and specifically a shorter colon length. The HG-fed mice may have more severe inflammation, but this did not appear to lead to a significantly greater DAI score.

Diet-induced changes in the microbial community of the cecum might have impacted recovery. SCFAs produced in the cecum may be absorbed in the colon [163-164]. The contribution of the cecum to colitis is shown in a study by Brown et al. (2017) [165]. They had a group of sham surgery mice and another group of mice with their cecum removed. The mice lacking a cecum had less fecal SCFAs, and a colonic microbiota with reduced diversity in terms of richness and evenness. They had a decrease in *Lachnospiraceae* and *Ruminococcaceae* and an increase in *Enterobacteriaceae* in the colon. After 7 days of exposure to *Citrobacter rodentium*, cecectomized mice had greater concentrations of IFN-γ, TNF-α, and IL-10 in the proximal colon and greater IFN-γ in the distal colon compared to sham surgery mice. The mice also experienced greater weight loss than sham surgery mice after 13 days [165]. The findings show that the bacterial community in the cecum can influence the production of SCFAs. The absorption of cecal SCFAs by colonocytes can also influence the inflammatory environment in the colon and recovery processes.

The high sugar diets caused a reduction in SCFA-producing bacteria such as *S24-7*, *Clostridiales*, and *Lachnospiraceae* in cecum contents. The low amounts of SCFA-producing bacteria may have been due to the fiber content present in the high sugar diets compared to the control diet. Control mice would have benefited from having a greater production of SCFAs such

as butyrate in the cecum. Absorption of cecal SCFAs in the colon would stimulate proliferation of colonocytes, improvement in gut barrier integrity, and a reduction in pro-inflammatory cytokines through the production of regulatory T cells [18-21,163]. The control mice may have had a lower DAI on day 9 as a result of having more SCFA-producing bacteria in the cecum.

Higher levels of *Enterobacteriaceae* and *Akkermansia* were observed in the cecal contents of mice on the high sugar diets. It is known that endogenous microbes that thrive in the hostile inflamed gut are those with abilities to survive antimicrobial stress and persist in the oxidative environment [166]. Overall, the evidence shows that inflammation depletes commensal anaerobes and production of butyrate leading to increased epithelial oxygenation that potentiates pathogen colonization and dysbiosis [167]. *Enterobacteriaceae* may have increased in the cecum of high sugar diet-fed mice due to a lack of production of butyrate by SCFA-producing bacteria such as *Lachnospiraceae*. Butyrate levels were not measured in the cecum, but may have been lower in the high sugar diet-fed mice. Lack of PPAR-γ activation may have led to an increase in oxygen in the cecum and growth of *Enterobacteriaceae* [56-57,147]. The lack of easily fermentable fibers in the high sugar diets may have resulted in the increased *Akkermansia* seen. Desai et al. (2016) found that when a fiber-free diet was given to gnotobiotic mice with a human gut microbiome, there was an increase in *Akkermansia* in the cecum and stool [168]. *Akkermansia* consumed mucin O-glycans, causing a smaller mucus layer and less protection against *C.rodentium*-induced colitis. They also found a decrease in SCFA-producing bacteria such as *E.rectale* and *Bacteroides ovatus* [168]. In our study, the high sugar diets were not fiber-free but contained cellulose as the only fiber type. Cellulose is not as easily fermented as other fibers such as pectin [169]. Van den Abbeele et al. (2011) provided rats with a control diet consisting of cellulose as the only fiber type, or a diet with additional inulin or long-chain arabinoxylan [170]. The rats on the control diet had more *Akkermansia muciniphila* in the cecum than rats on the other diets. The finding shows that the bacterial community present in the cecum is more reliant on mucus with the consumption of a low fiber diet or when easily fermentable fibers are lacking [170].

3.5. Conclusions

Mice on all the high sugar diets showed generally similar results in terms of increased susceptibility to colitis. The lack of significant differences between the sugar diets suggests that the increased susceptibility may have been due to the lack of complex fiber rather than the direct effects of the sugars. The high sugar diets and control diets have similar fiber percentage, but different fiber types. The control diet had a mixture of hemicellulose, cellulose, lignin, and pectin [136] whereas the high sugar diets only had cellulose. The findings suggest that the consumption of diverse fibers may be protective against DSS-induced colitis through effects on gut microbial metabolism.

A limitation of this study was that only indirect permeability measurements were taken. Future studies may involve measurements of the lactulose/mannitol ratio, the expression of proteins involved in barrier function, or changes in mucus production after two days on the high sugar diets.

Future studies might involve the administration of exogenous butyrate, such as in the form of tributyrin, with high sugar diets during DSS. If butyrate administration leads to improvement in DSS-induced colitis, this would support the proposition that low butyrate levels increased susceptibility to colitis. Butyrate oxidation or concentrations of derivatives produced during butyrate metabolism could be measured with colon tissue from mice after 5 days of DSS. The measurements may either support or reject the idea that butyrate oxidation was impaired in high sugar diet-fed mice after 5 days of DSS.

Other differences between the high sugar diets and chow may need to be considered, such as reported differences in the amounts of vitamins, minerals, proteins and fats [171-172]. A study could be conducted with a control diet that is more similar to high sugar diets, instead of a chow diet. The control diet should have the same composition of the high sugar diets but the sugar component may be replaced with starch. The results of this study would either support or reject the idea that the fiber content impacted susceptibility to DSS-induced colitis, not the high sugar content.

Chapter 4: General Discussion, Limitations and Future Directions

4.1. General Discussion

Consumption of high sugar diets increased the severity of DSS-induced colitis and caused a lack of repair. The high sugar diets caused a decrease in butyric acid levels, but this was not seen with the consumption of chow diets and high sugar water treatments. The high sugar diets had different fiber content from chow, whereas the fiber content did not differ between the high sugar water treatments. Furthermore, the lack of significant differences between the high sugar diets suggests that the increased colitis severity are associated with the lack of diverse and easily fermentable fibers in the diet rather than the sugar content.

The association between sugars and soft drinks and IBD risk are contradictory. Some studies show no association [173-175], whereas others show an increased risk of IBD with higher consumption of sugars and soft drinks [38,176-180]. Consumption of soft drinks has also been linked to increased mortality to digestive diseases [105]. The consumption of fibers has also been found to show either no association with IBD risk [181] or decreased risk [48,182].

The findings of this thesis suggest that the consumption of diverse and easily fermentable fibers may be protective against colitis. However, mice studies show the differential effects of fibers on colitis severity. Fibers such as psyllium have been shown to reduce disease severity with continuous consumption, [183] whereas inulin was found to increase colitis severity [155]. Fiber supplementation studies conducted in humans also show either improvement in IBD symptoms or no change [184-185].

Fiber supplementation may impact disease severity through microbial composition changes and the production of metabolic products such as butyrate [186]. Specific bacteria will increase in abundance based on the chemical structure of the fiber. Bacteria containing the properties and enzymes to bind and degrade the fiber may increase in abundance [186]. For example, the supplementation of resistant starch 2 in humans has been found to increase *Ruminococcus bromii* [186-187]. However, the pre-existing microbial community in individuals can influence the effects of fiber supplementation on butyrate production [186-189]. Venkataraman et al. (2016) found that supplementation with resistant starch 2 did not lead to an increase in butyrate in all human participants [187]. All participants had similar levels of the SCFA-producing bacteria *Bifidobacterium adolescentis* and *Ruminococcus bromii* prior to the treatment. An increase *B. adolescentis* and *R. bromii* were associated with higher fecal butyrate

levels in some participants, but not in participants that already had high levels prior to supplementation. In those participants, the microbial community may have already been producing butyrate near its maximum capacity. In another group of participants, fecal butyrate levels were low prior to supplementation and continued to remain low. Butyrate levels may not have changed due to the lack of change in the abundance of *B. adolescentis* or *R. bromii* [187]. Competition with other bacteria in the microbial community or the lack of synergistic interactions may have prevented the increase in *B. adolescentis* or *R. bromii* [187-189]. The presence of low amounts of acetate-producing bacteria prior to supplementation and lack of changes with resistant starch 2 may have prevented an increase in butyrate-producing bacteria. The findings show that a personalized approach involving the analysis of individuals' microbial composition may be needed when attempting to use fiber to change metabolic products and ameliorate disease [186-189].

The impaired repair seen with high sugar diets suggests that the consumption of fiber may be beneficial for repair. This is supported by a study that found that CD patients who consumed greater amounts of fiber during remission had a lower likelihood of experiencing flares than participants with lower fiber intake [190]. However, IBD patients tend to avoid consuming fibers during active disease and remission [191-193]. Patients will avoid high fiber foods such as fruits, beans, and nuts because they tend to cause adverse symptoms such as bloating, abdominal pain and flatulence [194-196]. Low fiber composition prevents adverse symptoms in the patients but may lead to low butyrate levels and lack of improvement in the intestinal environment. IBD patients might be able to consume more fiber and experience an improvement in symptoms. In a study conducted by Hallert et al. (2003), UC patients were able to increase their fecal butyrate levels by consuming additional oat bran with their diet [197]. They did not experience an increase in adverse symptoms or relapses [197]. Similarly, Chiba et al. (2015) provided a small cohort of active CD patients with a semi-vegetarian diet with high fiber content (32.4 g in 2 000 kcal) [198]. Remission was induced in 100% of the patients with the diet and biologic treatment. 95% maintained remission for 2 years with the diet and without biologic treatment [198]. Decreased disease activity was also observed when a small cohort of 10 mildly active CD patients consumed 15 g of fructo-oligosaccharide (FOS) with their diet daily for 3 weeks [199]. The patients also experienced an increase in fecal *Bifidobacteria* and IL-10 producing dendritic cells in the rectal mucosa [199]. In contrast to these findings, FOS did not

improve disease activity or intestinal inflammation in active CD patients enrolled in a randomized controlled trial involving 103 participants [200]. FOS did not significantly increase fecal *Bifidobacteria* or *Faecalibacterium prausnitzii*, but there was an increase in IL-10 and a decrease in IL-6 production by dendritic cells in the rectal mucosa. The production of SCFAs by bacteria other than *F. prausnitzii* might have led to these effects on cytokine production. The contrasting results of these two studies may be associated with differences in the cohorts used. Patients in the randomized control trial had more severe disease before starting the study, compared to the small cohort of 10 patients. The patients also experienced worsening of symptoms such as abdominal pain and flatulence with the FOS. These findings show that fiber supplementation may benefit patients with milder forms of the disease [200].

4.2. Limitations and Future Directions

Only the DSS-induced colitis model was used for this thesis, but the model may not reflect what occurs in humans. In IBD patients, a combination of genetic and environmental factors cause increased disease susceptibility [100]. However, the DSS-induced colitis model is beneficial because it is possible to mimic periods of relapse and remission seen with IBD patients. Genetically-induced colitis models, such as IL-10-deficient mice, can be used to observe the effect of high sugar diets on spontaneous rather than induced colitis. The high sugar diets would need to be administered for a longer period of time. Models involving inflammation in other parts of the gastrointestinal tract may also be used, such STAT4 transgenic mice or $TNF^{\Delta ARE}$ mice which experience transmural ileitis [100].

Future studies may include IBD models that involve inflammation in the small intestine and mimic CD to see if the sugar content of diets causes differential effects. The high glucose water treatment caused a significant increase in gastroduodenal permeability. There can be further investigation to see if increased permeability in upper regions of the gastrointestinal tract due to high sugar content will exacerbate colitis in other IBD models.

Future studies might involve an investigation into the effects of different sugar and fiber combinations on colitis. High sugar intake has been found to be associated with increased IBD risk along with low vegetable intake [38]. Future studies could see if increased fiber intake can protect against colitis despite a higher sugar intake. Ritchie et al. (1987) conducted a 2-year long study in which CD patients were fed a low fiber diet with no restriction on sugar consumption, or a high fiber diet with low sugar intake [201]. No differences were found in clinical outcomes, such as the number of patients that were admitted to a hospital or received surgery [201]. Issues with the experimental design, such as the use of dietary advice rather than diets, and the long period of the study may have prevented differences from being seen.

References

1. Kmiec, Z., Cyman, M. and Slebioda T.J. **Cells of the innate and adaptive immunity and their interactions in inflammatory bowel disease**. *Adv Med Sci*. 2017; 62: 1–16
2. Corridoni, D., Arseneau K.O. and Cominelli F. **Inflammatory bowel disease**. *Immunol Lett*. 2014; 161: 231-235.
3. Kaplan G.G. and Ng S.C. **Understanding and preventing the global increase of inflammatory bowel disease**. *Gastroenterology*. 2017; 152: 313-321.
4. Kaplan G.G., Bernstein C.N., Coward S. et al. **The impact of inflammatory bowel disease in Canada 2018: epidemiology**. *J Can Assoc Gastroenterol*. 2019; 2: S6-16
5. Hillman E.T., Lu H., Yao T. and Nakatsu C.H. **Microbial ecology along the gastrointestinal tract**. *Microbes Environ*. 2017; 32: 300-313
6. Mowat A.M. and Agace W.W. **Regional specialization within the intestinal immune system**. *Nat Rev Immunol*. 2014; 14: 667-685
7. Buckley A. and Turner J.R. **Cell biology of tight junction barrier regulation and mucosal disease**. *Cold Spring Harb Perspect Biol*. 2018; 10: a029314
8. Abreu M.T. **Toll-like receptor signalling in the intestinal epithelium: how bacterial recognition shapes intestinal function**. *Nat Rev Immunol*. 2010; 10: 131-144
9. Li H., Limenitakis J.P., Fuhrer T. et al. **The outer mucus layer hosts a distinct intestinal microbial niche**. *Nat Commun*. 2015; 6: 8292
10. Johansson M.E., Larsson J.M. and Hansson G.C. **The two mucus layers of colon are organized by the MUC2 mucin, whereas the outer layer is a legislator of host-microbial interactions**. *Proc Natl Acad Sci USA*. 2011; 108: 4659-4665
11. Slomiany A., Grabska M., and Slomiany B.L. **Essential components of antimicrobial gastrointestinal epithelial barrier: specific interaction of mucin with an integral apical membrane protein of gastric mucosa**. *Mol Med*. 2001; 7: 1-10
12. Peterson L.W. and Artis D. **Intestinal epithelial cells: regulators of barrier function and immune homeostasis**. *Nat Rev Immunol.* 2014; 14: 141-153
13. Turner J.R. **Intestinal mucosal barrier function in health and disease**. *Nat Rev Immunol*. 2009; 9: 799-809
14. Louis P., Scott K.P., Duncan S.H., Flint H.J. **Understanding the effects of diet on bacterial metabolism in the large intestine**. *J Appl Microbiol*. 2007; 102: 1197-1208

15. James S.L., Muir J.G., Curtis S.L., and Gibson P.R. **Dietary fibre: a roughage guide**. *Intern Med J*. 2003; 33: 291-296
16. Parada Venegas D., De la Fuente M.K., Landskron G. et al. **Short chain fatty acids (SCFAs)-mediated gut epithelial and immune regulation and its relevance for inflammatory bowel diseases**. *Front Immunol*. 2019; 10: 277
17. Duncan S.H., Holtrop G., Lobley G.E. et al. **Contribution of acetate to butyrate formation by human faecal bacteria**. *Br J Nutr*. 2004; 91: 915-923
18. Louis P., Hold G.L. and Flint H.J. **The gut microbiota, bacterial metabolites and colorectal cancer**. *Nat Rev Microbiol*. 2014; 12: 661-672
19. Willemsen L.E., Koetsier M.A. van Deventer S.J. and van Tol E.A. **Short chain fatty acids stimulate epithelial mucin 2 expression through differential effects on prostaglandin E1 and E2 production by intestinal myofibroblasts**. *Gut*. 2003; 52: 1442-1447
20. Wang H.B., Wang P.Y., Wang X. et al. **Butyrate enhances intestinal epithelial barrier function via up-regulation of tight junction protein claudin-1 transcription**. *Dig Dis Sci*. 2012; 57: 3126-3135
21. Arpaia N., Campbell C., Fan X. et al. **Metabolites produced by commensal bacteria promote peripheral regulatory T-cell generation**. *Nature*. 2013; 504: 451-455
22. Smith P.D., Ochsenbauer-Jambor C. and Smythies L.E. **Intestinal macrophages: unique effector cells of the innate immune system**. *Immunol Rev*. 2005; 206: 149-159
23. Smythies L.E., Sellers M., Clements R.H. **Human intestinal macrophages display profound inflammatory anergy despite avid phagocytic and bacteriocidal activity**. *J Clin Invest*. 2005; 115: 66-75
24. Hakansson A. and Molin G. **Gut microbiota and inflammmation**. *Nutrients*. 2011; 3: 637-682
25. Schiffrin E.J. and Blum S. **Interactions between the microbiota and the intestinal mucosa**. *Eur J Clin Nutr*. 2002; 56: S60-64
26. Abraha C. and Medzhitov R. **Interactions between the host innate immune system and microbes in inflammatory bowel disease**. *Gastroenterology*. 2011; 140: 1729-1737
27. Weber B., Saurer L., and Mueller C. **Intestinal macrophages: differentiation and involvement in intestinal immunopathologies**. *Semin Immunopathol*. 2009; 31: 171-184

28. Taupin D. and Podolsky D.K. **Trefoil factors: initiators of mucosal healing**. *Nat Rev Mol Cell Biol*. 2003; 4: 721-732
29. Sturm A. and Dignass A.U. **Epithelial restitution and wound healing in inflammatory bowel disease**. *World J Gastroenterol*. 2008; 14: 348-353
30. Halme L., Paavola-Sakki P., Turunen U. et al. **Family and twin studies in inflammatory bowel disease**. *World J Gastroenterol*. 2006; 12: 3668-3672
31. Turpin W., Goethel A., Bedrani L., Croitoru Mdcm K. **Determinants of IBD heritability: genes, bugs and more**. *Inflamm Bowel Dis*. 2018; 18: 1133-1148
32. McCole D.F. **IBD candidate genes and intestinal barrier regulation**. *Inflamm Bowel Dis*. 2014; 20: 1829-1849
33. Barreiro-de Acosta M., Alvarez Castro A., Souto R. et al. **Emigration to western industrialized countries: a risk factor for developing inflammatory bowel disease**. *J Crohns Colitis*. 2011; 5: 566-569
34. Benchimol E.I., Mack D.R., Guttmann A. et al. **Inflammatory bowel disease in immigrants to Canada and their children: a population-based cohort study**. *Am J Gastroenterol*. 2015; 110: 553-563
35. Benchimol E.I., Manuel D.G., To T. et al. **Asthma, type 1 and type 2 diabetes mellitus, and inflammatory bowel disease amongst South Asian immigrants to Canada and their children: a population-based cohort study**. *PLos One*. 2015; 10: e0123599
36. Zuo T., Kamm M.A., Colombel J.F. and Ng S.C. **Urbanization and the gut microbiota in health and inflammatory bowel disease**. *Nat Rev Gastroenterol Hepatol*. 2018; 15: 440-452
37. Ananthakrishnan A.N., Khalili H., Konijeti G.G. et al. **Long-term intake of dietary fat and risk of ulcerative colitis and Crohn's disease**. *Gut*. 2014; 63: 776-784
38. Racine A., Carbonnel F., Chan S.S. et al. **Dietary patterns and risk of inflammatory bowel disease in Europe: results from the EPIC study**. *Inflamm Bowel Dis*. 2016; 22: 345-354
39. Agus A., Denizot J., Thevenot J. et al. **Western diet induces a shift in microbiota composition enhancing susceptibility to adherent-invasive E.coli infection and intestinal inflammation**. *Sci Rep*. 2016; 6: 19032

40. Gruber L., Kisling S., Lichti P. et al. **High fat diet accelerates pathogenesis of murine Crohn's disease-like ileitis independently of obesity**. *PloS One*. 2013; 8: e71661
41. Tjonneland A., Overvad K., Bergmann M.M. et al. **Linoleic acid, a dietary n-6 polyunsaturated fatty acid, and the aetiology of ulcerative colitis: a nested case-control study within a European prospective cohort study**. *Gut*. 2009; 58:1606-1611
42. Hwang D.H., Kim J.A. and Lee, J.Y. **Mechanisms for the activation of toll-like receptor 2/4 by saturated fatty acids and inhibition by docosahexaenoic acid**. *Eur J Pharmacol*. 2018; 785: 24-25
43. Limdi J.K. **Dietary practices and inflammatory bowel disease**. *Indian Journal of Gastroenterology*. 2018; 37: 284-292
44. Devkota S., Wang Y., Musch M.W. et al. **Dietary-fat-induced taurocholic acid promotes pathobiont expansion and colitis in IL10-/- mice**. *Nature*. 2012; 487: 104-108
45. Teigen L.M., Geng Z., Sadowsky M.J. et al. **Dietary factors in sulfur metabolism and pathogenesis of ulcerative colitis**. *Nutrients*. 2019; 11: 931
46. Jantchou P., Morois S., Clavel-Chapelon F. et al. **Animal protein intake and risk of inflammatory bowel disease: the E3N prospective study**. *Am J Gastroenterol*. 2010; 105: 2195-2201
47. Marion-Letellier R., Amamou A., Savoye G. and Ghosh S. **Inflammatory bowel diseases and food additives: To add fuel on the flames!** *Nutrients*. 2019; 11: 1111
48. Ananthakrishnan A.N., Khalili H., Konijeti G.G. et al. **A prospective study of long-term intake of dietary fiber and risk of Crohn's disease and ulcerative colitis.** *Gastroenterology*. 2013; 145: 970-977
49. Jakobsen C., Paerregaard A., Munkholm P. and Wewer V. **Environmental factors and risk of developing paediatric inflammatory bowel disease – A population based study 2007-2009**. *J Crohns Colitis*. 2013; 7: 79-88
50. Lewis J.D. and Abreu M.T. **Diet as a trigger or therapy for inflammatory bowel diseases**. *Gastroenterology*. 2017; 152: 398-414
51. Andersen V., Olsen A., Carbonnel F. et al. **Diet and risk of inflammatory bowel disease**. *Dig Liver Dis*. 2012; 44: 185-194

52. Ott S.J., Musfeldt M., Wenderoth D.F. et al. **Reduction in diversity of the colonic mucosa associated bacterial microflora in patients with active inflammatory bowel disease**. *Gut.* 2004; 53: 685-693

53. Gophna U., Sommerfeld K., Gophna S. et al. **Differences between tissue-associated intestinal microfloras of patients with Crohn's disease and ulcerative colitis**. *J Clin Microbiol*. 2006; 44: 4136-4141

54. Sokol H., Seksik P., Furet J.P. et al. **Low counts of Faecalibacterium Prausnitzii in colitis microbiota**. *Inflamm Bowel Dis.* 2009; 15: 1183-1189

55. Ni J., Wu G.D., Albenberg L. and Tomov V.T. **Gut microbiota and IBD: causation or correlation**. *Nat Rev Gastroenterol Hepatol*. 2017; 14: 573-584

56. Byndloss M.X., Pernitzsch S.R. and Baumler A.J. **Healthy hosts rule within: ecological forces shaping the gut microbiota**. *Mucosal Immunol*. 2018; 11: 1299-1305

57. Litvak Y., Byndloss M.X., Baumler A.J. **Colonocyte metabolism shapes the gut microbiota**. *Science*. 2018; 362: eaat9076

58. Sellon R.K., Tonkonogy S., Schultz M. et al. **Resident enteric bacteria are necessary for development of spontaneous colitis and immune system activation in interleukin-10-deficient mice**. *Infect Immun*. 1998; 66: 5224-5231

59. Wang S.L., Wang Z.R. and Yang C.Q. **Meta-analysis of broad-spectrum antibiotic therapy in patients with active inflammatory bowel disease**. *Exp Ther Med*. 2012; 4: 1051-1056

60. Zeng L., Hu S., Chen P. et al. **Macronutrient intake and risk of Crohn's disease: systematic review and dose-response meta-analysis of epidemiological studies**. *Nutrients.* 2017; 15: E500

61. Wang F., Feng J., Gao Q. et al. **Carbohydrate and protein intake and risk of ulcerative colitis: systematic review and dose-response meta-analysis of epidemiological studies**. *Clin Nutr*. 2017; 36: 1259-1265

62. Fedorak R., Hotte N., Park H. et al. **High sugar diets promote an inflammatory microbiota and reduce gene expression related to intestinal barrier function**. *Gastroenterology*. 2016; 150: S114-115

63. Laffin M., Fedorak R., Zalasky A. et al. **A high-sugar diet rapidly enhances susceptibility to colitis via depletion of luminal short-chain fatty acids in mice**. *Sci Rep*. 2019; 9: 12294

64. Cheng M.W., Chegeni M., Kim K.H. et al. **Different sucrose-isomaltase response of caco-2 cells to glucose and maltose suggests dietary maltose sensing**. *J Clin Biochem Nutr*. 2014; 54: 55-60

65. Skovbjerg H. **Immunoelectrophoretic studies on human small intestinal brush border proteins-the longitudinal distribution of peptidases and disaccharidases**. *Clinic Chimica Acta*. 1981; 112: 205-212

66. Karasov W.H. **Integrative physiology of transcellular and paracellular intestinal absorption**. *J Exp Biol*. 2017; 220: 2495-2501

67. Ferraris R.P., Choe J.Y. and Patel C.R. **Intestinal absorption of fructose**. *Annu Rev Nutr*. 2018; 38: 41-67

68. Kellett G.L. and Helliwell P.A. **The diffusive component of intestinal glucose absorption is mediated by the glucose-induced recruitment of GLUT2 to the brush-border membrane**. *Biochem J*. 2000; 350: 155-162

69. Patel C., Douard V., Yu S. et al. **Fructose-induced increases in expression of intestinal fructolytic and gluconeogenic genes are regulated by GLUT5 and KHK**. *Am J Physiol Regul Integr Comp Physiol*. 2015; 309: R499-509

70. Patel C., Douard V., Yu S. et al. **Transport, metabolism, and endosomal trafficking-dependent regulation of intestinal fructose absorption**. *FASEB J*. 2015; 29: 4046-4058

71. Das U.N. **Sucrose, fructose, glucose, and their link to metabolic syndrome and cancer**. *Nutrition*. 2015; 31: 249-257

72. Rutledge A.C. and Adeli K. **Fructose and the metabolic syndrome: pathophysiology and molecular mechanisms**. *Nutr Rev*. 2007; 65: S13-S23

73. McGuinness O.P. and Cherrington A.D. **Effects of fructose on hepatic glucose metabolism**. *Curr Opin Clin Nutr Metab Care*. 2003; 6: 441-448

74. Adeva-Andany M.M., Perez-Felpete N., Fernandez-Fernandez C. et al. **Liver glucose metabolism in humans**. *Biosci Rep*. 2016; 36: e00416

75. Zhang D.M., Jiao R.Q. and Kong L.D. **High dietary fructose: direct or indirect dangerous factors disturbing tissue and organ functions**. *Nutrients*. 2017; 9: E335

76. Patel C., Sugimoto K., Douard V. et al. **Effect of dietary fructose on portal and systemic serum fructose levels in rats and in KHK-/- and GLUT5-/- mice**. *Am J Physiol Gastrointest Liver Physiol*. 2015; 309: G779-790

77. Volynets V., Rings A., Bardos G. et al. **Intestinal barrier analysis by assessment of mucins, tight junctions, and alpha-defensins in healthy C57BL/6J and BALB/cJ mice**. *Tissue Barriers*. 2016; 4: e1208468

78. Wang N., Yu H., Ma J. et al. **Evidence for tight junction protein disruption in intestinal mucosa of malignant obstructive jaundice patients**. *Scand J Gastroenterol*. 2010; 45: 191-199

79. Lee J.Y., Wasinger V.C., Yau Y.Y. et al. **Molecular pathophysiology of epithelial barrier dysfunction in inflammatory bowel diseases**. *Proteomes*. 2018; 6: E17

80. Wang L., Llorente C., Hartmann P. et al. **Methods to determine intestinal permeability and bacterial translocation during liver disease**. *J Immunol Methods*. 2015; 421: 44-53

81. Woting A. and Blaut M. **Small intestinal permeability and gut-transit time determined with low and high molecular weight fluorescein isothiocyanate-dextrans in C3H mice**. *Nutrients*. 2018; 10: E685

82. Arrieta M.C., Madsen K., Doyle J. and Meddings J. **Reducing small intestinal permeability attenuates colitis in the IL10 gene-deficient mouse**. *Gut*. 2009; 58: 41-48

83. Arrieta M.C., Bistritz L., and Meddings J.B. **Alterations in intestinal permeability**. *Gut*. 2006; 55: 1512-1520

84. Clarke L.L. **A guide to Ussing chamber studies of mouse intestine**. *Am J Physiol Gastrointest Liver Physiol*. 2009; 296: G1151-66

85. Srinivasan B., Kolli A.R., Esch M.B. et al. **TEER measurement techniques for in vitro barrier model systems**. *J Lab Autom*. 2015; 20: 107-126

86. Do M.H., Lee E., Oh M.J. et al. **High-glucose or -fructose diet cause changes of the gut microbiota and metabolic disorders in mice without body weight change**. *Nutrients*. 2018; 10: E761

87. d'Hennezel E., Abubucker S., Murphy L.O. and Cullen T.W. **Total lipopolysaccharide from the human gut microbiome silences toll-like receptor signaling**. *mSystems*. 2017; 2: e00046-17

88. Vatanen T., Kostic A.D., d'Hennezel E. et al. **Variation in microbiome LPS immunogenicity contributes to autoimmunity in humans**. *Cell*. 2016; 165: 1551
89. Turner J.R., Rill B.K., Carlson S.L. et al. **Physiological regulation of epithelial tight junctions is associated with myosin light-chain phosphorylation**. *Am J Physiol*. 1997; 273: C1378-1385
90. Johnson R.J., Rivard C., Lanaspa M.A. et al. **Fructokinase, fructans, intestinal permeability, and metabolic syndrome: an equine connection?** *J Equine Vet Sci*. 2013; 33: 120-126
91. Low D., Nguyen D.D., and Mizoguchi E. **Animal models of ulcerative colitis and their application in drug research**. *Drug Des Devel Ther*. 2013; 7: 1341-1357
92. Koroleva E.P., Halperin, S., Gubernatorova E.O. et al. **Citrobacter rodentium-induced colitis: A robust model to study mucosal immune responses in the gut**. *J Immunol Methods*. 2015; 421: 61-72
93. Mizoguchi A., Takeuchi T., Himuro H. et al. **Genetically engineered mouse models for studying inflammatory bowel disease**. *J Pathol*. 2016; 238: 205-219
94. Chassaing B., Aitken J.D., Malleshappa M. and Vijay-Kumar M. **Dextran sulfate sodium (DSS)-induced colitis in mice**. *Curr Protoc Immunol*. 2014; 104: Unit 15.25
95. Poritz L.S., Garver K.I., Green C. et al. **Loss of the tight junction protein ZO-1 in dextran sulfate sodium induced colitis**. *J Surg Res*. 2017; 140: 12-19
96. Whittem C.G., Williams A.D. and Williams C.S. **Murine colitis modeling using dextran sulfate sodium (DSS)**. *J Vis Exp*. 2010; 35: 1652
97. Yan Y., Kolachala V., Dalmasso G. et al. **Temporal and spatial analysis of clinical and molecular parameters in dextran sodium sulfate induced colitis**. *PLoS One*. 2009; 4: e6073
98. Hall L.J., Faivre E., Quinlan A. et al. **Induction and activation of adaptive immune populations during acute and chronic phases of a murine model of experimental colitis**. *Dig Dis Sci*. 2011; 56: 79-89
99. Wirtz S., Popp V., Kindermann M. et al. **Chemically induced mouse models of acute and chronic intestinal inflammation**. *Nat Protoc*. 2017; 12: 1295-1309

100. Valatas V., Vakas M. and Kolios G. **The value of experimental models of colitis in predicting efficacy of biological therapies for inflammatory bowel diseases**. *Am J Physiol Gastrointest Liver Physiol*. 2013; 305: G763-785
101. Popkin B.M. and Nielsen S.J. **The sweetening of the world's diet**. *Obes Res*. 2003; 11: 1325-1332
102. Rosinger A., Herrick K., Gahche J and Park S. **Sugar-sweetened beverage consumption among U.S. Adults, 2011-2014**. *NCHS Data Brief*. 2017; 270; 1-8
103. Mock K., Lateef S., Benedito V.A. and Tou J.C. **High-fructose corn syrup-55 consumption alters hepatic lipid metabolism and promotes triglyceride accumulation**. *J Nutr Biochem*. 2017; 39: 32-39
104. Parker K., Salas M., and Nwosu V.C. **High fructose corn syrup: production, uses and public health concerns**. *Biotechnol Mol Biol Rev*. 2010; 5: 71-78
105. Mullee A., Romaguera D., Pearson-Stuttard J. et al. **Association between soft drink consumption and mortality in 10 European countries**. *Jama Intern Med*. 2019; [Epub ahead of print]. doi: 10.1001/jamainternmed.2019.2478
106. Bergheim I., Weber S., Vos M. et al. **Antibiotics protect against fructose-induced hepatic lipid accumulation in mice: role of endotoxin**. *J Hepatol*. 2008; 48: 983-992
107. Mastrocola R., Ferrocino I., Liberto E. et al. **Fructose liquid and solid formulations differently affect gut integrity, microbiota composition and related liver toxicity: a comparative in vivo study**. *J Nutr Biochem*. 2018; 55: 185-199
108. Kuzma J.N., Cromer G., Hagman D.K. et al. **No differential effect of beverages sweetened with fructose, high-fructose corn syrup, or glucose on systemic or adipose tissue inflammation in normal-weight to obese adults: a randomized controlled trial**. *Am J Clin Nutr*. 2016; 104: 306-314
109. Malik V.S., Li Y., Pan A. et al. **Long-term consumption of sugar-sweetened and artificially sweetened beverages and risk of mortality in US adults**. *Circulation*. 2019; 139; 2113-2125
110. Lindqvist A., Baelemans A., Erlanson-Albertsson C. **Effects of sucrose, glucose and fructose on peripheral and central appetite signals**. *Regul Pept*. 2008; 150: 26-32
111. Van der Borght K., Kohnke R., Goransson N. et al. **Reduced neurogenesis in the rat hippocampus, following high fructose consumption**. *Regul Pept*. 2011; 167: 26-30

112. Melanson K.J., Angelopoulos T.J., Nguyen V. et al. **High-fructose corn syrup, energy intake and appetite regulation**. *Am J Clin Nutr*. 2008; 88: 1738S-1744S
113. Sternini C., Anselmi L. and Rozengurt E. **Enteroendocrine cells: a site of 'taste' in gastrointestinal chemosensing**. *Curr Opin Endocrinol Diabetes Obes*. 2008; 15: 73-78
114. Kong M.F., Chapman I., Goble E. et al. **Effect of oral fructose and glucose on plasma GLP-1 and appetite in normal subjects**. *Peptides*. 1999; 20: 545-551
115. Hasegawa H., Shirohara H., Okabayashi Y. et al. **Oral glucose ingestion stimulate cholecystokinin release in normal subjects and patients with non-insulin dependent diabetes mellitus**. *Metabolism*. 1996; 45: 196-202
116. Ritze Y., Bardos G., D'Haese J.G. et al. **Effect of high sugar intake on glucose transporter and weight regulating hormones in mice and humans**. *PLoS One*. 2014; 9: e101702
117. Sclafani A., Cardieri C., Tucker K. et al. **Intragastric glucose but not fructose conditions robust flavor preferences in rat**. *Am J Physiol*. 1993; 265: R320-5
118. Zukerman S., Ackroff K. and Sclafani A. **Post-oral appetite stimulation by sugars and nonmetabolizable sugar analogs**. *Am J Physiol Regul Integr Comp Physiol*. 2013; 305: R840-853
119. Glendinning J.I., Beltran F., Benton L. et al. **Taste does not determine daily intake of dilute sugar solutions in mice**. *Am J Physiol Regul Integr Comp Physiol*. 2010; 299: R1333-1341
120. Meddings J.B., Sutherland L.R., Byles N.I. and Wallace J.L. **Sucrose a novel permeability marker for gastroduodenal disease**. *Gastroenterology*. 1993;104: 1619–26.
121. Madunic I.V., Breljak D., Karaica D. et al. **Expression profiling and immunolocalization of Na+ -D-glucose-cotransporter 1 in mice employing knockout mice as specificity control indicate novel locations and differences between mice and rats**. *Pflugers Arch*. 2017; 469: 1545-1565
122. Stearns A.T., Balakrishnan A., Rhoads D.B. and Tavakkolizadeh A. **Rapid upregulation of sodium-glucose transporter SGLT1 in response to intestinal sweet taste stimulation**. *Ann Surg*. 2010; 251: 865-871

123. Weber S., Volynets V., Kanuri G. et al. **Treatment with the 5-HT3 antagonist tropisetron modulates glucose-induced obesity in mice**. *Int J Obes (Lond)*. 2009; 33: 1339-1347

124. Mihai B.M., Mihai C., Cijevschi-Prelipcean C. et al. **Bidirectional relationship between gastric emptying and plasma glucose control in normoglycemic individuals and diabetic patients**. *J Diabetes Res*. 2018; 2018: 1736959

125. Elias E., Gibson G.J., Greenwood L.F. et al. **The slowing of gastric emptying by monosaccharides and disaccharides in test meals**. *J Physiol*. 1968; 194: 317-326

126. Hewetson M., Cohen N.D., Love S. et al. **Sucrose concentration in blood: a new method for assessment of gastric permeability in horses with gastric ulceration**. *J Vet Intern Med*. 2006; 20: 388-394

127. Abazia C., Ferrara R., Corsaro M.M. et al. **Simultaneous gas-chromatographic measurement of rhamnose, lactulose and sucrose and their application in the testing gastrointestinal permeability**. *Clin Chim Acta*. 2003; 338: 25-32

128. Volynets V., Louis S., Pretz D. et al. **Intestinal barrier function and the gut microbiome are differentially affected in mice fed a western-style diet or drinking water supplemented with fructose**. *J Nutr*. 2017; 147: 770-780

129. Forsyth C.B., Shannon K.M., Kordower J.H. et al. **Increased intestinal permeability correlates with sigmoid mucosa alpha-synuclein staining and endotoxin exposure markers in early parkinson's disease**. *PLoS One*. 2011; 6: e28032

130. Zhang G.Y., Nie S.P., Huang X.J. et al. **Study on Dendrobium officinale O-Acetyl-glucomannan (Dendronan). 7. Improving Effects on Colonic Health of Mice**. *J Agric Food Chem*. 2016; 64: 2485-2491

131. Hu J.L., Nie S.P., Min F.F and Xie M.Y. **Polysaccharide from seeds of plantago asiatica L. increases short-chain fatty acid production and fecal moisture along with lowering pH in mouse colon**. *J Agric Food Chem*. 2012; 60: 11525-11532

132. Statovci, D., Aguilera, M., MacSharry J. and Melgar S. **The impact of western diet and nutrients on the microbiota and response at mucosal interfaces**. *Front Immunol*. 2017; 8: 838

133. Uranga J.A., Lopez-Miranda, V., Lombo F. and Abalo R. **Food, nutrients and nutraceuticals affecting the course of inflammatory bowel disease**. *Pharmacol Rep*. 2016; 68: 816-826
134. Chan S.S., Luben R., van Schaik F. et al. **Carbohydrate intake in the etiology of Crohn's disease and ulcerative colitis**. *Inflamm Bowel Dis*. 2014; 20: 2013-2021
135. Macia L., Tan J., Vieira A.T. et al. **Metabolite-sensing receptors GPR43 and GPR109A facilitate dietary fibre-induced gut homeostasis through regulation of the inflammasome**. *Nat Commun*. 2015; 6: 6734
136. Pellizzon M.A. and Ricci M.R. **The common use of improper control diets in diet-induced metabolic disease research confounds data interpretation: the fiber factor**. *Nutr Metab (Lond)*. 2018; 15: 3
137. Van der Laan L.J., Dopp E.A., Haworth R. et al. **Regulation and functional involvement of macrophage scavenger receptor MARCO in clearance of bacteria in vivo**. *J Immunol*. 1999; 162: 939-947
138. Yoshimatsu M., Terasaki Y., Sakashita N. et al. **Induction of macrophage scavenger receptor MARCO in nonalcoholic steatohepatitis indicates possible involvement of endotoxin in its pathogenic process**. *Int J Exp Pathol*. 2004; 85: 335-343
139. Caporaso J.G., Kuczynski J., Stombaugh J. et al. **QIIME allows analysis of high-throughput community sequencing data**. *Nat Methods*. 2010; 7: 335-336
140. Callahan B.J., McMurdie P.J., Rosen M.J. et al. **DADA2: High-resolution sample inference from Illumina amplicon data**. *Nat Methods*. 2016; 13: 581-583
141. Segata N., Izard J., Waldron L. et al. **Metagenomic biomarker discovery and explanation**. *Genome Biol*. 2011; 12: R60
142. Chong J., Soufan O., Li C. et al. **MetaboAnalyst 4.0: towards more transparent and integrative metabolomics analysis**. *Nucleic Acids Res*. 2018; 46: W486-W494
143. Stirling G. and Wilsey B. **Empirical Relationships between Species Richness, Evenness, and Proportional Diversity**. *Am Nat*. 2001; 158: 286-299
144. Flint H.J., Duncan S.H., Scott K.P. and Louis P. **Links between diet, gut microbiota composition and gut metabolism**. *Proc Nutr Soc*. 2015; 74: 13-22

145. Ormerod K.L., Wood D.L., Lachner N. et al. **Genomic characterization of the uncultured Bacteroidales family S24-7 inhabiting the guts of homeothermic animals**. *Microbiome*. 2016; 4: 36

146. Peng X., Li S., Luo J. et al. **Effects of dietary fibers and their mixtures on short chain fatty acids and microbiota in mice guts**. *Food Funct*. 2013; 4: 932-938

147. Byndloss, MX, Olsan E.E., Rivera-Chavez F. et al. **Microbiota-activated PPAR-γ signaling inhibits dysbiotic Enterobacteriaceae expansion**. *Science*. 2017; 357: 570–575

148. Power K.A., Lepp D., Zarepoor L. et al. **Dietary flaxseed modulates the colonic microenvironment in healthy C57Bl/6 male mice which may alter susceptibility to gut-associated diseases**. *J Nutr Biochem*. 2016; 28: 61-69

149. De Preter V., Arijs I., Windey K. et al. **Decreased mucosal sulfide detoxification is related to an impaired butyrate oxidation in ulcerative colitis**. *Inflamm Bowel Dis*. 2012; 29: 2371-2380

150. Thibault R., De Coppet P., Daly K. et al. **Down-regulation of the monocarboxylate transporter 1 is involved in butyrate deficiency during intestinal inflammation**. *Gastroenterology*. 2007; 133: 1916-1927

151. Ahmad M.S., Krishnan S., Ramakrishna B.S. et al. **Butyrate and glucose metabolism by colonocytes in experimental colitis in mice**. *Gut*. 2000; 46: 493-499

152. Vieira E.L., Leonel A.J., Sad A.P. et al. **Oral administration of sodium butyrate attenuates inflammation and mucosal lesion in experimental acute ulcerative colitis**. *J Nutr Biochem*. 2012; 23: 430-436

153. Mishiro T., Kusunoki R., Otani A et al. **Butyric acid attenuates intestinal inflammation in murine DSS-induced colitis model via milk fat globule-EGF factor 8**. *Lab Invest*. 2013; 93: 834-843

154. Venkatraman A., Ramakrishna B.S., Shaji R.V. et al. **Amelioration of dextran sulfate colitis by butyrate: role of heat shock protein 70 and NF-kappaB**. *Am J Physiol Gastrointest Liver Physiol*. 2003; 285: G177-84

155. Singh V., Yeoh B.S., Walker R.E. et al. **Microbiota fermentation-NLRP3 axis shapes the impact of dietary fibres on intestinal inflammation.** *Gut*. 2019; [Epub ahead of print]. doi: 10.1136/gutjnl-2018-316250

156. Kaiko G.E., Ryu S.H., Koues O.I. et al. **The colonic crypt protects stem cells from microbiota-derived metabolites**. *Cell*. 2016; 165: 1708-1720

157. Eastaff-Leung N., Mabarrack N., **Barbour A. et al. Foxp3+ regulatory T cells, Th17 effector cells, and cytokine environment in inflammatory bowel disease**. *J Clin Immunol*. 2010; 30: 80-89

158. Alex P., Zachos N.C., Nguyen T. et al. **Distinct cytokine patterns identified from multiplex profiles of murine DSS and TNBS-induced colitis**. *Inflamm Bowel Dis*. 2009; 15: 341-352

159. Melgar S., Karlsson A. and Michaelsson E. **Acute colitis induced by dextran sulfate sodium progresses to chronicity in C57BL/6 but not in BALB/c mice: correlation between symptoms and inflammation**. *Am J Physiol Gastrointest Liver Physiol*. 2005; 288: G1328-1338

160. Zheng L., Kelly C.J., Battista K.D. et al. **Microbial-Derived Butyrate Promotes Epithelial Barrier Function through IL-10 Receptor-Dependent Repression of Claudin-2**. *J Immunol*. 2017; 199: 2976-2984

161. Zadori Z.S., Toth V.E., Feher A. et al. **Inhibition of alpha2A-adrenoceptors ameliorates dextran sulfate sodium-induced acute intestinal inflammation in mice**. *J Pharmacol Exp Ther*. 2016; 358: 483-491

162. Moreau N.M., Martin L.J., Toquet C.S. et al. **Restoration of the integrity of rat caeco-colonic mucosa by resistant starch, but not by fructo-oligosaccharides, in dextran sulfate sodium-induced experimental colitis**. *Br J Nutr*. 2003; 90: 75-85

163. Kripke S.A., Fox A.D., Berman J.M. et al. **Stimulation of intestinal mucosal growth with intracolonic infusion of short-chain fatty acids**. *JPEN J Parenter Enteral Nutr*. 1989; 13: 109-116

164. Den Besten G., van Eunen K., Groen A.K. et al. **The role of short-chain fatty acids in the interplay between diet, gut microbiota, and host energy metabolism**. *J Lipid Res*. 2013; 54: 2325-2340

165. Brown K., Abbott D.W., Uwiera R.R.E. and Inglis G.D. **Removal of the cecum affects intestinal fermentation, enteric bacterial community structure, and acute colitis in mice**. *Gut Microbes*. 2018; 9: 218-235

166. Winter S.E., Lopez C.A. and Baumler A.J. **The dynamics of gut-associated microbial communities during inflammation.** *EMBO Rep*. 2013; 14: 319-327

167. Rivera-Chavez F., Zhang L.F., Faber F. et al. **Depletion of butyrate-producing clostridia from the gut microbiota drives an aerobic luminal expansion of Salmonella.** *Cell Host Microbe*. 2016; 19: 443-454

168. Desai M.S., Seekatz A.M., Koropatkin N.M. et al. **A dietary fiber-deprived gut microbiota degrades the colonic mucus barrier and enhances pathogen susceptibility**. *Cell*. 2016; 167: 1339-1353

169. Gray D.F., Eastwood M.A., Brydon W.G. and Fry S.C. **Fermentation and subsequent disposition of 14C-labelled plant cell wall material in the rat**. *Br J Nutr*. 1993; 69: 189-197

170. Van den Abbeele P., Gerard P., Rabot S. et al. **Arabinoxylans and inulin differentially modulate the mucosal and luminal gut microbiota and mucin-degradation in humanized rats**. *Environ Microbiol*. 2011; 13: 2667-2680

171. Tordoff M.G., Pilchak D.M., Williams J.A. et al. **The maintenance diets of C57BL/6J and 129X1/SvJ mice influence their taste solution preferences: implications for large-scale phenotyping projects**. *J Nutr*. 2002; 132: 2288-2297

172. Reeves P.G., Nielsen F.H. and Fahey G.C. Jr. **AIN-93 purified diets for laboratory rodents: final report of the American Institute of Nutrition ad hoc writing committee on the reformulation of the AIN-76A rodent diet.** *J Nutr*. 1993; 123: 1939-1951

173. Khalili H., Hakansson N., Chan S.S. et al. **No association between consumption of sweetened beverages and risk of later-onset Crohn's disease or ulcerative colitis**. *Clin Gastroenterol Hepatol*. 2019; 17: 123-129

174. Chan S.S., Luben R., van Schaik F. et al. **Carbohydrate intake in the etiology of Crohn's disease and ulcerative colitis.** *Inflamm Bowel Dis*. 2014; 20: 2013-2021

175. Hart A.R., Luben R., Olsen A. et al. **Diet in the aetiology of ulcerative colitis: a European prospective cohort study.** *Digestion*. 2008; 77: 57-64

176. Nie J.Y. and Zhao Q. **Beverage consumption and risk of ulcerative colitis: Systematic review and meta-analysis of epidemiological studies.** *Medicine (Baltimore)*. 2017; 96: e9070

177. Yang X.Y., Chen P.F., and He J.H. **High consumption of sweetened beverages might increase the risk of inflammatory bowel diseases.** *Clin Gastroenterol Hepatol*. 2019; 17: 1417-1418

178. Opstelten J.L., de Vries J.H.M., Wools A. et al. **Dietary intake of patients with inflammatory bowel disease: A comparison with individuals from a general population and associations with relapse.** *Clin Nutr*. 2019; 38: 1892-1898

179. Reif S., Klein I., Lubin F. et al. **Pre-illness dietary factors in inflammatory bowel disease.** *Gut*. 1997; 40: 754-760

180. Sakamoto N., Kono S., Wakai K. et al. **Dietary risk factors for inflammatory bowel disease: a multicenter case-control study in Japan.** *Inflamm Bowel Dis*. 2005; 11: 154-163

181. Andersen V., Chan S., Luben R. et al. **Fibre intake and the development of inflammatory bowel disease: A European prospective multi-centre cohort study (EPIC-IBD).** *J Crohns Colitis*. 2018; 12: 129-136

182. Liu X., Wu Y. and Zhang D. **Dietary fiber intake reduces risk of inflammatory bowel disease: result from a meta-analysis.** *Nutr Res*. 2015; 35: 753-758

183. Llewellyn S.R., Britton G.J., Contijoch E.J. et al. **Interactions between diet and the intestinal microbiota alter intestinal permeability and colitis severity in mice.** *Gastroenterology*. 2018; 154: 1037-1046

184. Wedlake L., Slack N., Andreyev H.J. and Whelan K. **Fiber in the treatment and maintenance of inflammatory bowel disease: a systematic review of randomized controlled trials.** *Inflamm Bowel Dis*. 2014; 20: 576-586

185. Wong C., Harris P.J. and Ferguson L.R. **Potential benefits of dietary fibre intervention in inflammatory bowel disease.** *Int J Mol Sci*. 2016; 17: 919

186. Martinez I., Kim J., Duffy P.R. et al. **Resistant starches types 2 and 4 have differential effects on the composition of the fecal microbiota in human subjects**. *PLoS One*. 2010; 5: e15046

187. Venkataraman A., Sieber J.R., Schmidt A.W. et al. **Variable responses of human microbiomes to dietary supplementation with resistant starch**. *Microbiome*. 2016; 4: 33

188. Deehan E.C., Duar R.M., Armet A.M. et al. **Modulation of the gastrointestinal microbiome with nondigestible fermentable carbohydrates to improve human health**. *Microbiol Spectr*. 2017; 5. doi: 10.1128/microbiolspec.BAD-0019-2017
189. Baxter N.T., Schmidt A.W., Venkataraman A. et al. **Dynamics of human gut microbiota and short-chain fatty acids in response to dietary interventions with three fermentable fibers**. *mBio*. 2019; 10: e02566-18
190. Brotherton C.S., Martin C.A., Long M.D. et al. **Avoidance of fiber is associated with greater risk of Crohn's disease flare in a 6 month period.** *Clin Gastroenterol Hepatol*. 2016; 14: 1130-1136
191. Bergeron F., Bouin M., D'Aoust L. et al. **Food avoidance in patients with inflammatory bowel disease: What, when and who?** *Clin Nutr*. 2018; 37: 884-889
192. Zallot C., Quilliot D., Chevaux J.B. et al. **Dietary beliefs and behavior among inflammatory bowel disease patients.** *Inflamm Bowel Dis*. 2013; 19: 66-72
193. Vagianos K., Clara I., Carr R. et al. **What are adults with inflammatory bowel disease (IBD) eating? A closer look at the dietary habits of a population-based Canadian IBD cohort**. *JPEN J Parenter Enteral Nutr*. 2016; 40: 405-411
194. Triggs C.M., Munday K., Hu R. et al. **Dietary factors in chronic inflammation: food tolerances and intolerances of a New Zealand Caucasian Crohn's disease population.** *Mutat Res*. 2010; 690: 123-138
195. Bueno-Hernandez N., Nunez-Aldana M., Ascano-Gutierrez I. and Yamamoto-Furusho J.K. **Evaluation of diet pattern related to the symptoms of Mexican patients with Ulcerative Colitis (UC): through the validity of a questionnaire.** *Nutr J*. 2015; 14: 25
196. Cohen A.B., Lee D., Long M.D. et al. **Dietary patterns and self-reported associations of diet with symptoms of inflammatory bowel disease.** *Dig Dis Sci*. 2013; 58: 1322-1328
197. Hallert C., Bjorck I., Nyman M. et al. **Increasing fecal butyrate in ulcerative colitis patients by diet: controlled pilot study.** *Inflamm Bowel Dis*. 2003; 9: 116-121
198. Chiba M., Tsuji T., Nakane K, and Komatsu M. **High amount of dietary fiber not harmful but favorable for Crohn disease**. *Perm J*. 2015; 19: 58-61.
199. Lindsay J.O., Whelan K., Stagg A.J., et al. **Clinical, microbiological, and immunological effects of fructo-oligosaccharide in patients with Crohn's disease**. *Gut*. 2006; 55: 348-55

200. Benjamin J.L., Hedin C.R., Koutsoumpas A. et al. **Randomised, double-blind, placebo-controlled trial of fructo-oligosaccharides in active Crohn's disease**. *Gut*. 2011; 60: 923-929.

201. Ritchie J.K., Wadsworth J., Lennard-Jones J.E., and Rogers E. **Controlled multicentre therapeutic trial of an unrefined carbohydrate, fibre rich diet in Crohn's disease**. *Br Med J (Clin Res Ed)*. 1987; 295: 517-520